SILICON SOLAR CELL PROCESS
DEVELOPMENT, FABRICATION AND ANALYSIS

FOR PERIOD COVERING

15 June 1978 to 15 June 1979

PHOTOELECTRONICS DIVISION
15251 EAST DON JULIAN ROAD
CITY OF INDUSTRY, CA 91746

SILICON SOLAR CELL PROCESS
DEVELOPMENT, FABRICATION AND ANALYSIS

Annual Report (Phase I)

FOR PERIOD COVERING

15 June 1978 to 15 June 1979

BY

H.I. YOO, P.A. ILES AND D.P. TANNER

JPL CONTRACT NO. 955089

OPTICAL COATING LABORATORY, INC.
PHOTOELECTRONICS DIVISION
15251 EAST DON JULIAN ROAD
CITY OF INDUSTRY, CA 91746

ABSTRACT

This program has investigated, developed and utilized technologies appropriate and necessary for improving the efficiency of solar cells made from various unconventional silicon sheets. During this reporting period, work has progressed in fabrication and characterization of solar cells from RTR ribbons (Motorola), EFG (RF and RH) ribbons (Mobil-Tyco), dendritic webs (Westinghouse), "Silso" wafers (Wacker), cast silicon by HEM (Crystal Systems), silicon on ceramic (Honeywell) and continuous Czochralski ingots (Hamco). Solar cells were fabricated using a standard process typical of those used currently in the silicon solar cell industry. Also back surface field (BSF) processing and other process modifications were included to give preliminary indications of possible improved performance.

The parameters measured included open circuit voltage, short circuit current, curve fill factor, and conversion efficiency (all taken under AMO illumination). Also measured for typical cells were spectral response, dark I-V characteristics, minority carrier diffusion length, and photoresponse by fine light spot scanning. The results were compared to the properties of cells made from conventional single crystalline Czochralski silicon with an emphasis on statistical evaluation. Limited efforts were made to identify growth defects which will influence solar cell performance and discussion is given on the difficulties experienced in processing the sheets using near-conventional methods.

TABLE OF CONTENTS

LIST OF FIGURES (Continued)

LIST OF FIGURES (Continued)

LIST OF TABLES

LIST OF TABLES (Continued)

I. <u>INTRODUCTION</u>

This contract was intended to evaluate several different silicon
sheet forms for their promise as solar cell materials. Conventional
solar cell processing methods were used, to ensure good control of
processes. A conservative sequence was selected, to give all sheets
a good chance of providing cells with good performance. Because the
intent was to evaluate the silicon, no attempt was made to reduce
the cost of the processes. The rationale was proved that the
most direct and effective way to evaluate materials for solar cells
is to fabricate cells. For continuity with earlier work the photo-
voltaic properties were evaluated at AMO. In addition sufficient
back-up physical measurements were made to confirm the solar cell
performance. Limited attempts were made to improve the performance
of each sheet candidate. The results below show that consistent
evaluation was obtained, and enabled specific suggestions to be
made to the silicon sheet suppliers as to future directions likely
to improve their sheets.

The following section (II) describes work on separate sheet forms,
in the order received.

These forms were:

A. "Silso" Silicon   (Wacker)

B. EFG (RF) Ribbon Silicon   (Mobil Tyco)

C. EFG (RH) Ribbon Silicon   (Mobil Tyco)

D. RTR Silicon   (Motorola)

E. Dendritic Web Silicon   (Westinghouse)

F. Cast (HEM) Silicon   (Crystal Systems)

G. Silicon on Ceramic (SOC)   (Honeywell)

H. Continuous Czochralski   (Hamco)

For each form, the solar cell performance (and other properties)
for conventional and other improvements are described. At the end of
Section II (in paragraph I), some summaries, comments, figures and tables
are given. Section III gives conclusions and recommendations and
Section IV gives the Work Plan Status. Section V contains References.
The Appendices include:

I. Time Schedule

II. Abbreviations

III. Description of Solar Cell Fabrication

IV. OCLI AMO Solar Simulator

V. Other Measurement Techniques

II. TECHNICAL DISCUSSION

A. WACKER "SILSO" SOLAR CELLS

1.0 SOLAR CELL FABRICATION

Preparation and Description of Blanks

Wacker wafers were sliced into 2x2 cm silicon blanks using an O.D.
diamond saw. The wafers and the location of the blanks in each wafer
were identified with letters and numerals, respectively. Figure 1
shows how these blanks were prepared from a "Silso" wafer (in this
case wafer A). Identification of each blank on a wafer is very
important since the cell blanks have different grain size depending
on the location of the blanks on the original wafers (10x10 cm).
Edges of the wafer showed smaller grain size than the middle since
nucleation starts at edges during solidification of molten silicon.
Grains were mm size in the middle and were less than mm in areas close
to edges. [Refer to reference (1) for detailed information on Wacker
"Silso" casting process.]

The blanks were chemically polished in planar etch (2:15:5 = HF:HNO$_3$:
CH$_3$COOH) for about 10 minutes, which removed about 1.5 mils of silicon
from each face of the blanks. Four point probe measurement indicated
that resistivities were in the range of 5-11 ohm-cm with P-type
conductivity (four point probe measurement of polycrystalline material
might introduce error in bulk resistivity reading due to the potential
drop at the grain boundaries).

Surface photovoltage measurement for these "Silso" blanks indicated
minority carrier diffusion lengths in the range of 40 to 80 μm
(measurement used a light beam size of around 3-4 mm in diameter).
Single crystalline control blanks were prepared in the same way with
the measured resistivity range 1-3 ohm-cm and minority carrier diffusion
length between 100-200 μm.

Standard Process

The prepared blanks were processed to fabricate standard solar cells,
along with control cells from Czochralski silicon. [Refer Appendix III
for the detailed description of the standard process.] The sheet
resistance of the diffused layer (N-type) was measured to be about
30 ohm/square for Wacker "Silso" silicon and 22-25 ohm/square for
the single crystalline controls. Final mechanical yield, ratio between
unbroken cells and initial starting blanks, was about 94%. Table 1
shows the number and cause of the broken cells during processing.

Back Surface Field (BSF) Process

The detailed description of the BSF process is given in Appendix III
and two "Silso" wafers were processed using this process. The sheet
resistance of the diffused layer (N-type) was 27-31 ohm/square for the
controls and 26-28 ohm/square for the "Silso" wafers. One cell was
broken in the metallization process and two cells were damaged in
electrical testing, resulting in an overall mechanical yield of around
90%.

Grain Boundary Passivation Process

Tests were made to try and increase the carrier collection efficiency in polycrystalline silicon by means of a heavily doped region near (or in) the grain boundaries (2). Phosphorus dopant is preferentially introduced into the grain boundaries of P-type material by a low temperature diffusion process. A subsequent high temperature diffusion forms a heavily doped skin which covers the surface of each grain. The resulting junction around each grain surface collects electrons which might otherwise recombine at the undoped grain boundaries. This grain boundary doping (passivation) scheme offers possibility of an increase of conversion efficiency in polycrystalline silicon solar cells especially if the grain structure is columnar.

An experiment was performed in an effort to improve the conversion efficiency using this method. An N-type, (phosphorus-dopant) source (Emulsitone) was spun on 2x2 cm wafers. After drying on a hot plate, those wafers were loaded in a furnace and heated at 600°C for about 24 hours in N_2 atmosphere. After removing glass layers on the spin-on side of the wafers, standard process was used to complete the cells.

One "Silso" wafer was fabricated using this process with no breakage (mechanical yield of 100%). Sheet resistance of the diffused layers of both control and "Silso" wafers were in the range of 23-38 ohm/square and 28-30 ohm/square, respectively.

2.0   SOLAR CELL PERFORMANCE AND CHARACTERIZATION

Characteristics Under Illumination

Parameters of the finished solar cells were measured under AMO conditions* (135 mW/cm^2, tungsten-xenon lamps with red and blue filters) before and.after applying anti-reflective coating. The measurement block temperature was 25°C and the input light intensity was calibrated using a standard balloon-flown solar cell.

The detailed parameter of the individual control cells and. Wacker "Silso" cells are given in reference (3) electrical data sheets. One "Silso" wafer was processed and the average values, standard deviation and ranges are summarized in Table 2, showing 9.6% for "Silso" cells and 11.2% for the control cells. To see the dependence of the parameters on the location of the cells on each "Silso" wafer, mainly due to the difference in grain structure, solar cells were classified as corner cells, edge cells, and middle cells, depending on the location (see Figure 1; 1 corner cell, 6 edge cells, and 9 middle cells were obtained from each wafer). The data obtained from the standard process dependence of cell parameters on location is summarized in Table 3. As expected, due to smaller grain size at the corners and edges of Wacker wafer, solar cell efficiency clearly increases in order corner-edge-middle. Some "Silso" wafers contained visible

*Detailed description of OCLI AMO Solar Simulator is given in Appendix IV.

inclusions near the middle of the wafer, showing fine grain structures surrounding the inclusions and consequently producing poor solar cell performance compared with the rest of the wafer area; i.e. see cells A-10 and D-11 in Appendix III of reference (3). Figure 2 shows a microscopic photograph of these inclusions which might have been introduced from the container used for casting of Wacker silicon.

Back surface field solar cells showed an average efficiency of about 9.5%, about the same efficiency as the standard solar cells. Slightly improved short circuit current was offset by the decrease in open circuit voltage. However, efficiencies of the controls increased to 12.1% (about 1% conversion efficiency increase over the standard process cells) by improvement in both short circuit current and open circuit voltage. Individual cell parameters are listed in reference (3) and statistics are summarized in Table 4. In an effort to see the upper limit of efficiency of the Wacker sheets, fine contact lines (active area of the cell is around 93%) and multilayer antireflective coating were applied to three of the BSF cells, resulting in an average conversion efficiency of 10.7%. Results are summarized at the bottom of the table. Positional dependence of BSF cell performance is given in Table 5 with the similar results with the solar cells from the standard processes.

Solar cells from the grain boundary passivation process showed very close performance characteristics with the cells from the standard process, indicating no improvement was achieved by using this process modification. Electrical data sheets and summary tables are given in reference (3).

Dark I-V Characteristics

Dark I-V characteristics (forward and reverse) were obtained from selected solar cells. The plot was made by point-by-point measurement using digital multimeters. Room temperature plots of the dark I-V curves for solar cells from various processes are given in Figures 3 and 4. Sometimes dark diode currents of a solar cell can be expressed in a simple way,

$$I_D = I_o \left(\exp \frac{qV}{AkT} - 1\right).$$

This could be the case at high forward bias condition ($V > 0.4$ volts) in which the diffusion component dominates the diode current. In this case "A" factor in the equation shows deviation from ideal diode characteristics, i.e. it indicates the degree of influence from the space charge recombination and shunt component of the current, and effect of series resistance of solar cells. Calculated "A" values from the curves ranged from 1.4 to 2.2, indicating significant deviation from the ideal diode case in which the "A" factor is unity. I_o was also obtained from the plots. A relatively wide range of I_o was observed, from 10^{-6} A/cm^2 to 10^{-9} A/cm^2; solar cells with small grain structure, such as corner cells and edge cells, showed larger values. This indicates that low open circuit voltage of the cells with small grain size is due to the large value of I_o.

Spectral Response

Absolute spectral response (A/W) was measured using a filter wheel which is a combination of a set of narrow bandwidth filters and a light source.

Detailed measurement techniques are described in Appendix V-A and Figures 5 through 7 show spectral response of Wacker cells and typical control cells of different process modification. Cells made from Wacker wafers indicated lower spectral response than single crystalline control cells at longer wavelengths (>0.6 μm), mainly ·due to smaller minority carrier diffusion length caused by grain boundary effects. The Wacker cells with lower spectral response were located in the edge (small grain size) while Wacker cells with higher response were located in the middle (large grain size) of the Wacker wafers, confirming the effect of grain size on spectral response of solar cells. The spectral response variations also agreed with the cell performance variations. However, no significant difference in spectral response was noticed from Wacker cells taken through the process variations tried (BSF, GB passivation).

Minority Carrier Diffusion Length

Minority carrier diffusion length (D.L.) was measured using the surface photovoltage (SPV) method on both bulk "Silso" wafers and diffused wafers, and a short circuit current method for the finished solar cells. Detailed description of the techniques used are given in Appendix V-B. Table 6 summarizes results of SPV measurements. Generally middle blanks showed higher D.L., showing D.L. in some spots approaching those of single crystalline silicon. No significant change in D.L. before and just after the diffusion step was observed. The whole area of a solar cell was illuminated to measure minority carrier diffusion length.

Table 7 summarizes the diffusion length of solar cells made from four Wacker wafers (A,B,C, and D) and Table 8 indicates the dependence of diffusion length on location of each cell in a wafer, such as corners, edges and middle. Diffusion length of solar cells (2x2 cm) ranged from 30-65 μm, showing lower diffusion length for the cells fabricated from either corners or edges of a wafer. Diffusion length measurement using small beam size (∿3-4 mm beam diameter) indicated that significant variation in the values are observed even within a single cell (2x2 cm). These are well illustrated in Figure 8, again indicating smaller diffusion length at spots close to the edges due to small grain structure.

Photoresponse by Small Light Spot Scanning

Localized photoresponse of solar cells (standard) were obtained by light spot scanning. Detailed measurement techniques are described in Appendix V.C and Figure 9 is the result of the scanning. The Wacker cell showed lower response than the control cell everywhere and the width of electrically active boundaries was estimated to be less than 0.2 mm for small crystallites and about 2 mm for large crystallites.

2-4 mm Edge Trim

A-1	A-2	A-3	A-4	
A-5	A-6	A-7	A-8	
A-9	A-10	A-11	A-12	
A-13	A-14	A-15	A-16	
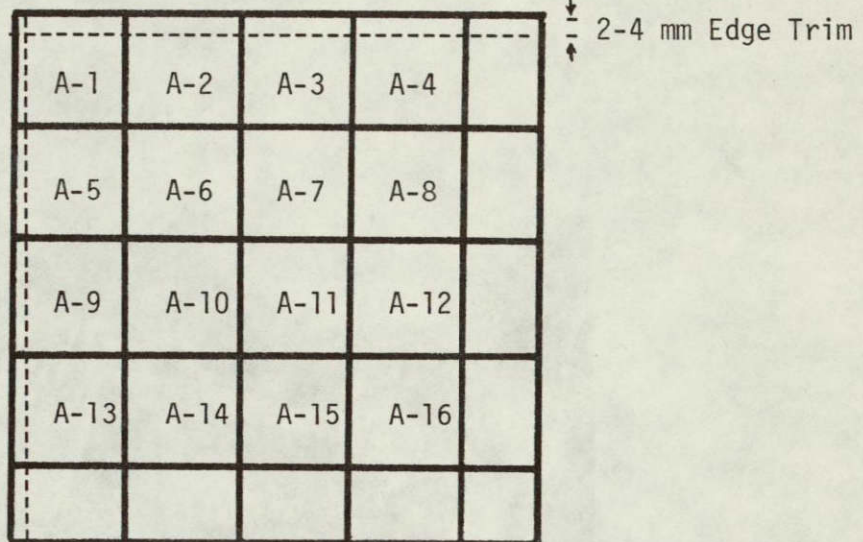
Classification of Blanks

Corner: A-1

Edge: A-2, A-3, A-4, A-5, A-9,
         and A-13

Middle: A-6, A-7, A-8, A-10,
         A-11, A-12, A-14, A-15,
         and A-16

FIGURE 1

Preparation and Classification of Silicon Blanks
(2x2 cm) From a Wacker "Silso" Wafer (A Wafer, 10x10 cm)

FIGURE 2

A Microscopic Photograph of Inclusions
in Wacker Wafer (200X Magnification)

FIGURE 3

Dark I-V Characteristics of Wacker Solar Cells
(2x2 cm, Standard Process) at R.T.

x = Forward Characteristics
o = Reverse Characteristics
⸱⸱⸱⸱ Wacker Cells
— A Control Cell (Single Crystalline)
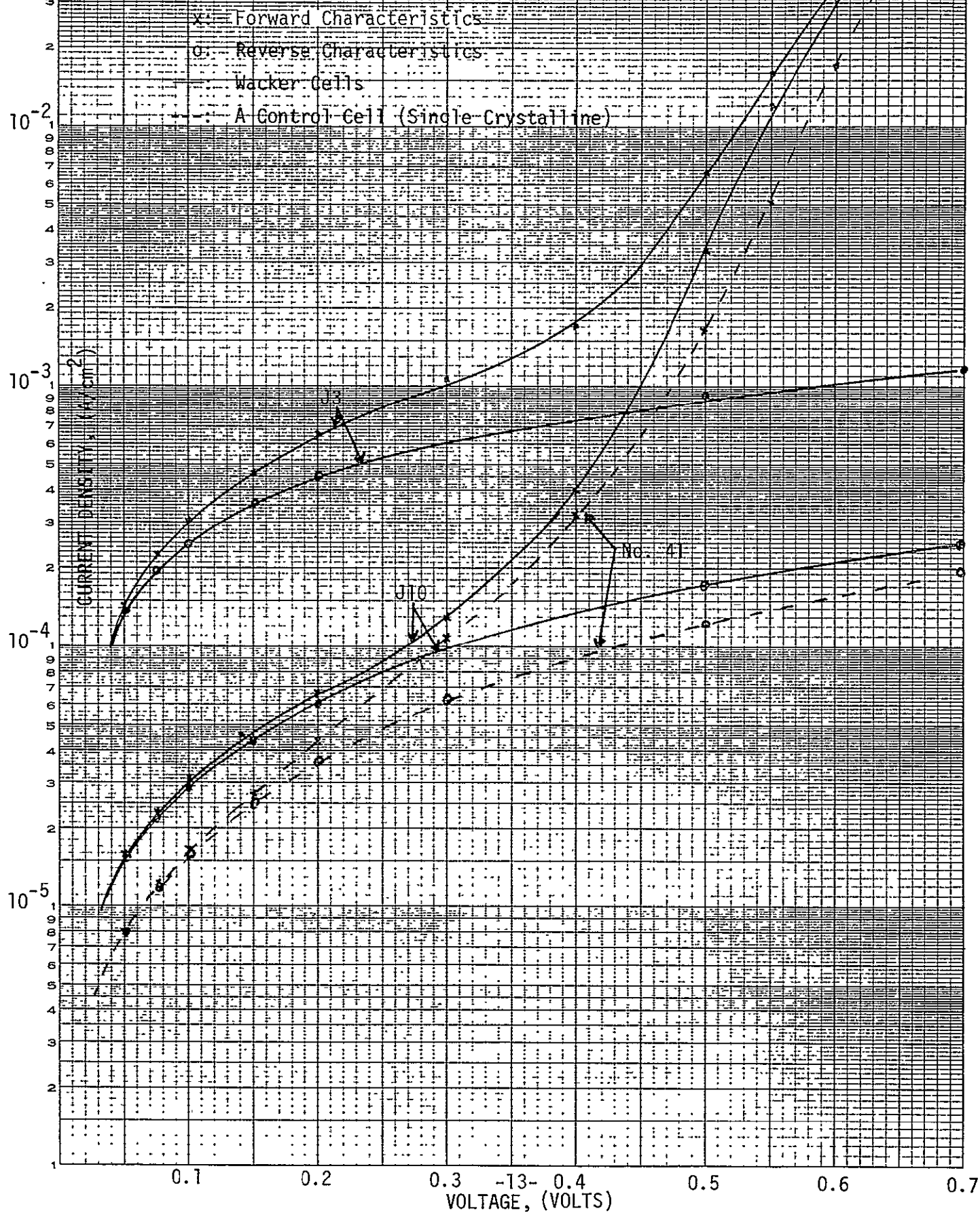
FIGURE 4

Dark I-V Characteristics of Wacker Solar Cells
(2x2cm, BSF Process) at R.T.

x: Forward Characteristics
o: Reverse Characteristics
——: Wacker Cells
—·—: A Control Cell (Single Crystalline)
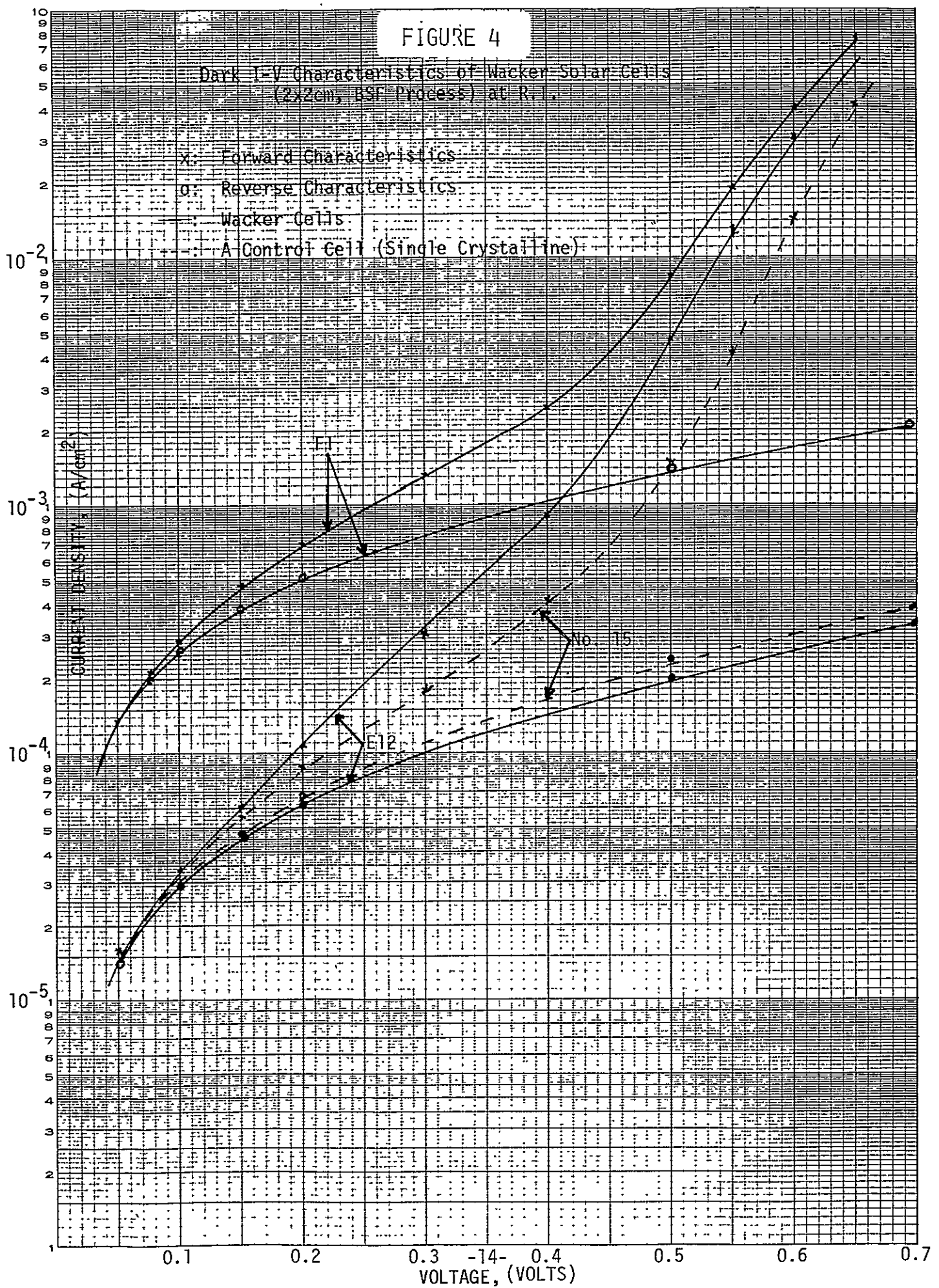
FIGURE 5

Spectral Response of Wacker Solar Cells
(Standard Process)
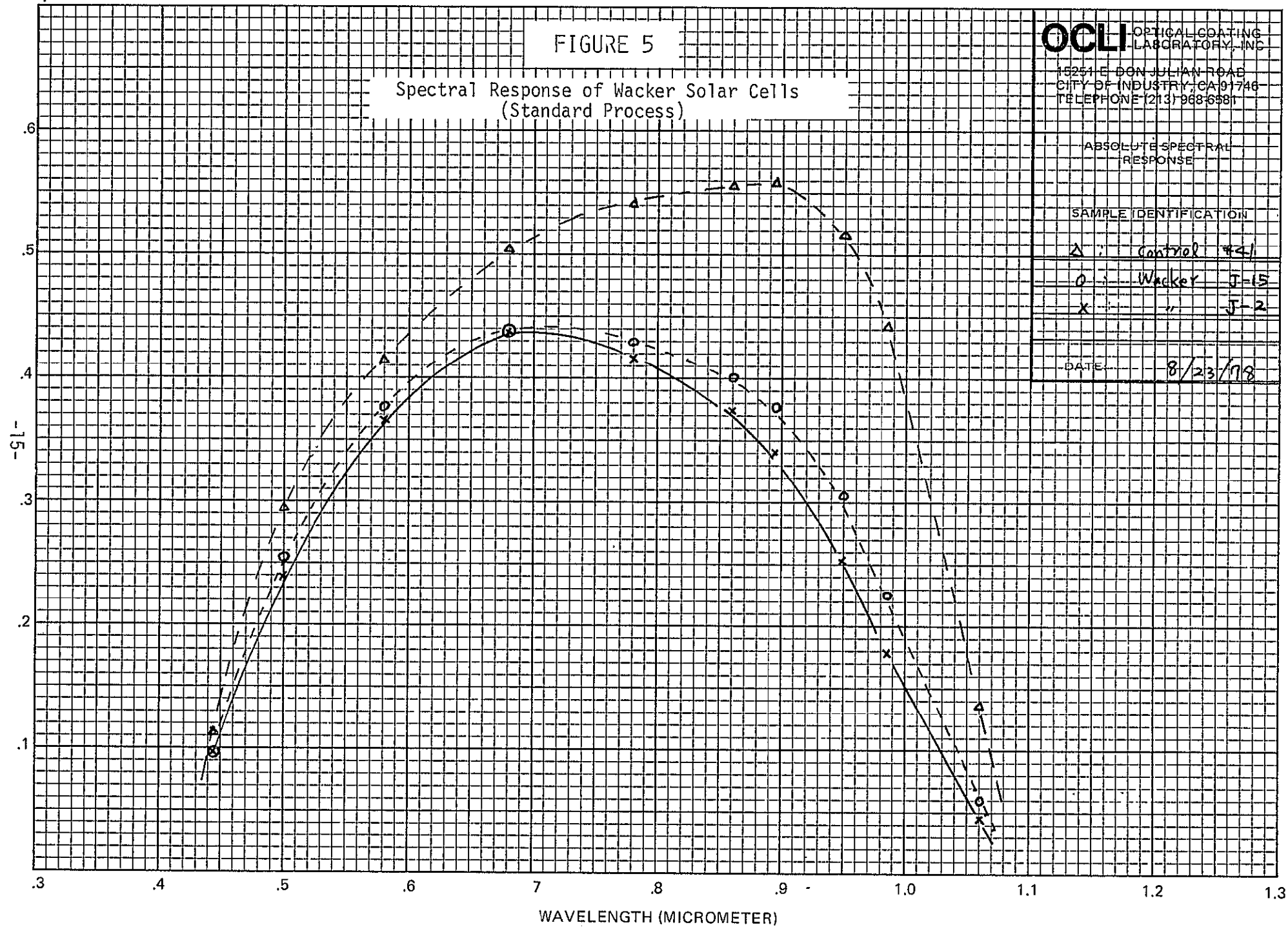
FIGURE 6

Spectral Response of Wacker Solar Cells
(BSF Process)

WAVELENGTH (MICROMETER)

SPECTRAL RESPONSE (A/W)

-16-

OCLI OPTICAL COATING LABORATORY, INC.

15251 E. DON JULIAN ROAD
CITY OF INDUSTRY, CA 91746
TELEPHONE (215) 968-6581

ABSOLUTE SPECTRAL RESPONSE

SAMPLE IDENTIFICATION

X : Control # 3
o : E11
□ : E1
△ : E2

DATE 7/31/78
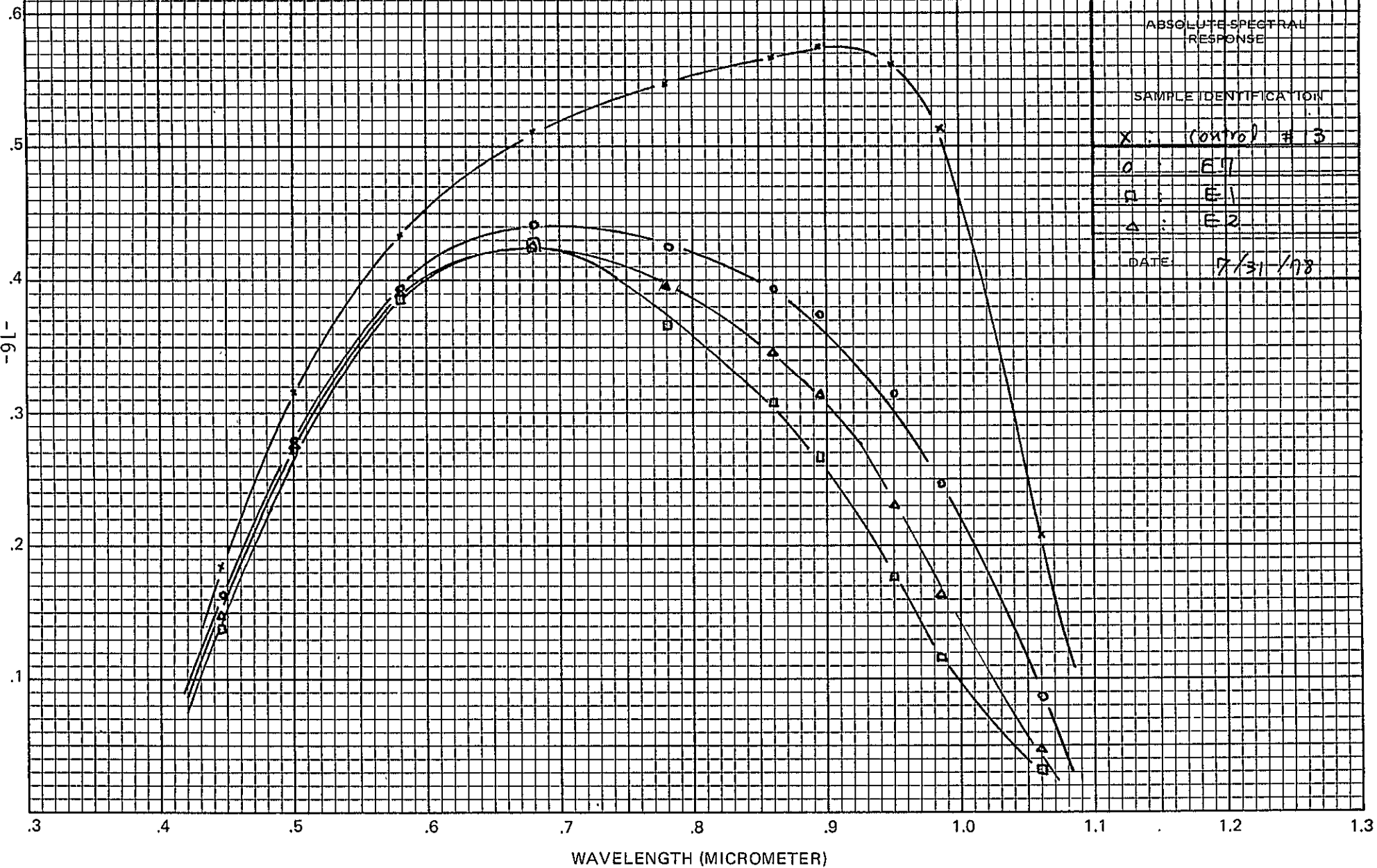
FIGURE 7

Spectral Response of Wacker Solar Cells
(G.B. Passivation Process)
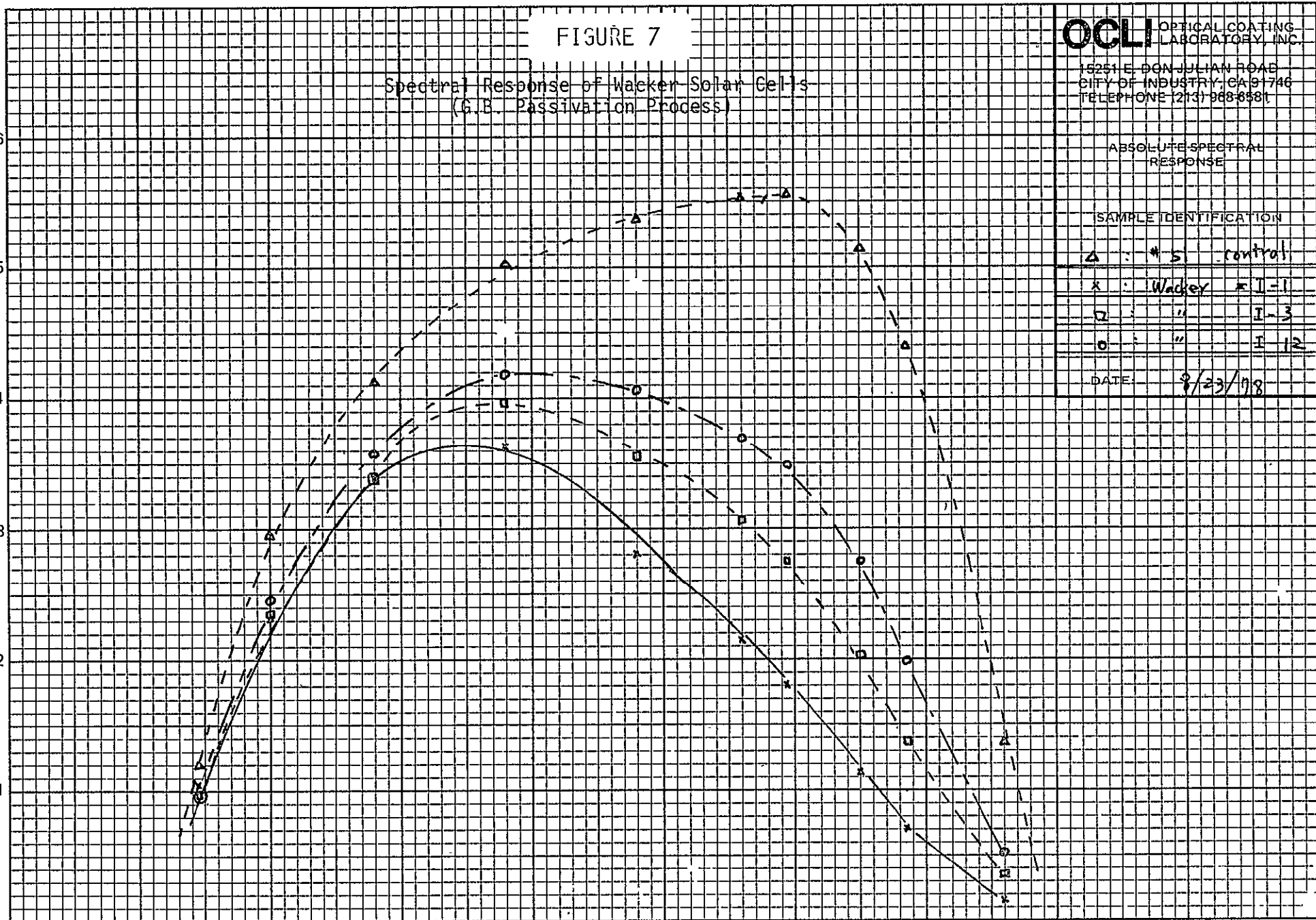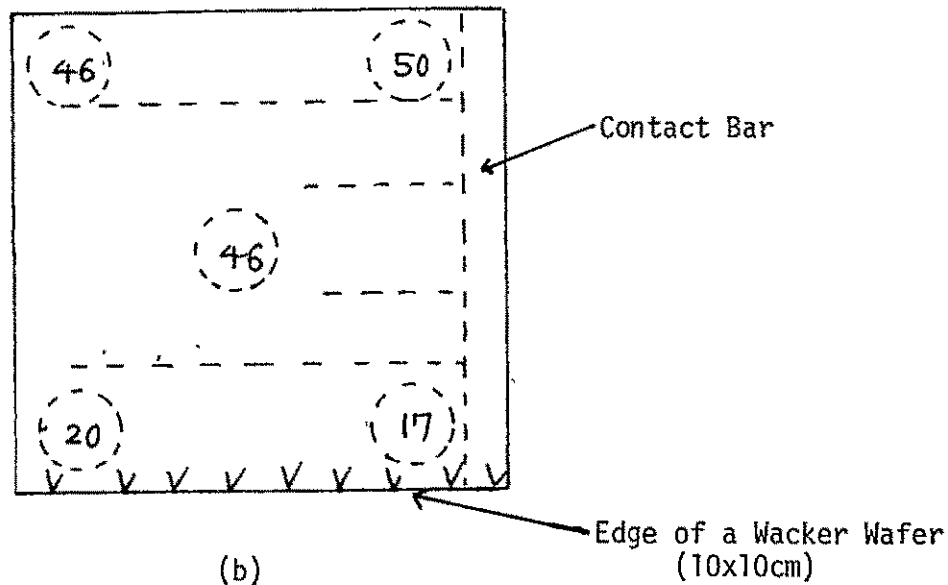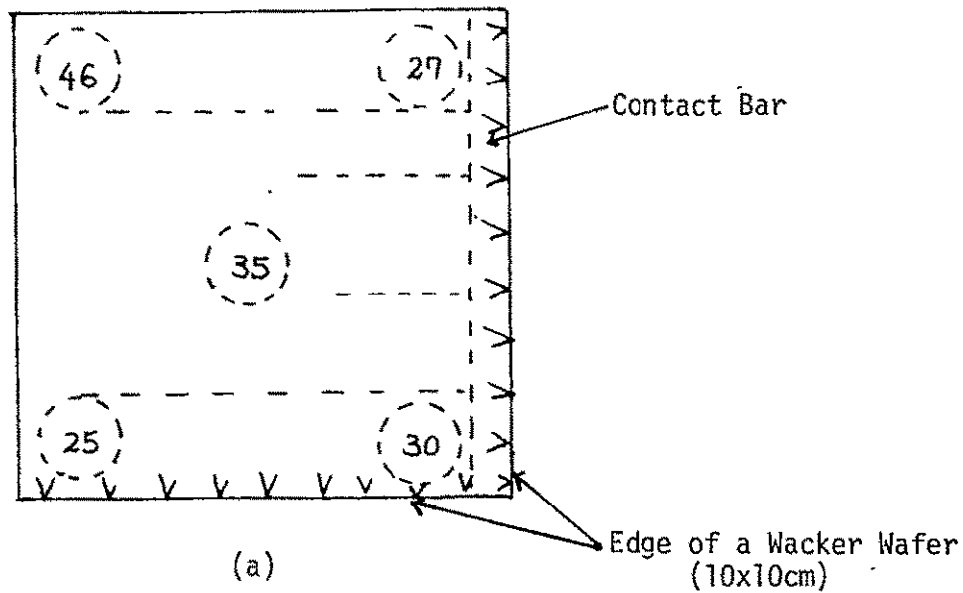
FIGURE 8

Minority Carrier Diffusion Length (μm) Variation
Within a Wacker Solar Cell (2x2cm), Measured by I_{sc} Method
With an Illuminated Beam Size of ~3-4mm Diameter

    a) A Corner Solar Cell (A1)

    b) A Edge Solar Cell (A3)
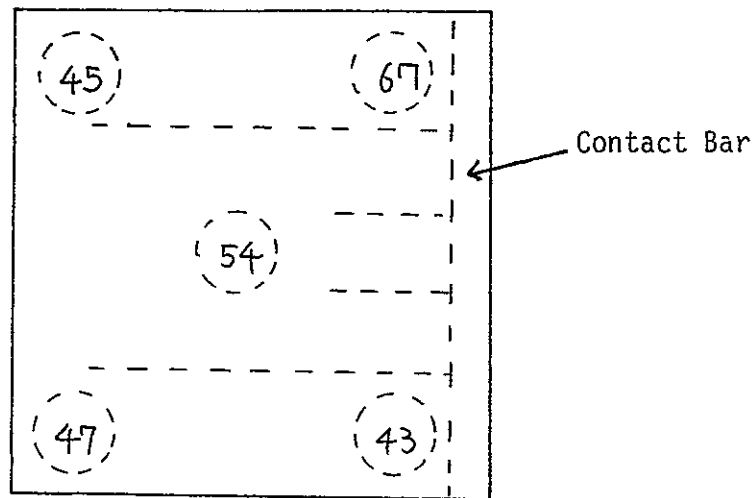
(c)

FIGURE 8

Minority Carrier Diffusion Length (μm) Variation
Within a Wacker Solar Cell (2x2cm), Measured by I_{sc} Method
With an Illuminated Beam Size of ∿3-4mm Diameter

c)   A Middle Solar Cell (A11)

FIGURE 9

SMALL LIGHT SPOT SCANNING OF A WACKER "SILSO" SOLAR CELL

CONTROL CELL

WACKER CELL

GRID LINES

← ~.6 mm →

RELATIVE PHOTORESPONSE

DISTANCE

-20-
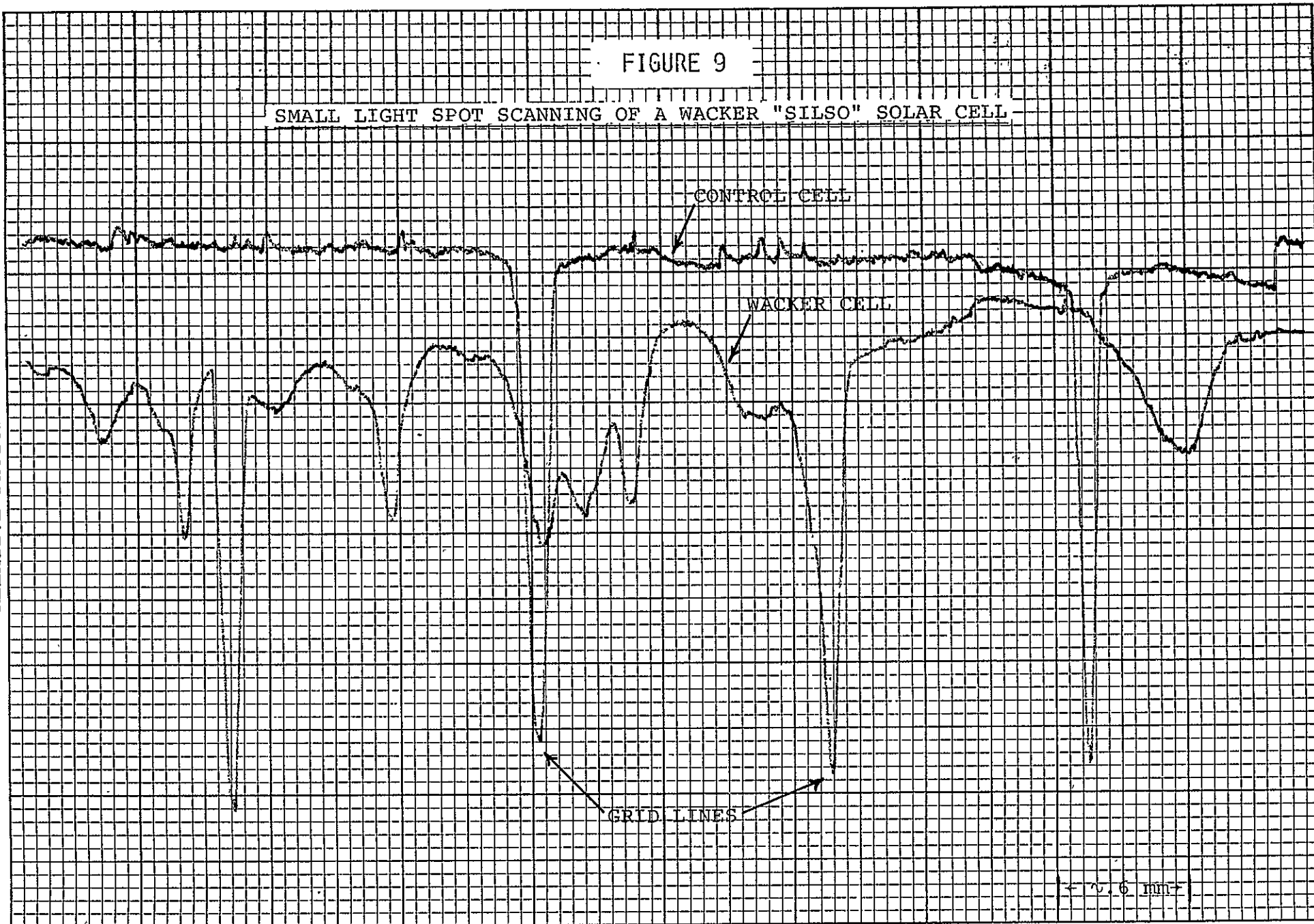
TABLE 1

Mechanical Failure of "Silso" Solar Cells
in the Process of Fabrication

NUMBER OF BROKEN CELLS	CAUSE
1	Dropped While Demounting 2x2 cm Blanks
2	Corner Chipped While Clamping Metal Shadow Mask In Evaporation Process
1	Shattered in Post-Metallization Heat Treatment in a Furnace

Standard Process   Starting Blanks: 64

NUMBER OF BROKEN CELLS	CAUSE
1	Metallization
2	Electrical Testing

BSF Process   Starting Blanks: 32

TABLE 2

Summary of Parameters of Solar Cells
Fabricated From a Wacker "Silso" Wafer; Standard Process

	V_{oc} (mV)	J_{sc} (mA/cm^2)	CFF (%)	η (%)
AVERAGE	558 (549)	30.5 (22.2)	77 (77)	9.6 (6.9)
STANDARD DEVIATION	6.1 (7.4)	0.8 (0.6)	1.3 (2.0)	0.5 (0.4)
RANGE	549-565 (539-555)	29.3-31.5 (21.3-23)	73-79 (72-79)	8.8-10.2 (6.3-7.3)

Control Cells

	V_{oc} (mV)	J_{sc} (mA/cm^2)	CFF (%)	η (%)
AVERAGE	593 (586)	32.9 (24)	78 (78)	11.2 (8.2)
STANDARD DEVIATION	N.A.	N.A.	N.A.	N.A.
RANGE	591-595 (584-588)	32.8-33 (23.8-24.3)	77-79 (76-80)	11.1-11.3 (8.0-8.2)

NOTE: 1. Measurement under AMO condition at 25°C.

2. Cells (2x2cm) with SiO AR coating, parenthesis numbers are for the parameters before AR coating.

-22-

TABLE 3

Dependence of Solar Cell Parameters on the Location of a
2x2 cm Blank Prepared From a Wacker "Silso" Wafer; Standard Process

		CORNER*	EDGE	MIDDLE
V_{oc} (mV)	AVERAGE	N.A.	551	563
	STANDARD DEVIATION	N.A.	1.8	1.5
	RANGE	N.A.	549~554	561~565
J_{sc} (mA/cm²)	AVERAGE	N.A.	29.6	31
	STANDARD DEVIATION	N.A.	0.2	0.2
	RANGE	N.A.	29.3~29.8	30.8~31.5
CFF (%)	AVERAGE	N.A.	76	78
	STANDARD DEVIATION	N.A.	1.5	0.7
	RANGE	N.A.	73~77	76~79
η (%)	AVERAGE	N.A.	9.2	10.0
	STANDARD DEVIATION	N.A.	0.2	0.2
	RANGE	N.A.	8.8~9.4	9.8~10.2

NOTE: Cells (2x2cm) with SiO AR coating measured under AMO condition
at 25°C.

*Cell broken, could not evaluate.

TABLE 4

Summary of Parameters of Solar Cells Fabricated From Wacker
"Silso" Wafers (E & F); Back Surface Field (BSF) Process

	V_{oc} (mV)	J_{sc} (mA/cm^2)	CFF (%)	η (%)
AVERAGE	545 (536)	31.5 (22.6)	75 (74)	9.5 (6.6)
STANDARD DEVIATION	8.4 (8.3)	0.9 (0.7)	1.8 (2.7)	0.5 (0.4)
RANGE	528-557 (518-547)	29.5-33 (21.3-23.8)	71-79 (66-77)	8.2-10.2 (5.7-7.2)

Control Cells

	V_{oc} (mV)	J_{sc} (mA/cm^2)	CFF (%)	η (%)
AVERAGE	602 (593)	35.5 (25.8)	77 (75)	12.1 (8.6)
RANGE	601-602 (591-593)	35.3-35.8 (25.8-26)	75-78 (72-78)	12.0-12.3 (8.2-8.9)

Cells With Fine Contact Line and MLAR Coating

	V_{oc} (mV)	J_{sc} (mA/cm^2)	CFF (%)	η (%)
AVERAGE	556	34.2	77	10.7
RANGE	550-561	33.6-34.8	75-78	10.6-10.8

NOTE: 1. Measured under AMO condition at 25°C.

2. Cells (2x2cm) with SiO AR coating, parenthesis numbers are for the parameters before AR coating.

TABLE 5

Dependence of Solar Cell Parameters on the Location of a 2x2cm Blank
Prepared From Wacker "Silso" Wafers (E & F): BSF Process

		CORNER	EDGE	MIDDLE
V_{oc} (mV)	AVERAGE	531	540	552
	STANDARD DEVIATION	N.A.	2.6	4.2
	RANGE	528∿533	534∿541	547∿557
J_{sc} (mA/cm²)	AVERAGE	29.6	31.0	32.0
	STANDARD DEVIATION	N.A.	0.4	0.5
	RANGE	29.5∿29.8	30.5∿31.8	31.3∿33
CFF (%)	AVERAGE	72	75	75
	STANDARD DEVIATION	N.A.	1.2	1.6
	RANGE	71∿72	74∿77	73∿79
η (%)	AVERAGE	8.4	9.4	9.9
	STANDARD DEVIATION	N.A.	0.2	0.3
	RANGE	8.2∿8.5	8.9∿9.6	9.4∿10.2

NOTE: Cells (2x2cm) with SiO AR coating measured under AMO condition
at 25°C.

TABLE 6

Minority Carrier Diffusion Length
Measurement on Bulk Wacker Wafers

	CORNER & EDGE	MIDDLE
AVERAGE	43 (35)	75 (88)
STANDARD DEVIATION	5 (5)	15 (19)
RANGE	40-55 (30-40)	60-130 (55-120)

NOTE: 1) Parenthesis numbers for the diffused wafers without contacts.

2) Measurement by SPV method with a light beam size $\sim$ 3 mm diameter.

3) Unit; μm.

TABLE 7

Minority Carrier Diffusion Length of Solar Cells (2x2cm)
Fabricated From Four Wacker Wafers (A, B, C and D)

WAFERS		CONTROL	A	B	C	D
Le (μm)	AVERAGE	135	47	46	52	51
	STANDARD DEVIATION	N.A.	7.7	11.7	10	9.5
	RANGE	130-140	33-56	33-61	35-65	31-60

TABLE 8

Dependence of Diffusion Length of Solar Cells on the
Location of a 2x2 cm Blank Prepared From a Wacker Wafer

LOCATION		CORNER	EDGE	MIDDLE
Le (μm)	AVERAGE	33	44	56
	STANDARD DEVIATION	1.6	5.4	5.4
	RANGE	31-35	34-51	49-65

NOTE: 1) Measurement by I_{sc} method.

2) Illuminated whole area of 2x2cm cells.

3) Unit; μm.

B.   EFG (RF) RIBBON SOLAR CELLS

1.0   SOLAR CELL FABRICATION

Preparation and Description of Blanks

The EFG ribbons delivered were of the R.F. furnace grown type with
visible surface undulations and inclusions from the die materials
[See reference (4) for detailed information on EFG process.]
The ribbon was about one inch wide and was sliced into approximately
1x1 inch blanks. Thickness was measured (by micrometer), at several
locations of each blank, indicating around 13 mils at the edges and
10 mils in the middle. To obtain detailed information on the surface
profile of the ribbons, a Dektak (Sloan) was used to scan thickness
across the width of the ribbons. Figure 10 shows a typical profile
of a ribbon surface, indicating significant variation in thickness
across the ribbon width.

NOTE: In the worst case, thickness was around 6 mils or less at
certain localized areas, indicating problems of handling in the process
of cell fabrication.

Since most of the blanks showed warpage, a bow gauge (Brown & Sharp)
was used to show the degree of warpage (this may not be the proper way
to check the warpage of such blanks). From 15 samples of 1" x 1"
blanks bows were averaged to be around 2.0 mils with the range of
0.4 - >3.0 mils.

Resistivity measurements by four point probe ranged between 0.8-2.8 ohm-cm with p-type conductivity. This might not necessarily indicate accurate bulk resistivity because of thickness variations and possible grain boundary effects. SPV measurement of minority carrier diffusion length from a number of measurements with the beam size of 3-4 mm in diameter indicated values between 30-70 μm.

Initial cleaning of the blanks was done by organic solvent in ultra-sonic cleaner, to remove most of the contaminants from wafer handling. However, a hazy color on the surface was difficult to eliminate without removing some silicon. The following efforts were made to remove surface features.

(1) Dip in HF.

(2) Boil in hot D.I. water followed by HF dip (since haze was suspected to be a thin SiO_2 layer).

(3) Clean in H_2SO_4; H_2O = 1:1

(4) Standard RCA Clean: Solution 1 - $NH_4OH;H_2O_2;H_2O$ = 1:1:5

Solution 2 - $HC;H_2O_2;H_2O$ = 1:1:5

None of the above procedures succeeded in removing the haze. Thus, the standard wafer cleaning procedure was chosen to be the initial organic solvent cleaning procedure which removed most of the surface contamination from wafer handling.

Standard Process

Cell fabrication has been done using standard process, described in Appendix III-A, with a change in contact formation process, caused by the uneven surface contours of the ribbon. Instead of using a metal shadow mask for the front contact, photolithographic techniques were used to accommodate the non-flat features and irregular size of the EFG sheets. Build-up of front contact thickness of silver layer was done later by electroplating. Since electroplated cells show leakage characteristics due to the deposition of metal (Ag) at the exposed junction of a cell (i.e., at the edges of a cell), edge trimming was carried out using a dicing saw (Tempress). The size of the finished solar cells varied, and was in the range of around 5-6 cm^2 in total area. Active area of the finished solar cells was about 88% of the total cell area, showing slightly less percentage in active area than those with the metal shadow mask (90%). This is mainly due to the relatively large contact bar area. Sheet resistance of the diffused layer was around 34 ohm/square for EFG ribbons and 28 ohm/square for the controls.

About 10 cells, out of 22 starting wafers, were broken in the process of cell fabrication, giving a mechanical yield of around 55%. Detailed causes of the breakage are listed in Table 9-A. An analysis indicated that most of the breakage is closely related to the non-flat features of the ribbons and possibly to residual stress in the blanks. This is considered to be a significantly lower yield compared to the single crystalline control cells.

Back Surface Field Process

The BSF process, described in Appendix III-B, was used for EFG sheets with the modification of front contact formation by photolithographic techniques as described in the previous standard process.

Finished EFG solar cells showed a mechanical yield of about 54%; again 13 cells out of 28 starting sheets were broken in this process. Detailed causes of the breakage are given in Table 9-B, and again are attributed to the properties of the starting ribbon.

SOLAR CELL PERFORMANCE AND CHARACTERIZATION

Characteristics Under Illumination

Solar cell parameters, such as I_{SC}, V_{OC}, CFF and η, were measured under AM0 solar simulation at 25°C. Electrical data sheets in the First Quarterly Report (3) give detailed information on individual cells and Table 10 and Table 11 summarize the results for cells of two process types, standard process and BSF process, respectively. BSF solar cells showed improved efficiency compared with standard solar cells, 8.5% versus 7.8%, with an overall increase in I_{SC}, V_{OC}, and CFF.

Conversion efficiency of EFG solar cells was less than those of "Silso" solar cells and also less than recently reported results with EFG ribbon, mainly due to lower V_{OC} and CFF. This was suspected to be due to shunting by SiC (die material), which could be detected visually on the surface of the ribbon in many cases. Thus, a number of experiments were done to eliminate the effect of those particles by isolating and dicing off the area possessing the inclusions. In one case open circuit voltage increased from 525 mV to 545 mV while curve fill factor improved from 58% to 66% after removal of some inclusions. A typical inclusion, which is presumed to have originated from the die material, is shown in Figure 11. However, improvement in either V_{OC} or CFF was not always obtained after the removal of specific surface inclusions. This indicated that either there are microscopic particles that cannot be detected at low magnifications or dependent on the way that the particle is embedded in the silicon matrix.

For example, a particle might not cause any shunting problem
if the particle is completely isolated by the coverage of a thin silicon
layer all over the surface of the particle (as in epitaxial cells).

Selected solar cells from BSF process were coated with MLAR coating
(instead of SiO AR coating) to show the improvement of the performance.
The results are given in the middle of Table 11. Although an
average efficiency of about 10.6% was obtained, improvement in short
circuit current after MLAR coating was only about 33%; (generally close
to 50% current gain after MLAR coating was achieved in single crystalline
solar cells.) This reduced coating gain could be the result of
the haze remaining on the starting blanks. The figures quoted for highest
efficiency can be characterized as "preliminary", because of limited
tests, and small sample size.

Limited solar cells were fabricated from the ribbons of chemically
etched surface to check the performance difference between cells with
and without an etching step (the ribbons were chemically etched in planar
solution for about two minutes, which removed about 10 μm of silicon
from each side of a ribbon). No significant differences in performance
were observed. However, these solar cells showed slightly lower short circuit
current density than the solar cells without chemical etching. Reasons
for this difference have not been identified yet.

Dark I-V Characteristics

Measurements carried out by point-by-point plots of the selected solar cells are given in Figure 12 for the standard process and Figure 13 for the BSF process. "A" factor and I_o in the diode equation (described in Section A, 2.0) were in the range of 1.5-3 and 10^{-7}-10^{-6} A/cm^2, respectively. These are slightly higher values compared with the "Silso" solar cells, and this result agrees with the slightly lower open circuit voltage and curve fill factor of EFG solar cells.

Spectral Response

Absolute spectral response (A/W) was measured using the same method described in Appendix V-A. Plots of the response are given in Figure 14 for the standard cells and in Figure 15 for the BSF cells. Spectral response of EFG cells at long wavelength (λ >0.6 μm) was significantly lower than those of the single crystalline control cells due to crystalline defects such as grain boundary, stacking faults, dislocations and perhaps inclusions. The slight dip at 0.78 μm was observed for both cells tested and the origin of the dip is not known at the present time.

Minority Carrier Diffusion Length

Diffusion length was measured on the finished solar cells using the short circuit current method described in Appendix V-B. Table 12 summarizes the results of the EFG solar cells, from both standard and BSF process, measured under illumination of the entire cell area, showing an average diffusion length between 40 and 50 μm.

Variation of diffusion length was also detected from small beam size measurement on two solar cells and Figure 16 show results of this, indicating significant variation from spot to spot; i.e. from 20 to 50 μm in case (b). This variation in diffusion length can affect the total cell short circuit current.

Photoresponse by Small Light Spot Scanning

Localized photoresponse of solar cells (standard) were obtained by light spot scanning. Detailed techniques are described in Appendix V-C and Figure 17 is the result of the scanning. The EFG cell indicated lower response than the control cell with the estimated "grain" size between 0.4 and 2 mm. Non-uniform response from crystallite-to-crystallite was often found in EFG cells, generally low response from small crystallites and this could possibly be due to the strain induced defects on small crystallites being more severe than those on the large crystallites.
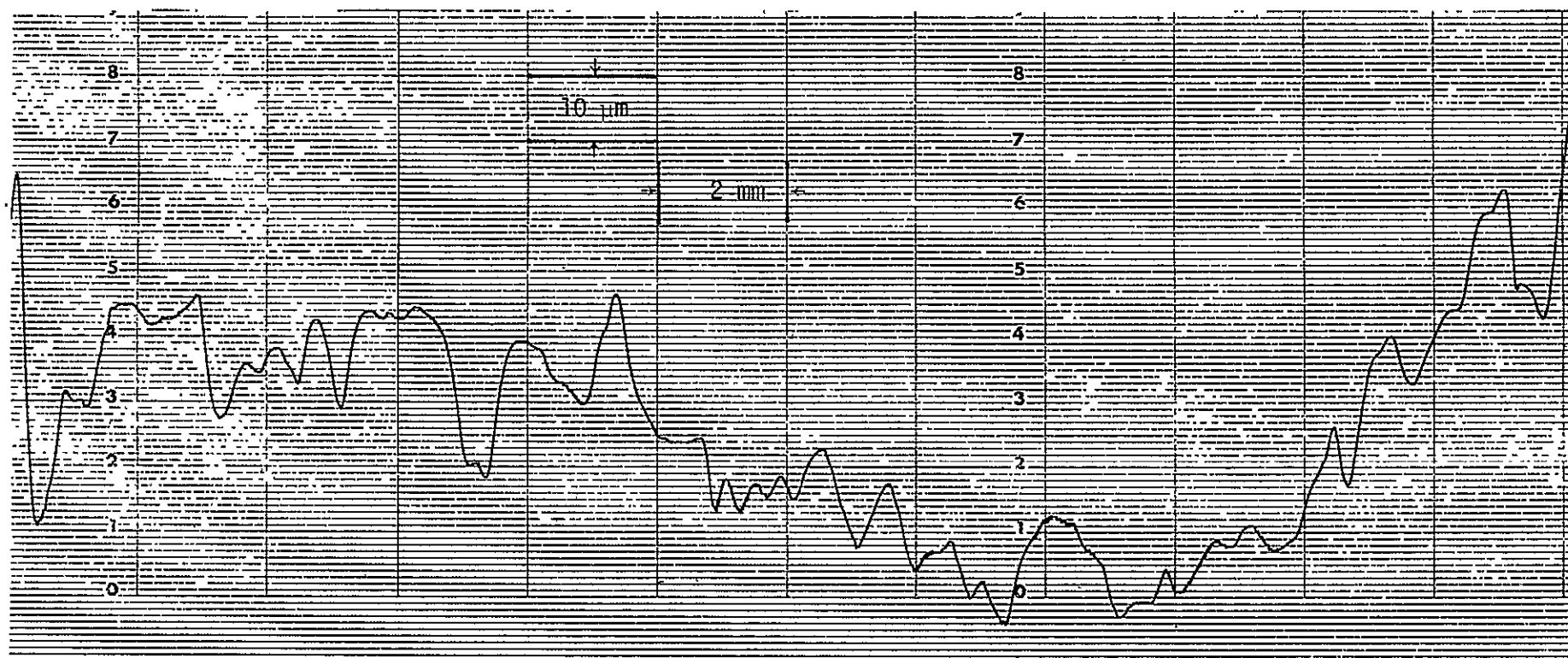
FIGURE 10

A Typical Surface Profile Across the Width of a EFG Ribbon
(Ribbon Width ~1") by Dektak (Sloan)
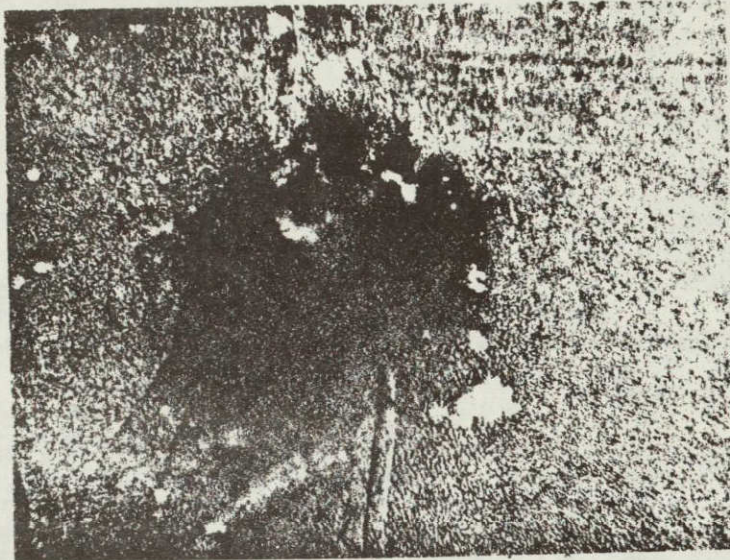
FIGURE 11

A Microscopic Photograph of a Typical Surface Inclusion
in EFG Ribbon (50x Magnification)

FIGURE 12

Dark I-V Characteristics of EFG (RF) Solar Cells
($\sim$5.5cm^2, Standard Process)

———: EFG Cells
- - -: A Control Cell (Single Crystalline)
o: Cell No. 7
x: Cell No. 14
$\triangle$: Control No. 70

FORWARD

REVERSE

REVERSE

CURRENT DENSITY, (A/cm^2)

-38-
VOLTAGE, (VOLTS)
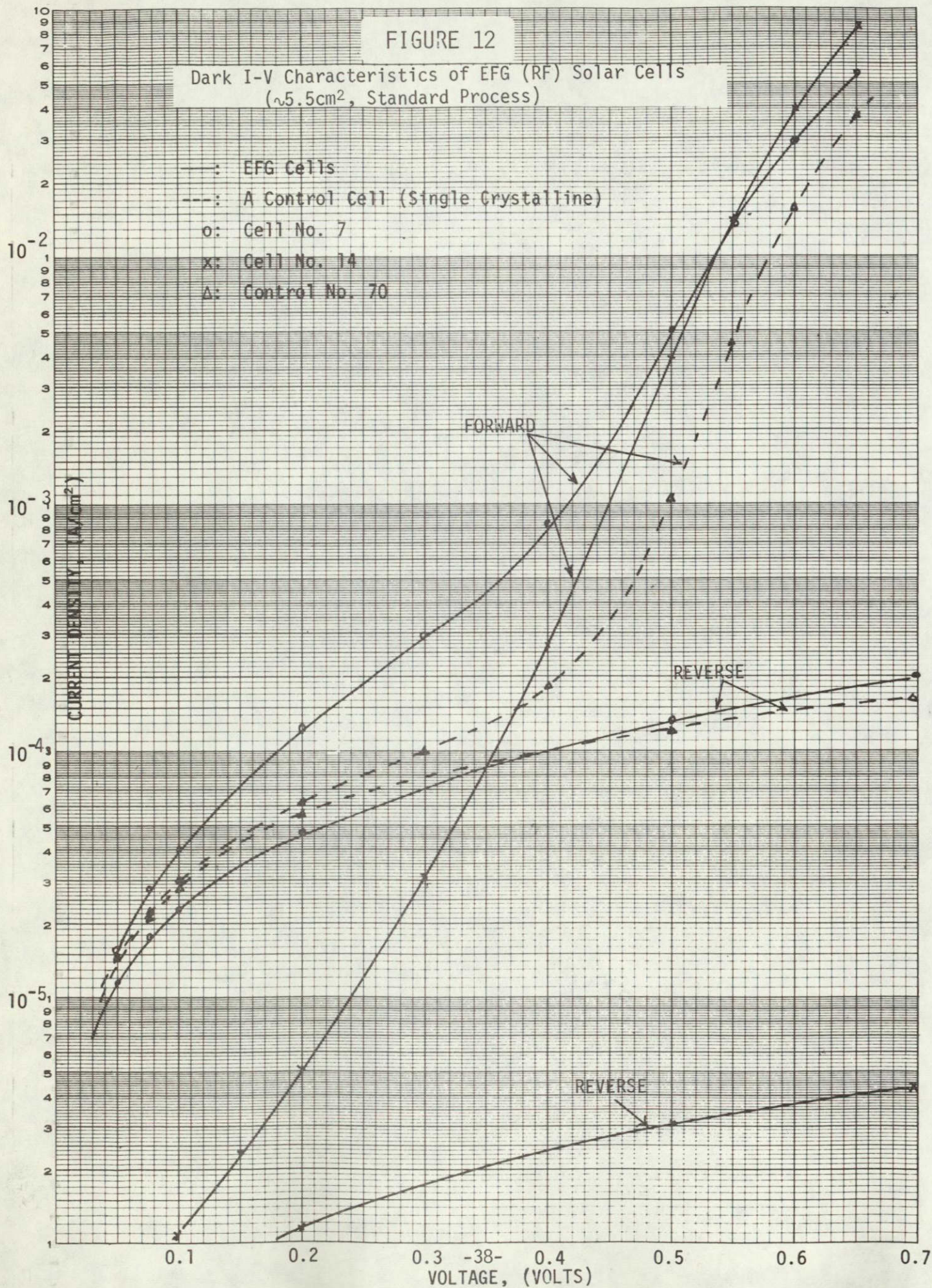
FIGURE 13

Dark I-V Characteristics of EFG (RF) Solar Cells
($\sim$5.5cm^2, BSF Process) at R.T.

x: Cell No. 50
o: Cell No. 29

FORWARD

REVERSE

CURRENT DENSITY (A/cm^2)

-39-
VOLTAGE, (VOLTS)
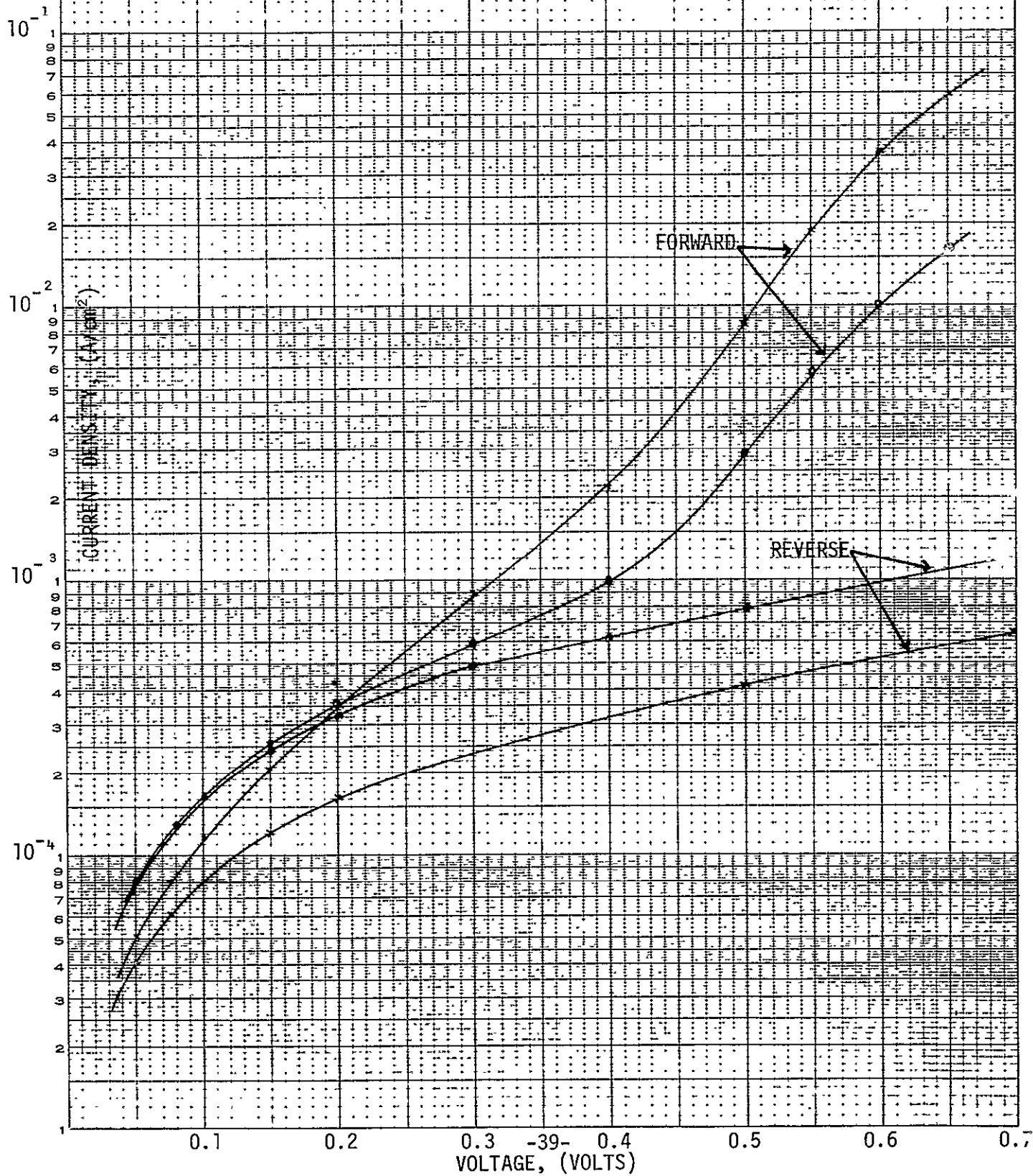
FIGURE 14

Spectral Response of EFG (RF) Solar Cells
(Standard Process)

ABSOLUTE SPECTRAL
RESPONSE

SAMPLE IDENTIFICATION

o	Cell #118
x	Cell # 3
Δ	Control #71

DATE: 9/18/78

SPECTRAL RESPONSE (A/W)
—40—

WAVELENGTH (MICROMETER)
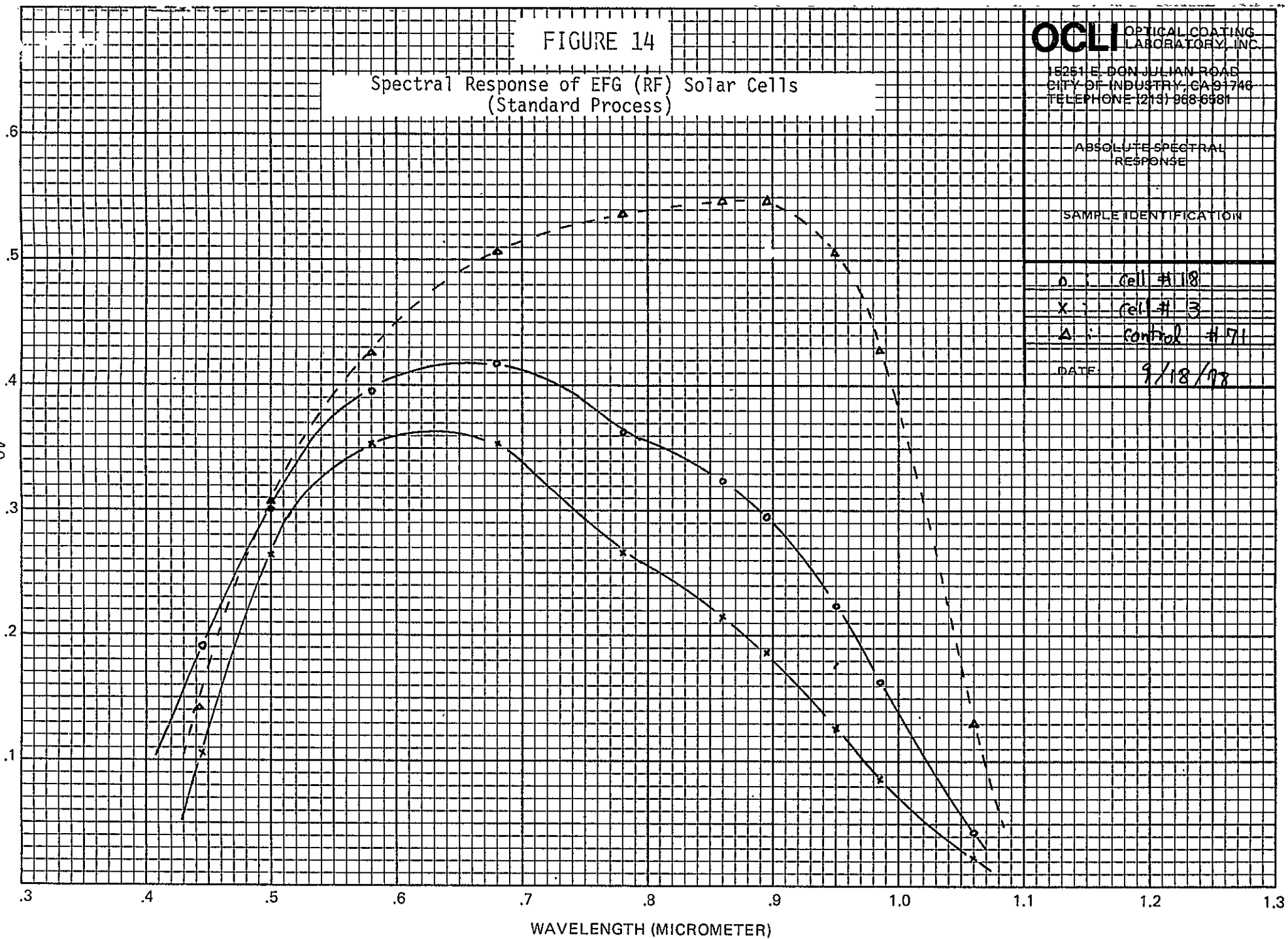
FIGURE 15

Spectral Response of EFG (RF) Solar Cells
(BSF Process)
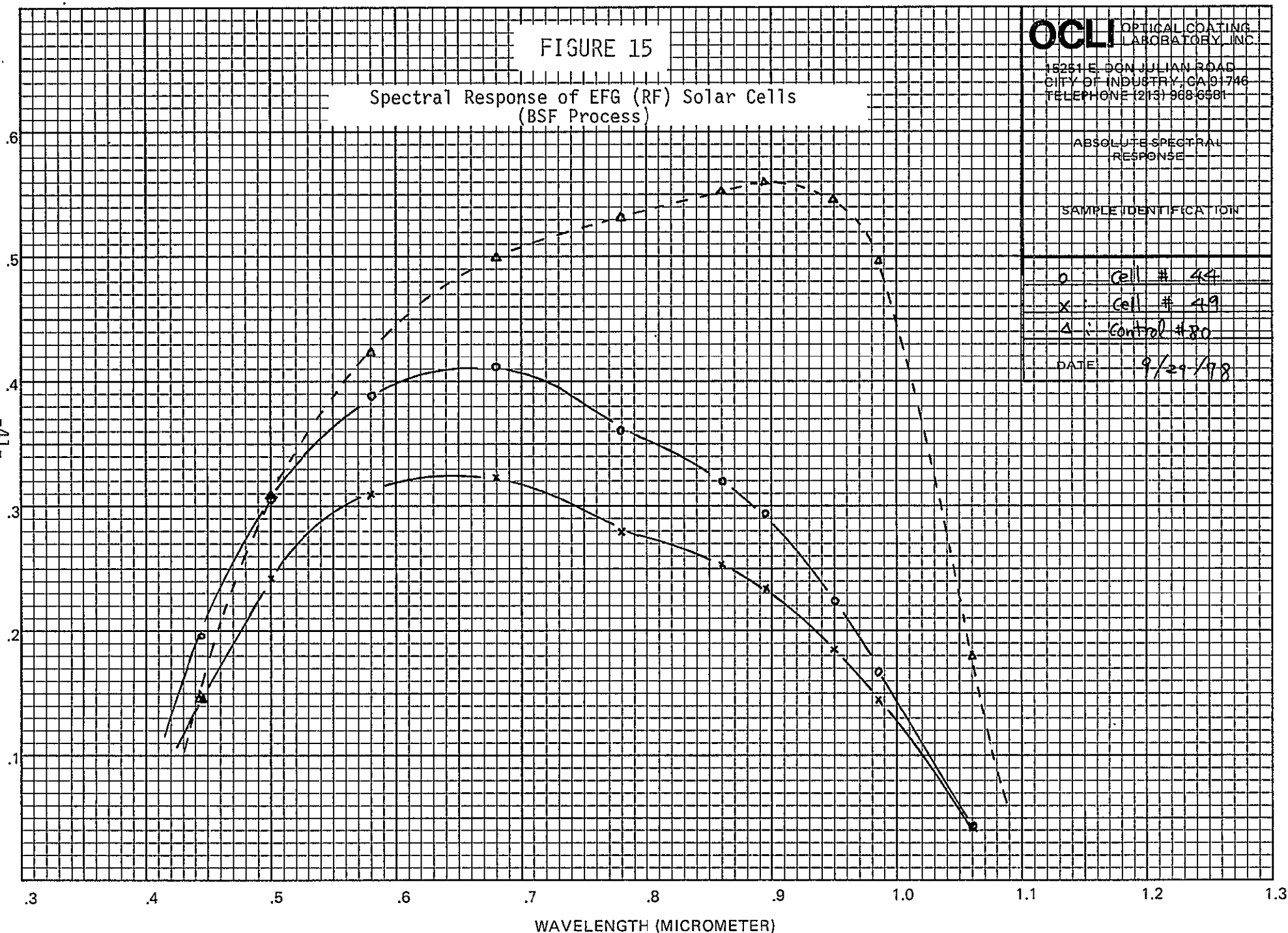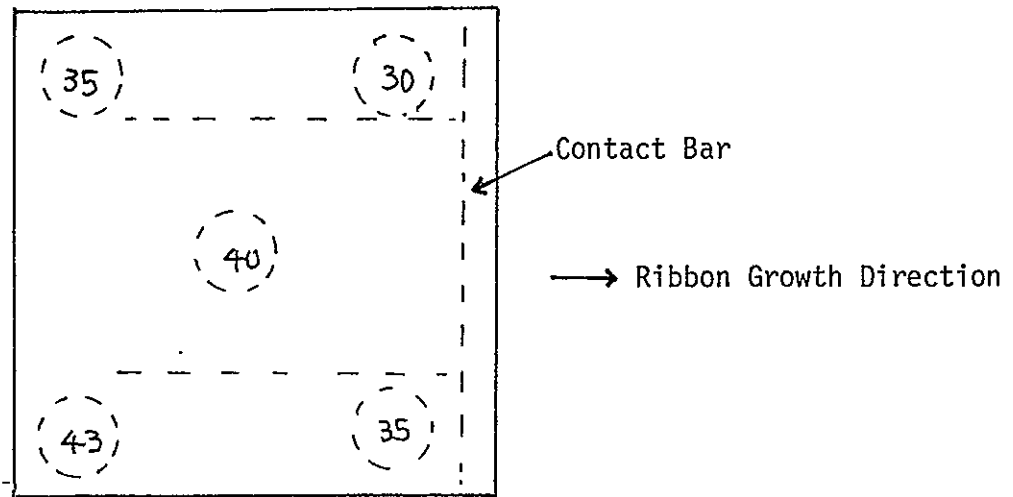
(a)
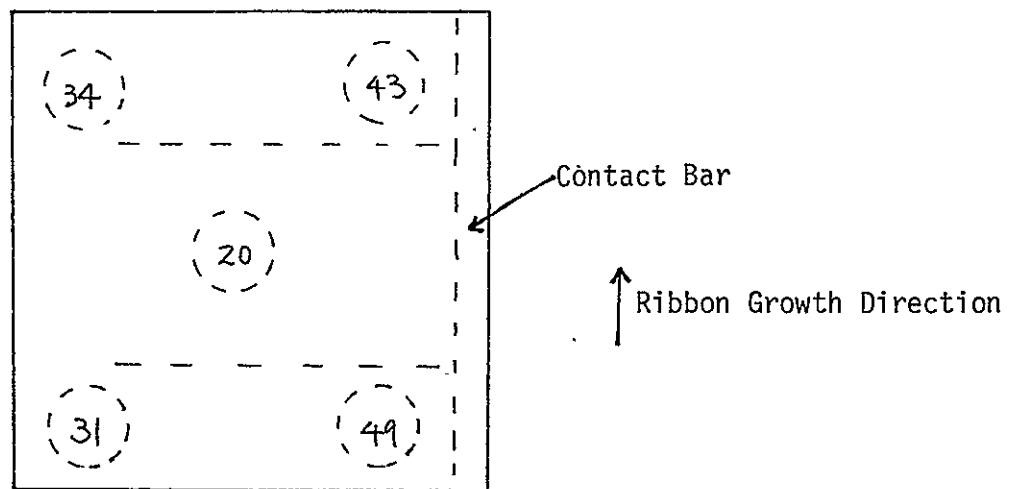
(b)

FIGURE 16

Minority Carrier Diffusion Length (μm) Variation
Within an EFG (RF) Solar Cell (∿5-6cm^2), Measured by I_{SC} Method
With an Illuminated Beam Size of ∿3-4mm Diameter

    a) An EFG Standard Cell (No. 7)

    b) An EFG BSF Cell (No. 40)

FIGURE 17

SMALL LIGHT SPOT SCANNING OF A EFG (RF) SOLAR CELL

CONTROL CELL

EFG CELL

GRID LINES

← ∿.6 mm →

RELATIVE PHOTORESPONSE

DISTANCE

-43-
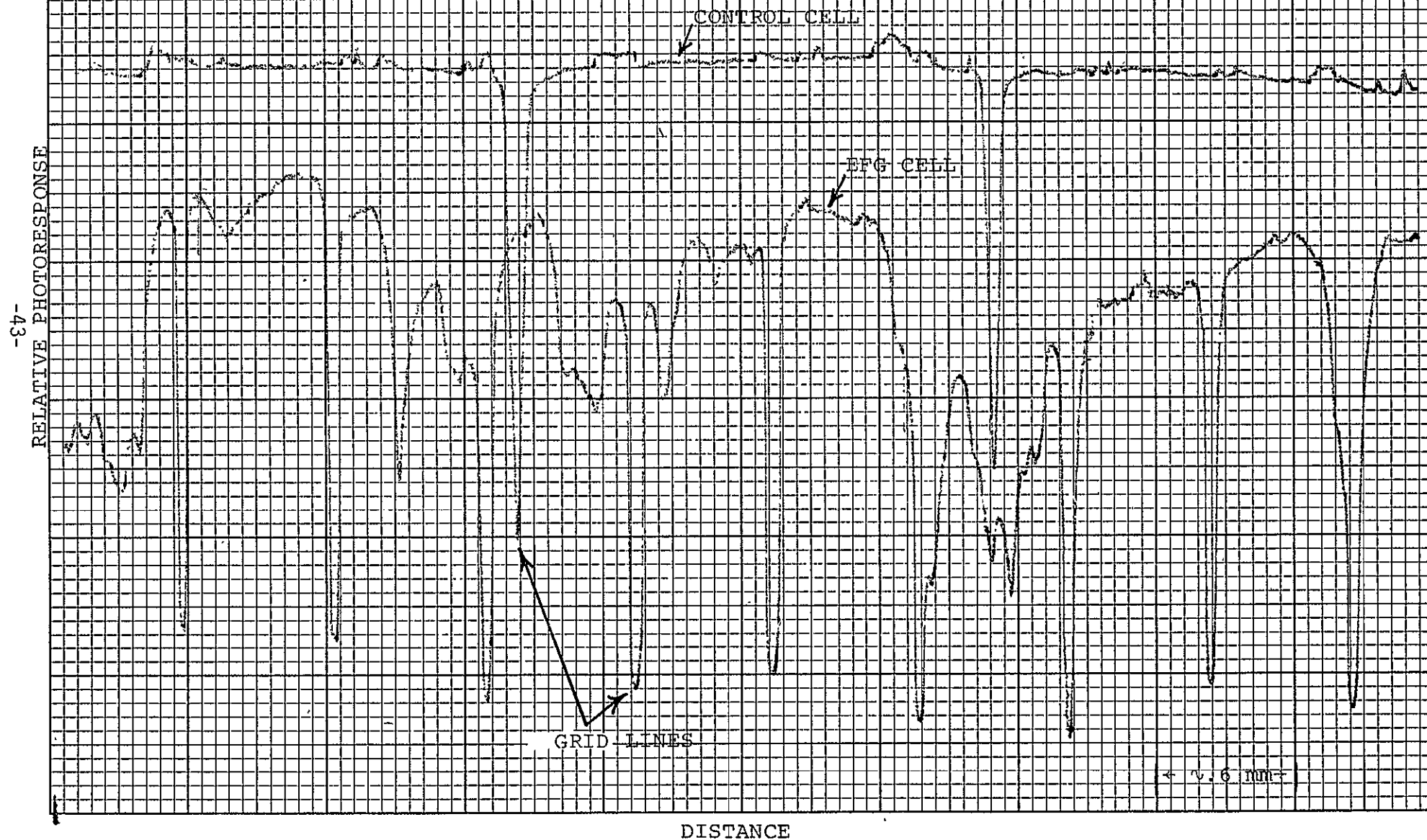
TABLE 9

Mechanical Failure of EFG (RF) Solar Cells
in the Process of Fabrication

A. Standard Process

NUMBER OF BROKEN CELLS	CAUSE
3	TEST Diamond Scribing 1 Back Contact 2
2	FRONT CONTACT Photoresist Spin 1 Develop & Rinse 1
1	BACK CONTACT
2	EDGE TRIMMING OR CUTTING USING DICING SAW
2	ELECTRICAL TEST

Starting: 22 Wafers

B. BSF Process

NUMBER OF BROKEN CELLS	CAUSE
1	INITIAL CLEANUP PROCESS
4	BSF PROCESS Al Screen Printing 1 Al Alloy (Al Penetration) 1 Al Scrubbing (Residual) 1 Acid Clean (Remove Excess Al) 1
2	FRONT CONTACT, PHOTORESIST EXPOSURE
4	ELECTRICAL TEST
1	EDGE TRIMMING
1	PROCESS MISTAKE

Starting: 28 Wafers

TABLE 10

Summary of Parameters of Solar cells
Fabricated From EFG (RF) Ribbons, Standard Process

	V_{oc} (mV)	J_{sc} (mA/cm^2)	CFF (%)	η (%)
AVERAGE	540 (529)	28.8 (21.4)	67.8 (64.8)	7.8 (5.5)
STANDARD DEVIATION	12.5 (14.4)	1.2 (1.4)	8.9 (11.6)	1.3 (1.2)
RANGE	517-556 (496-549)	26.3-30.2 (18.8-22.9)	52-79 (43-80)	5.8-9.6 (3.5-7.1)

Control Cells

	V_{oc} (mV)	J_{sc} (mA/cm^2)	CFF (%)	η (%)
AVERAGE	596 (589)	33.65 (24.3)	79 (78)	11.8 (8.3)
STANDARD DEVIATION	0 (0)	0.1 (0.1)	1.1 (1.8)	0.2 (0.2)
RANGE	596 (589)	33.5-33.8 (24.3-24.5)	78-80 (76-80)	11.6-12 (8.0-8.5)

NOTE: 1. Measured under AMO condition at 25°C.

2. Cells ($\sim$5-6cm^2 in area) with SiO AR coating, parenthesis numbers are for the parameters before AR coating.

TABLE 11

Summary of Parameters of Solar Cells
Fabricated From EFG (RF) Ribbon; BSF Process

	V_{oc} (mV)	J_{sc} (mA/cm^2)	CFF (%)	η (%)
AVERAGE	549 (538)	29.4 (22.4)	71 (70)	8.5 (6.2)
STANDARD DEVIATION	14 (17.5)	1.3 (1.2)	7.4 (7.5)	1.1 (0.9)
RANGE	533-572 (506-565)	26-31.2 (19.9-24.3)	55-78 (51-77)	6.5-10.3 (4.4-7.8)

Selected EFG Cells With MLAR Coating

	V_{oc} (mV)	J_{sc} (mA/cm^2)	CFF (%)	η (%)
AVERAGE	572 (562)	32.3 (24.2)	78 (76)	10.6 (7.7)

Control Cells

AVERAGE	603 (597)	33.9 (24.8)	76 (75)	11.5 (8.2)

NOTE: 1. Measured under AMO condition at 25°C.

2. Cells ($\sim$5-6cm^2 in area) with SiO AR coating (middle table is for the selected EFG cells with MLAR coating), parenthesis numbers are for the parameters before AR coating.

TABLE 12

Minority Carrier Diffusion Length (μm) of EFG (RF) Solar Cells

	AVERAGE	STANDARD DEVIATION	RANGE
STANDARD CELL	40	N/A	38-41
BSF CELLS	52	11	40-65

NOTE: 1) Measured by I_{SC} method illuminated whole solar cell area ($\sim$5.5cm^2).

       2) Samples:

Standard Cells: Nos. 7 and 18
BSF Cells: Nos. 29, 32, 40,45, 49 and 55

C.   EFG (RH) RIBBON SOLAR CELLS

1.0   SOLAR CELL FABRICATION

The EFG ribbons supplied had been grown in a resistance heated (RH) furnace. Two types were included, one with controlled silicon carbide (SiC) on one face of the ribbon using a displaced die and the other with an uncontrolled silicon carbide die. [See reference (4) for detailed information on EFG process.] The former ribbon was about 2 inches wide (thickness between 16-18 mils) while the latter ribbon was about 3 inches wide with thickness of about 10 mils. These ribbons were mounted on ceramic blocks using wax and sliced into 2x2 cm blanks for the convenience of cell fabrication. Resistivities ranged from 1-3 ohm-cm with P-type conductivity. Minority carrier diffusion lengths were measured to be around 15-40 (μm). Following a standard cleaning procedure, cells were fabricated using the standard and BSF processes with back contacts formed intentionally on the side containing the most SiC in both cases. Standard process resulted in about 80% mechanical yield (ratio of unbroken cells to starting blanks) in which most of the breakage occurred in the metallization steps, both front and back contacts; (this can be corrected, or minimized, by redesign of the mask fixture).

A limited number of cells were fabricated using BSF process. Heat treatments on back contacts (standard process) were also carried out in an effort to improve open circuit voltage. Temperature used for the heat treatment tests was 650°C (600°C in standard process) and cells were treated for 5 minutes and 10 minutes. [See Appendix III for the detailed information on standard and BSF processes.]

2.0   SOLAR CELL PERFORMANCE AND CHARACTERIZATION

Characterization Under Illumination

Finished solar cells had about 90% active area with a SiO AR coating.

Solar cell parameters, such as V_{OC}, I_{SC}, CFF, and η, were measured

at 25°C (test block temperature) under an AMO simulator. [Refer to

Appendix IV for description of the simulator.]

Third Quarterly Report (6) provides the parameters of individual

solar cells from EFG (RH) ribbons; standard and BSF cells, and solar

cells from the heat treatment test.

Solar cell parameters from the standard process are summarized in

Table 13. EFG "A" and "B" are cells from the controlled SiC while

EFG "C" are not. Average efficiencies of the controlled EFG ribbon

cells were about 6.6%, showing 6.2% for EFG "A" and 6.9% for EFG "B".

However, EFG cells from the uncontrolled SiC showed an average efficiency

of 5.4% which is a considerably lower value than those of the cells from

the controlled SiC. This is mainly due to the low curve fill factor

(CFF) which is likely to be caused by shunting problems from surface

inclusions (SiC). A lower V_{OC} of EFG "C" cells compared with those of

"A" and "B" cells also indicates the same problem: an average V_{OC} of

508 mV for the uncontrolled SiC ribbon cells versus 515-517 mV for the

controlled samples. Short circuit current density remains around

25 mA/cm^2 in all three ribbon cases, indicating consistent quality of

grown EFG ribbons.

A few cells were fabricated using BSF process. However, shunting problems from aluminum alloying step prevented the process from obtaining reliable statistical evaluation at present. [Note: Even control cells showed shunting chracteristics.] The solar cells from heat treatment on back contact did not show any improvement in V_{OC} or other cell parameters. Slight degradation of the cells at 10 minutes of sintering (650°C) was apparent in both EFG and control cells.

Dark I-V Characteristics

Dark diode I-V plots were obtained by using a semi-automatic dark I-V plotter for the cells in a reasonably short time. This has provided reliable statistical data on the cell characteristics which is otherwise very difficult to do by point-by-point measurement techniques. Based on this data, the characteristics of the cells of interest can be replotted by point-by-point measurement. Figure 18 shows the forward plots using the plotter and Figure 19 represents the characteristics of a typical good EFG cell measured by point-by-point techniques from which diode parameters ("A" factor and saturation current from simple diode equation) were derived. The "A" factor of EFG cell and the control cell (in Figure 19) was 1.6 and 1.4, respectively. Saturation current (I_o) of the EFG cell was considerably higher than that of the control, $2x10^{-8}$ A/cm^2 versus $6x10^{-10}$ A/cm^2. This seems to be the reason why V_{OC} of the EFG cells is relatively low, an average V_{OC} of 520 mV for EFG cells and an average 580 mV for the control cells. The higher value of the saturation current of

the EFG cell seems to be mainly due to low diffusion lengths of the EFG ribbons, 20-40 μm (EFG) versus 120-160 μm (control), with the doping levels of both materials about the same.

Spectral Response

Absolute spectral response (A/W) was made using a filter wheel set-up. [See Appendix V-A for the details.] Response versus wavelength of solar cells from the standard process is given in Figure 20. Generally EFG cells showed much lower response especially at long wavelength regions ($\lambda > 0.6$ μm) than those of the control cells. This indicates that the quality of the EFG ribbon is not as good as Czochralski controls, in other words low minority carrier lifetime.

Minority Carrier Diffusion Length

Minority carrier diffusion length was measured using the surface photovoltage (SPV) method for the bulk EFG and the short circuit current method (see Appendix V-B for details) for the finished solar cells. Bulk diffusion lengths were measured to be in the range between 20-40 μm (generally from spot-to-spot measurement) and diffusion lengths obtained from the solar cells by short circuit current method (illuminated on whole area of a cell) indicated similar results. Diffusion lengths were also obtained by measurement on a localized area (about 3-4 mm in diameter) by short circuit current method and the results showed a range between 15-40 μm. Table 14 summarizes the results of minority carrier diffusion length measurements by short circuit current method.

Photoresponse by Small Light Spot Scanning

Localized photoresponse of solar cells (standard) were obtained by light spot scanning. Scanned light source was a tungsten lamp filtered through thin film of silicon with a beam size estimated to be around 50-100 μm. [See Appendix V-C for the detailed description of the measurement.] Defocusing effect by the non-flat surface feature of EFG ribbons might have resulted in the modulation of beam size during scanning, consequently leading to loss of sharp contrast in response at electrically active defect sites. Figure 21 and Figure 22 are the results of the scanning. The first scanning direction was perpendicular to ribbon growth direction (across ribbon width) and the second was parallel to the growth direction. In both cases, some of the localized areas showed lower response than others of which areas of low response seemed to have a higher density of the electrically active defects. Response across the ribbon width showed a considerably high density of defect sites, which can be understood if we consider that grain boundaries and twins (or closely spaced parallel twins) exist in a direction parallel to the growth direction.

Defect Study

Besides crystallograhpic defects, such as grain boundaries and stacking faults, etc., dominant defects in EFG ribbon are the surface inclusions (SiC). These inclusions, especially when they exist in the surface of the shallow diffused layer (this is the case for the EFG ribbons of uncontrolled SiC), are likely to cause shunting or severe leakage

characteristics, consequently leading to a low curve fill factor and power output. The surface inclusions do not always seem to lead to shunting problems (same results were reported above in Section II-B). Figure 23 shows microscopic photographs of the inclusions, where case one (a) the inclusion caused severe shunting problems and in case two (b) the inclusion does not significantly influence cell performance, even though a front gridline fell across the top of the inclusion.

FIGURE 18

DARK FORWARD I-V PLOTS
EFG RH SOLAR CELLS (AREA ~41 cm²)
USING A DARK I-V PLOTTER

CELL NO. 5-868-4

CELL NO. 5-868-3

CELL NO. 5-868-2

CELL NO. 5-868-5

CELL NO. 5-868-6

CURRENT (AMPERE)

VOLTAGE (Volts)
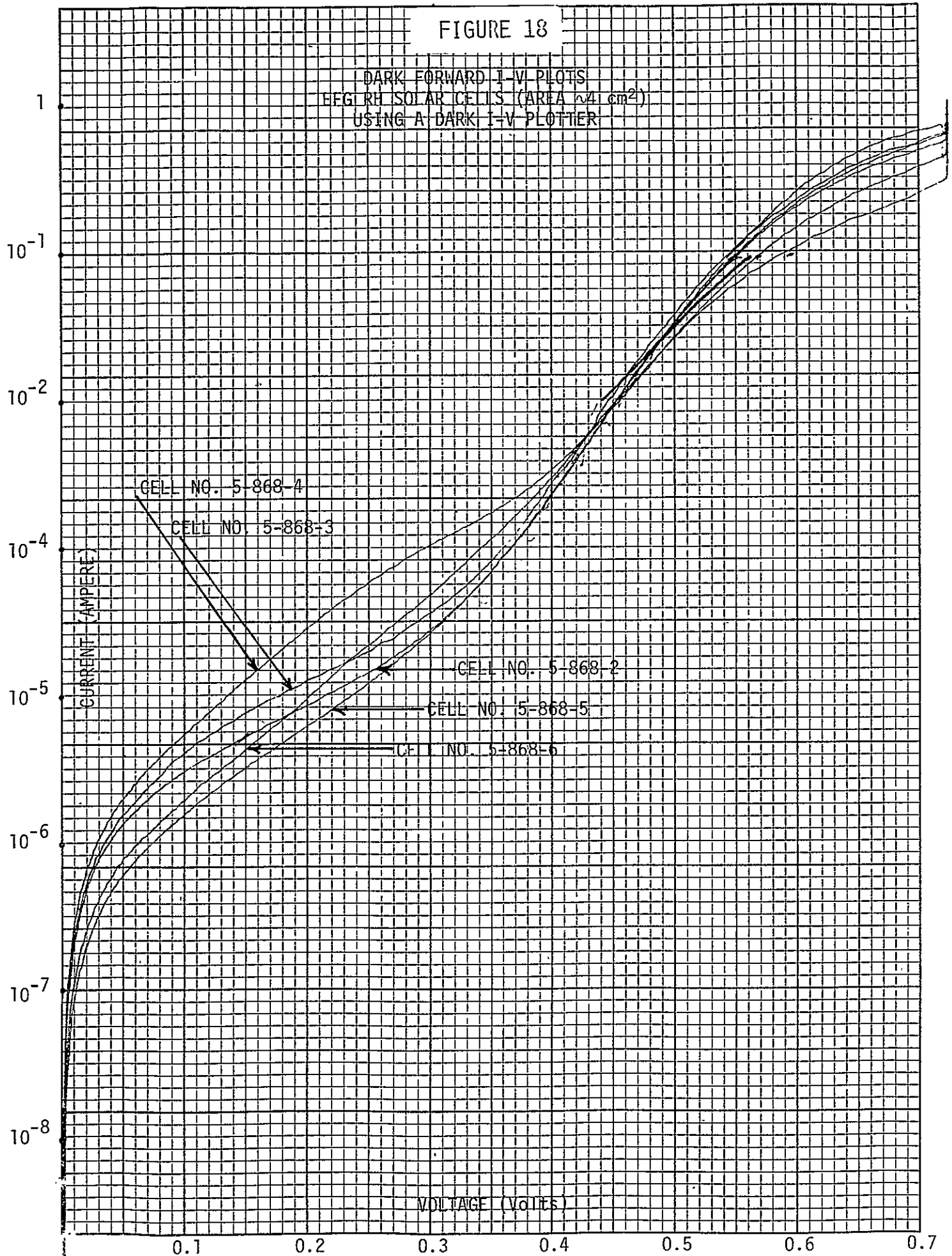
FIGURE 19

DARK I-V CHARACTERISTICS OF A EFG RH SOLAR CELL
(≈4 cm² in Area, Standard Process) AT R.T.

x: Control No. 7

o: EFG RH Cell No. 5-868-5

—: Forward Characteristics

---: Reverse Characteristics

CURRENT DENSITY, (A/cm²)

VOLTAGE, (VOLTS)

0.1   0.2   0.3   0.4   0.5   0.6   0.7

-55-
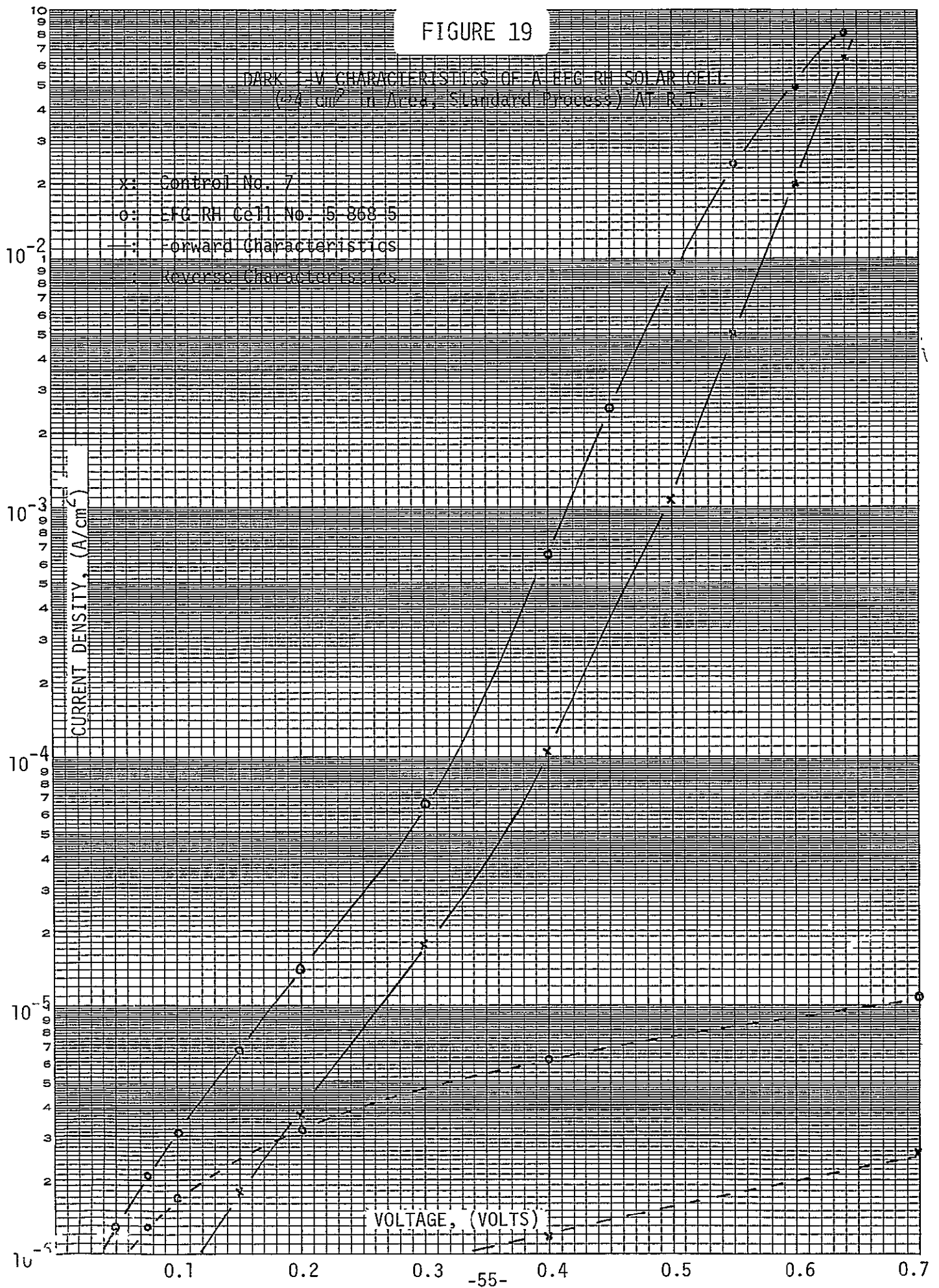
FIGURE 20

SPECTRAL RESPONSE OF EFG RH SOLAR CELLS
(Standard Process)

OCLI OPTICAL COATING LABORATORY, INC

15251 E. DON JULIAN ROAD
CITY OF INDUSTRY, CA 91746
TELEPHONE (213) 968-6581

ABSOLUTE SPECTRAL
RESPONSE

SAMPLE IDENTIFICATION

x: Control Cell No. 3
o: Cell No. 5-868-3
△: Cell No. 5-866-2

DATE: 5 March 79

-96-

SPECTRAL RESPONSE (A/W)

WAVELENGTH (MICROMETER)

FIGURE 21

SMALL LIGHT SPOT SCANNING OF A EFG (RH) SOLAR CELL
(Scanning Direction Perpendicular to Growth Direction)

CONTROL NO. 3

EFG RH NO. 6-868-2

GRID LINES

.6 mm

RELATIVE PHOTORESPONSE

DISTANCE

-57-
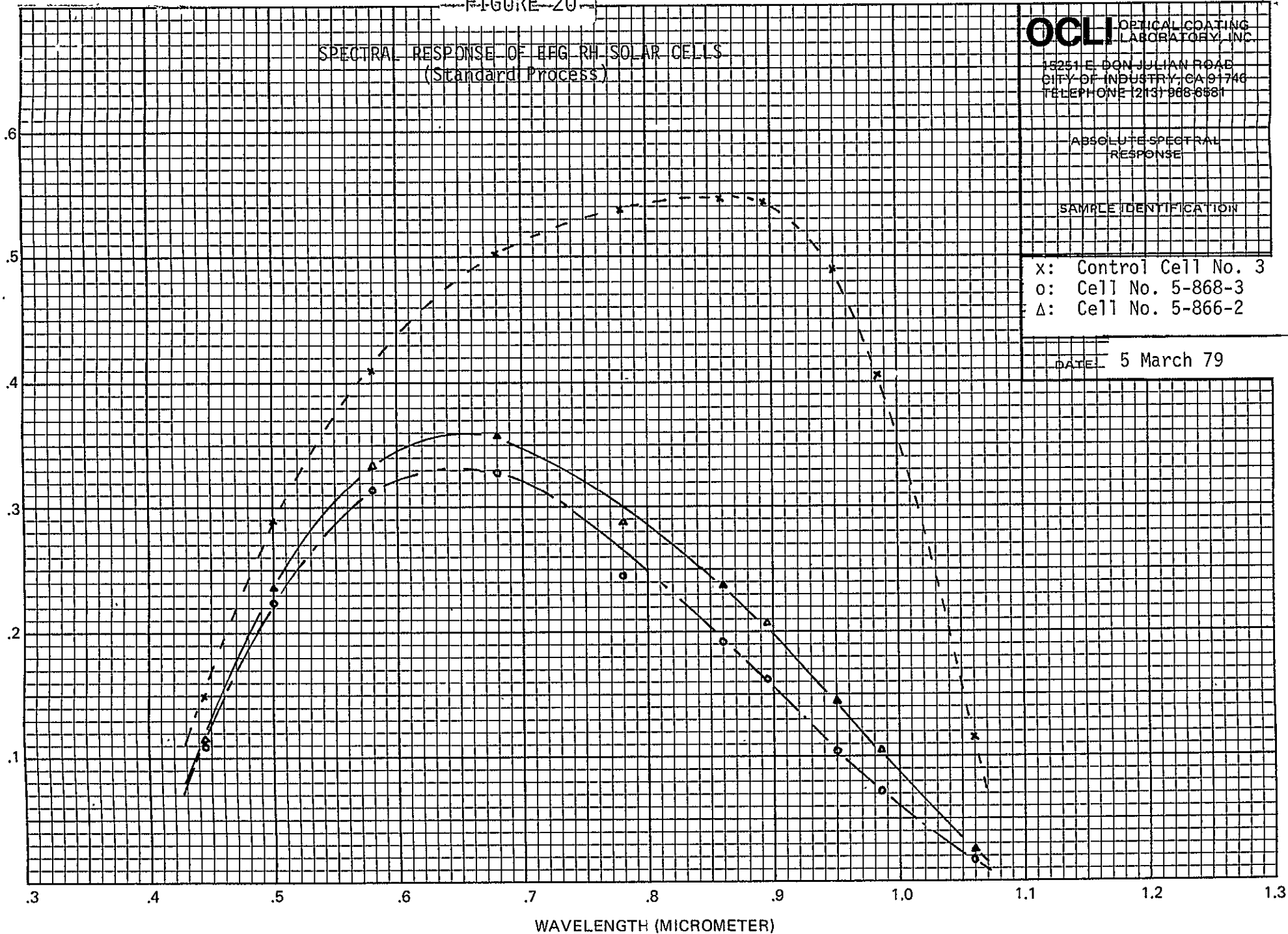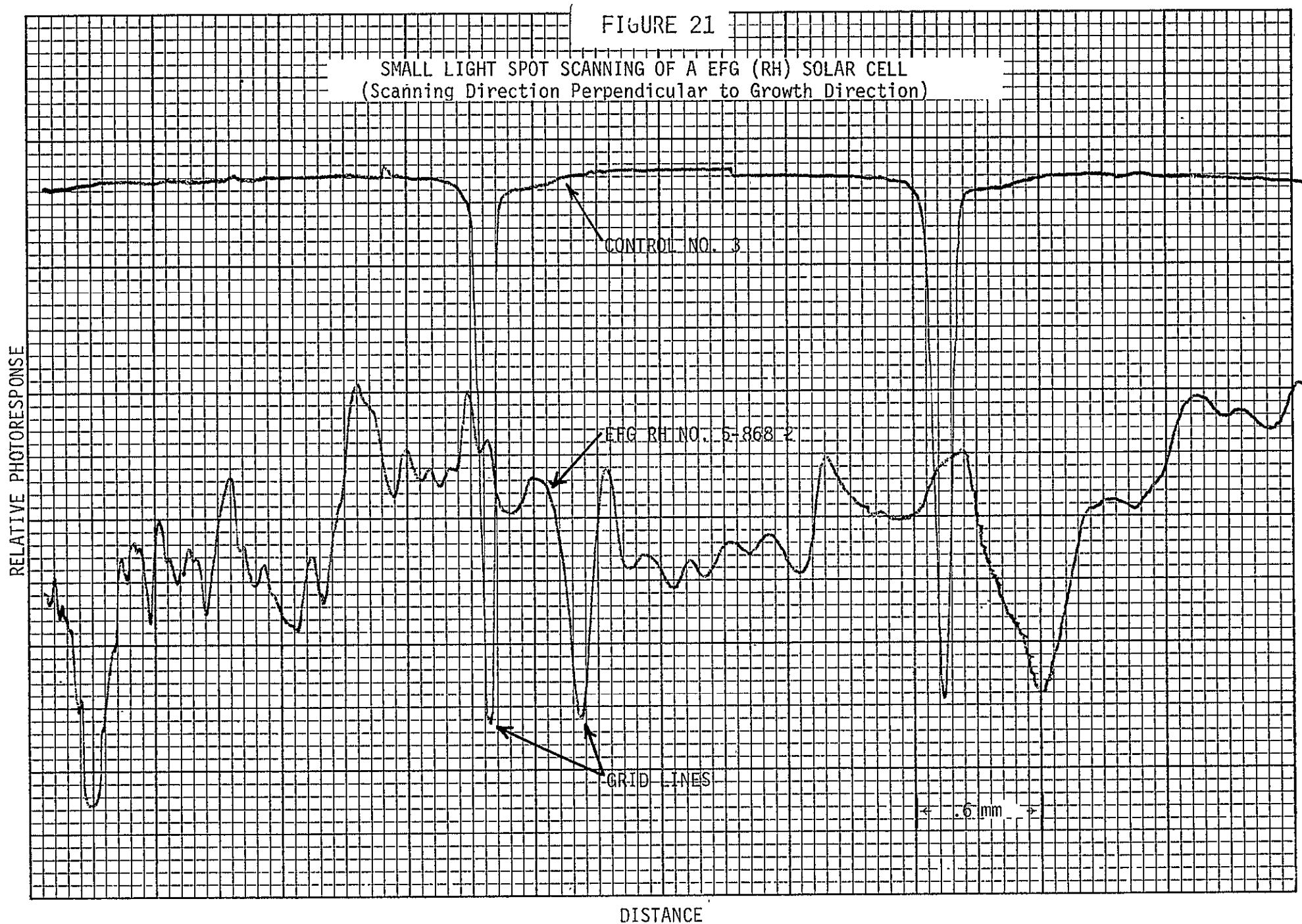
FIGURE 22

SMALL LIGHT SPOT SCANNING OF A EFG (RH) SOLAR CELL
(Scanning Direction Parallel to Growth Direction)

CONTROL NO. 3

EFG RH NO. 5-868-6

GRID LINES

.6 mm

RELATIVE PHOTORESPONSE

DISTANCE

-58-

FIGURE 23

(a)

(b)
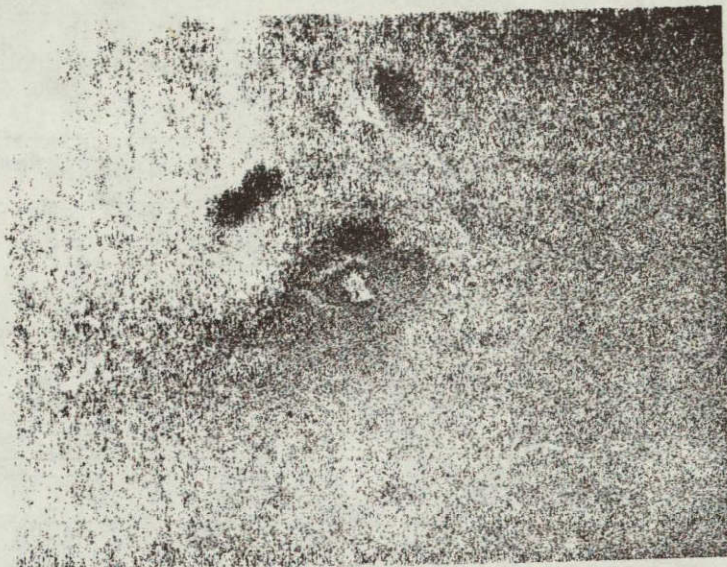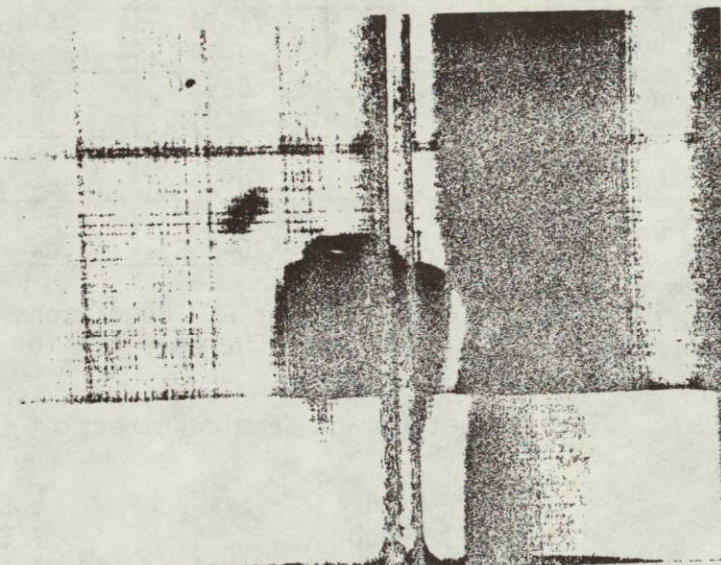
MICROSCOPIC PHOTOGRAPHS OF SURFACE INCLUSIONS IN EFG (RH) RIBBONS

(a) An inclusion found in Cell No. 5-370-2
(200X Magnification).

(b) An inclusion found in Cell No. 5-870-5
(200X Magnification).

TABLE 13

Summary of Parameters of Solar Cells
Fabricated From EFG (RH) Ribbon; Standard Process

		EFG "A"	EFG "B"	EFG "C"	CONTROL
V_{OC} (mV)	Average	517 (492)	515 (502)	508 (500)	580
	Standard Deviation	9 (19)	2 (2)	- -	-
	Range	490-526 (464-510)	510-508 (498-506)	480-527 (492-514)	576-588
J_{SC} (mA/cm^2)	Average	25.2 (17.9)	24.9 (17.6)	25 (18)	33.5
	Standard Deviation	0.6 (0.3)	0.7 (0.6)	- -	-
	Range	24.8-26.1 (17.5-18.4)	23.5-25.5 (16.5-18.2)	24-25.5 (17.2-18.6)	33-33.8
CFF (%)	Average	64 (60)	73 (72)	56 (60)	73
	Standard Deviation	12 (14)	1 (2)	- -	-
	Range	47-74 (42-73)	71-74 (69-74)	34-75 (49-72)	67-73
η (%)	Average	6.2 (4.0)	6.9 (4.8)	5.4 (4)	10.5
	Standard Deviation	1.4 (1.1)	0.2 (0.2)	- -	-
	Range	4.3-7.5 (2.6-5.1)	6.6-7.2 (4.5-5.0)	2.9-7.4 (3.0-4.9)	9.7-11.2

NOTE: 1. Measured at 25°C under AMO Conditions (cells with SiO AR). Parenthesis Numbers are for the Parameters Before AR Coating.

2. Identification and Sample Numbers of EFG RH Ribbon Cells:

"A":	5-866	-	5 Cells
"B":	5-868	-	7 Cells
"C":	5-870 Uncontrolled SiC	-	3 Cells
Control:	1-3 ohm-cm Czochralski	-	3 Cells

TABLE 14

SUMMARY OF MINORITY CARRIER DIFFUSION LENGTH OF
THE STANDARD CELLS FROM EFG (RH) RIBBON CELLS,
MEASURED BY I_{SC} METHOD

CELL NO.	POSITION					WHOLE AREA
	1	2	3	4	5	
5-866-2	38	40	19	20	28	26
5-868-3	18	22	14	18	18	18
5-870-5	--	--	--	--	--	24
5-870-7	--	--	--	--	--	14

NOTE: Units in µm.

IDENTIFICATION OF BEAM SPOT (BEAM SIZE 3-4 mm IN DIAMETER)
FOR DIFFUSION LENGTH MEASUREMENT ON LOCALIZED AREAS OF A 2x2 CM CELL
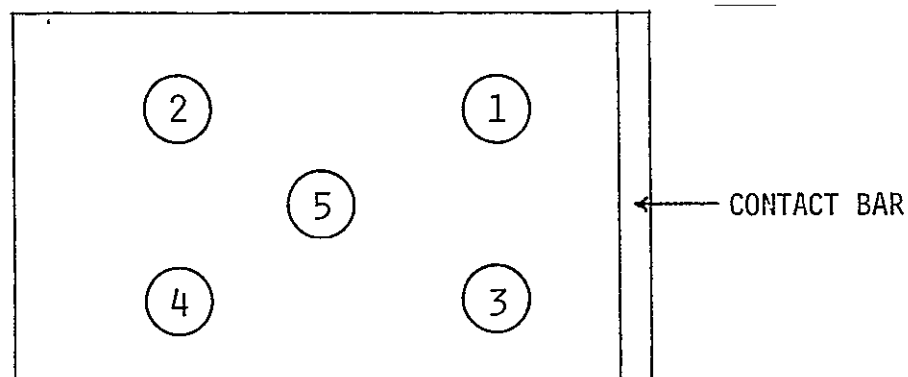
D. RTR SOLAR CELLS

1.0 SOLAR CELL FABRICATION

Blanks were prepared by waxing a ribbon on a ceramic block and slicing in size (2x2 cm). After removal of the individual blanks from the block, organic and chemical (standard RCA) solutions were used for cleaning the surface; the standard cell process followed thereafter. Blanks for the first batch were the ribbons from the annealed CVD feedstock while those for the second and third batches were ribbons from CVD feedstock with and without annealing, or from single crystalline feedstock. Thickness of ribbons was 6-7 mils and the resistivity measured by four point probe was in the range between 1-3 ohm-cm with p-type conductivity. Cells from the first two batches were processed without etching of silicon. In the third batch process, about 1 μm of silicon was removed from each side before the fabrication process by etching in planar etch solution for 15 seconds. Efforts were also made to include a BSF process. However, screen printing of aluminum paste was unsuccessful due to the shattering of ribbons during the squeezing operation. Overall mechanical yield (unbroken cells) obtained from three batch processes was about 50%, indicating very low yield considering the solar cells were handled with extreme care. Table 15 shows numbers and causes of the broken cells during the processes; the number of initial starting blanks was 52. In many cases broken cells were badly shattered possibly due to the excessive mechanical stresses in the ribbons induced in the process of laser recrystallization. [See reference (7) for detailed description of RTR process.]

2.0 SOLAR CELL PERFORMANCE AND CHARACTERIZATION

Characteristics Under AMO Illumination

Parameters of finished solar cells were measured under AMO conditions
(135 mW/cm^2, tungsten-xenon lamps with red and blue filters). The
block temperature was 25°C and input light intensity was calibrated
using a standard solar cell. The detailed parameters of the solar cells
from RTR ribbons* and control cells are given in Second Quarterly Report (5)
on the electrical data sheets. Solar cells made from CVD feedstock showed
maximum efficiency of 3.9% for the annealed ribbons and 5.6% for the
unannealed ribbons. Ribbon solar cells from single crystalline feedstock
showed slightly higher efficiency than those from polycrystalline CVD
feedstock, indicating maximum efficiency of about 6.6% with SiO AR
coating. Generally, solar cells processed from the etched blanks
(third batch) showed higher efficiency and more consistent results than
those from ribbon without removal of a thin silicon layer. Single
crystalline control cells showed 11-12% AMO efficiency. Large spread
in values, combined with the limited sample sizes, prevented these cells
from obtaining reliable summary tables or to provide statistical
evaluation.

Since significant variation in performance from cell to cell was observed
from these RTR cells, small mesa cells (2 mm in diameter) were fabricated
using masking techniques and the individual cells were illuminated by a
tungsten lamp to see the variation of cell performance within a single
2x2 cm cell. Figure 24 is the results of the mapping of open circuit
voltage, and significant differences in V_{OC} were noticed. Correlation

*Motorola considered these samples as poorly representative of the RTR
process. Hopefully some improved RTR samples can be evaluated later in
the program.

with crystal structure indicated that areas of low open circuit voltage
could be caused by fine details of the crystal structure.

Dark I-V Characteristics

Dark I-V characteristics (forward and reverse) were obtained from selected
RTR cells and a control cell. The plot was made by point-by-point
measurement and the results are plotted in Figure 25. "A" factor (in
simple diode equation) derived at high bias condition ranged from about
1.8 to 3 while a control cell showed "A" factor of 1.4. I_o was also
obtained from the plots, ranging from 10^{-7} A/cm^2 to 10^{-5} A/cm^2. This
suggests that shunting and space charge recombination effects are
serious problems in these cells.

Spectral Response

Absolute spectral response (A/W) was measured using a
method described in Appendix V-A. Response versus wavelength
are plotted in Figure 26, in which very poor response at
wavelengths beyond 0.6 μm can be seen. This can be
attributed to the poor quality (low lifetime or diffusion length) of the
bulk RTR ribbons, which was confirmed by minority carrier diffusion
length measurements (see next section).

Minority Carrier Diffusion Length

Minority carrier diffusion length was measured using a short circuit current
method for the finished solar cells. [See Appendix V-B for details.]
The whole area of a solar cell was illuminated by a light source
through a filter wheel and the diffusion length was obtained from
light intensity values at selected wavelengths.

Diffusion lengths of around 7-9 μm were obtained from
measurement on seven cells. Diffusion length was also measured
using small beam size illumination (∿3-4 mm beam diameter). Typical
results are given in Figure 27. No significant variations·from spot to
spot were observed, showing consistently low diffusion length. It is also
noteworthy that diffusion lengths of the cells from single crystalline
feedstock were not impressively better than those of the cells from
CVD feedstocks. This suggests there might be some problems associated
with the recrystallization process, either due to the contamination from
the process environment or the laser recrystallization process itself.*

Photoresponse by Small Spot Scanning

Localized photoresponse of the solar cells were obtained by light
spot scanning. [Refer to Appendix V-C for the detailed discussion
of the measurement.] A typical result is given in Figure 28. The
RTR cell showed very poor response everywhere, which made it
difficult to detect electrically active defect sites.

---

*Later reports from Motorola confirmed this speculation. Corrections
of these conditions led to RTR samples with significantly improved
performance, but these were not available within this reporting
period.

FIGURE 24

OPEN CIRCUIT VOLTAGE MAPPING OF MESA SOLAR CELLS
WITHIN A RTR SOLAR CELL (2x2 cm)

291	208	335				331
343	354		343	280	320	290
300	358	320	255	390	497	314
341	331	350	172	272	210	265
252	388	308	338	348	419	
300	310	354	352	358	393	
160	219	268	297	189	257	
210	194	184	194	142	246	70

NOTE: 1. ILLUMINATED TUNGSTEN LAMP WITH UNKNOWN LIGHT INTENSITY

2. DIAMETER OF MESA CELLS; 2 mm

3. UNIT; MILLIVOLTS

FIGURE 25

DARK I-V CHARACTERISTICS OF SOLAR CELLS
FROM RTR RIBBON (ROOM TEMPERATURE)

Forward Characteristics
Reverse Characteristics
o: Cell No. 811B-5
Δ: Cell No. 869-7
□: Cell No. 9872B-3
X: Control Cell No. 21

CURRENT DENSITY, (A/cm²)

VOLTAGE, (VOLTS)
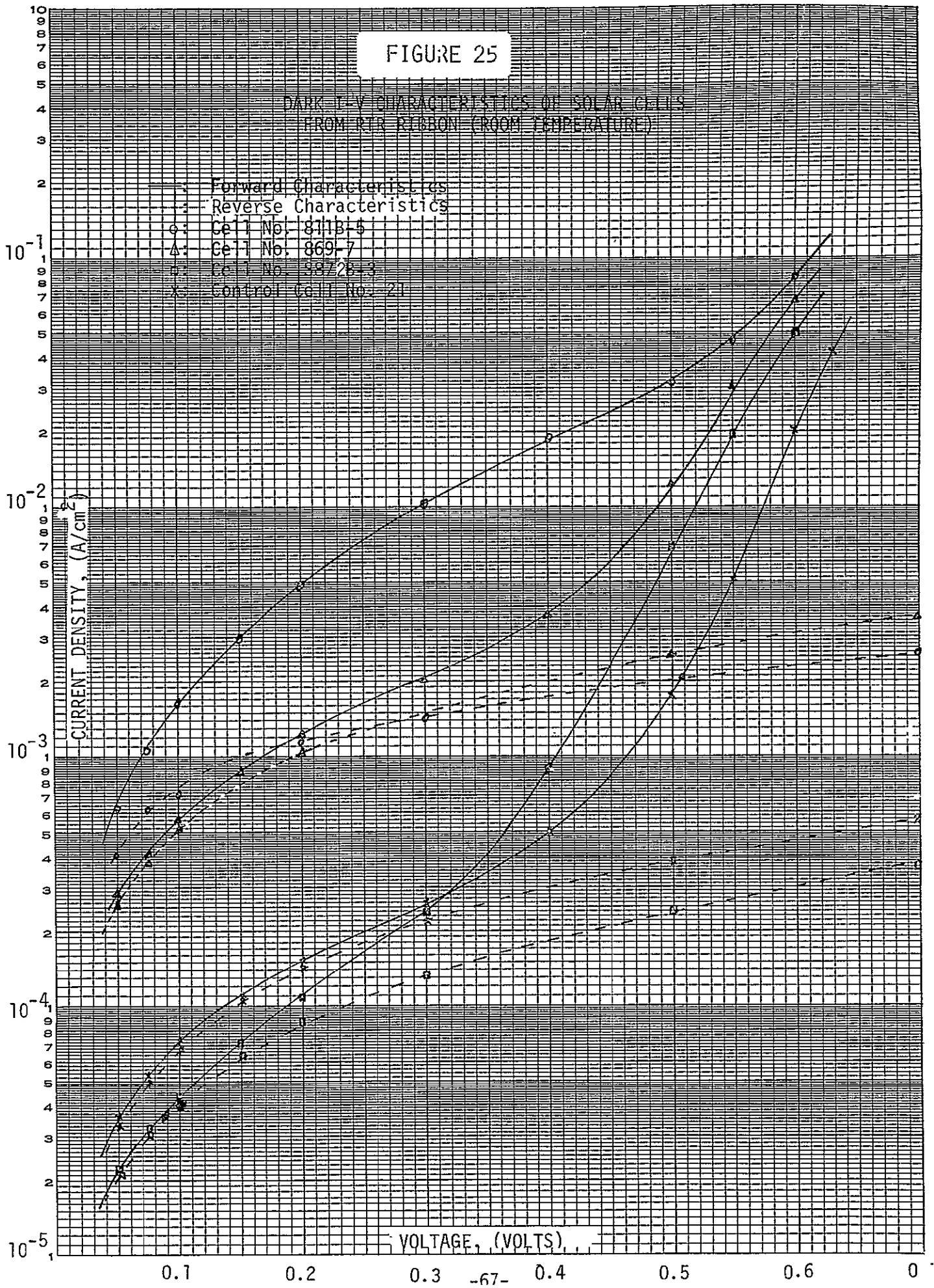
FIGURE 26

SPECTRAL RESPONSE OF RTR SOLAR CELLS AND A CONTROL SOLAR CELL
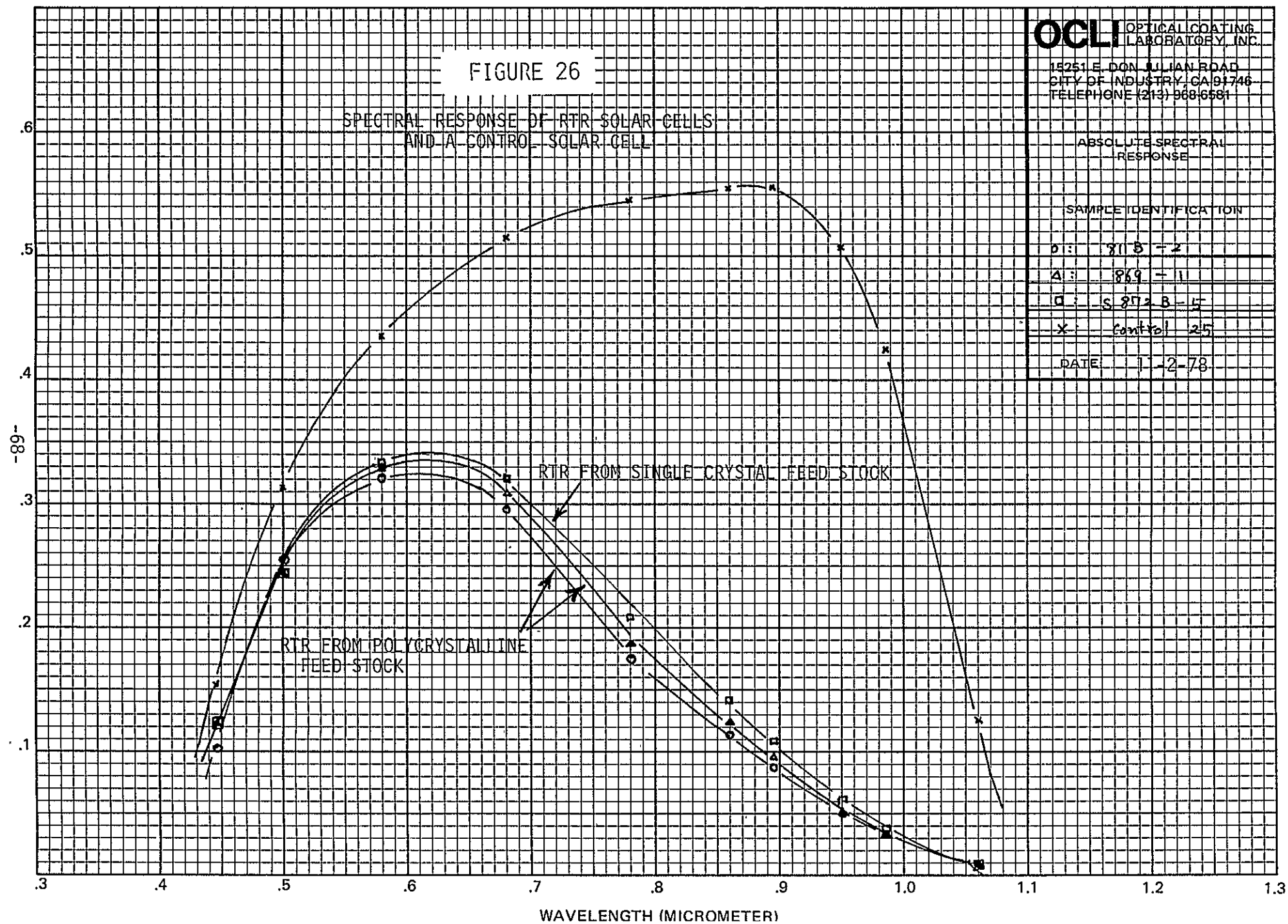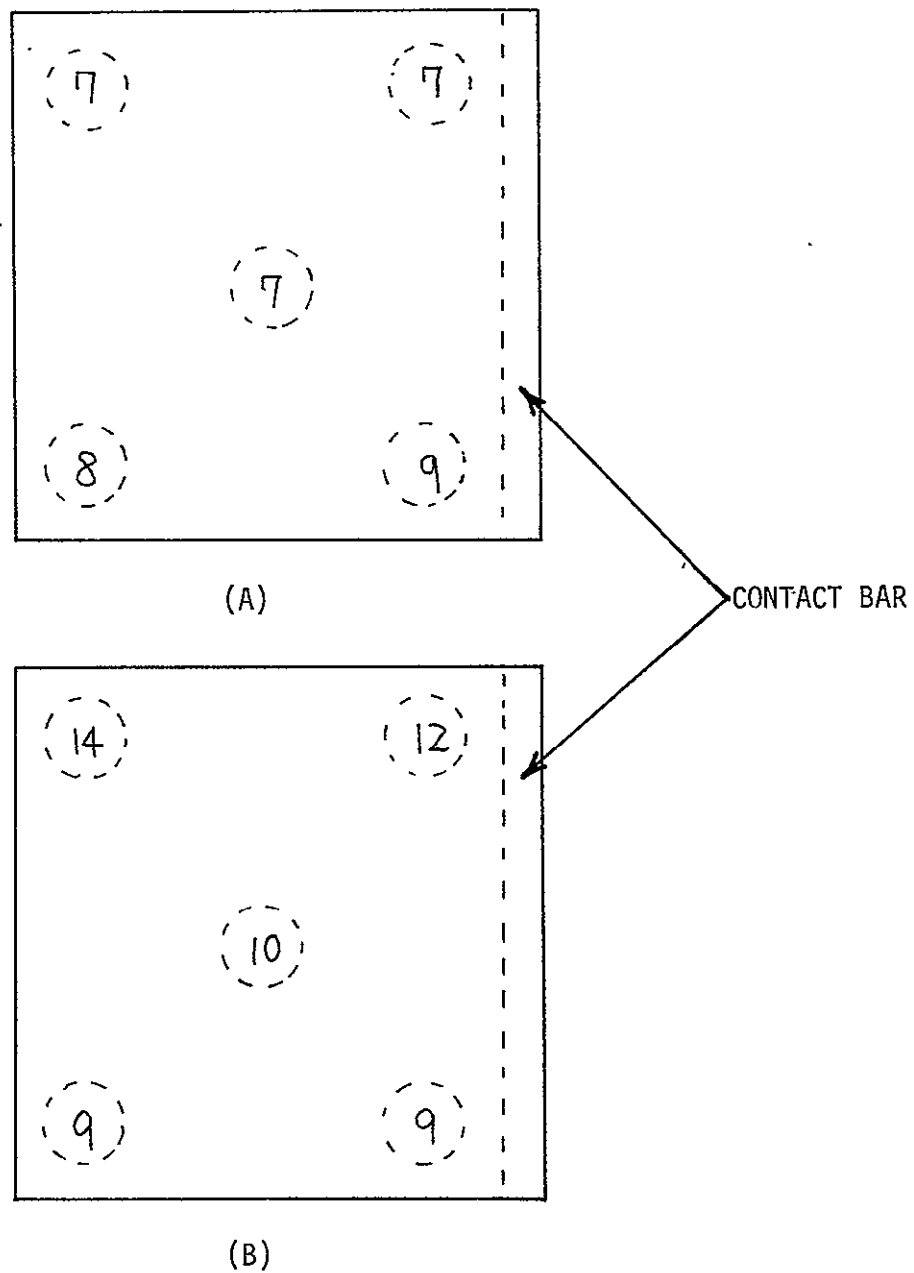
FIGURE 27

MINORITY CARRIER DIFFUSION LENGTH (μm)
VARIATION WITHIN RTR SOLAR CELLS (2x2 cm)

(A)   A CELL FROM CVD FEEDSTOCK (CELL NO. 869-7)

(B)   A CELL FROM SINGLE CRYSTALLINE FEEDSTOCK
      (CELL NO. S872B-3)

FIGURE 28

SMALL LIGHT SPOT SCANNING OF A RTR SOLAR CELL

CONTROL CELL

RELATIVE PHOTORESPONSE

-70-

RTR

GRID LINES

← ∿.6 mm →

DISTANCE
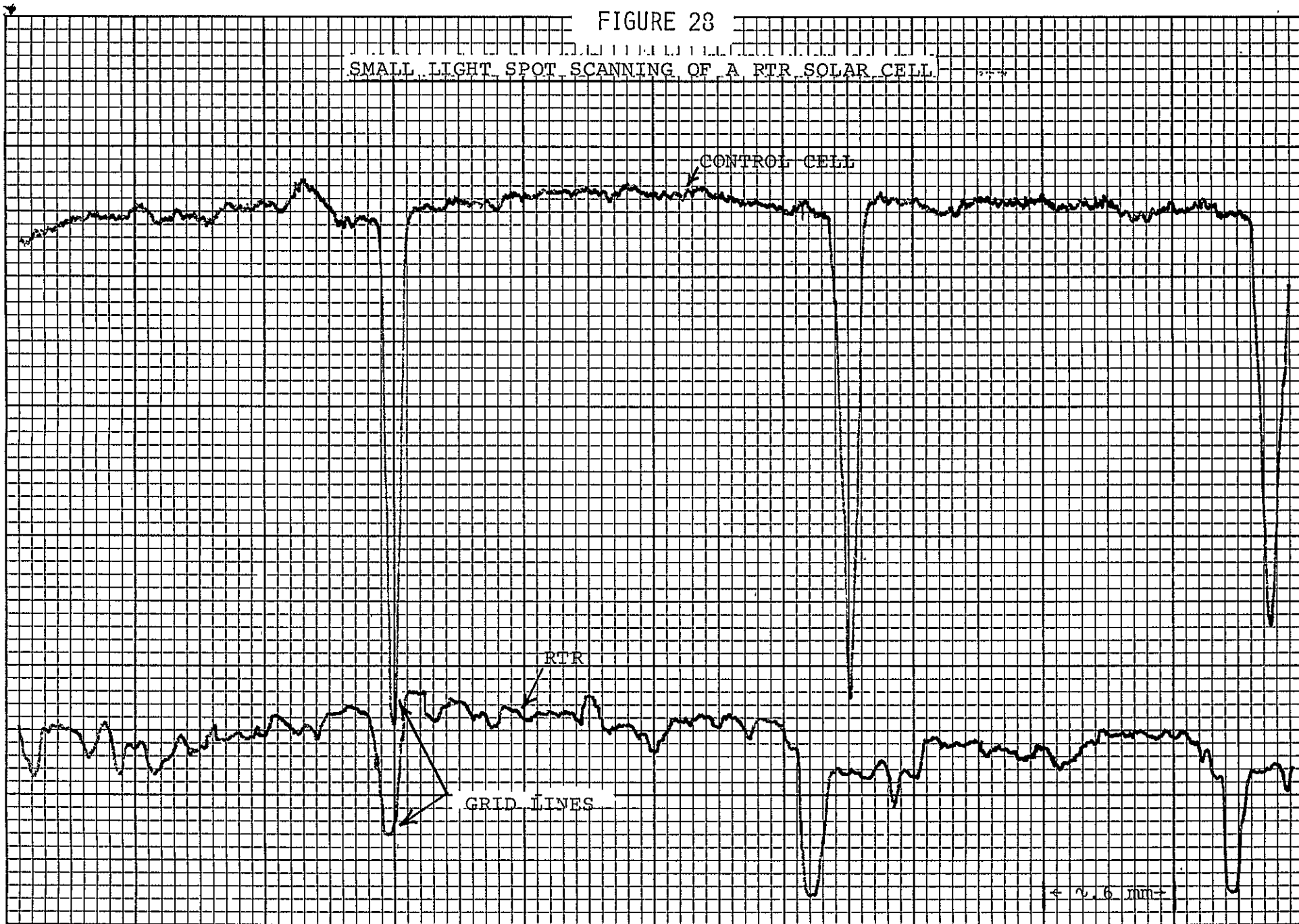
TABLE 15

MECHANICAL FAILURE OF RTR SOLAR CELLS (2x2 cm)
IN THE PROCESS OF FABRICATION

NUMBER OF BROKEN CELLS	CAUSE
6	Initial Slicing and Demounting
5	Cleaning
4	Evaporation; AR and Contact
1	Sintering
7	Electrical Test
23	TOTAL

Starting Blanks: 52

NOTE: Results are summarized from three batch processes

E.   DENDRITIC WEB SOLAR CELLS

1.0   SOLAR CELL FABRICATION

Blanks (2x2 cm) were prepared by waxing a web section on a ceramic block and slicing in size. After removal of the individual blanks from the block, efforts were made to remove SiO, deposited on the surface during the web growing process, by chemical methods, such as boiling in nitric and sulfuric acid followed by dipping in HF. None of the methods worked except scrubbing by a cotton tip, which caused some breakage of the webs, especially of thin webs (∿6 mils). The breakage could have been minimized if the scrubbing were done before the blank shaping process since bounding dendrites could provide mechanical support for the scrubbing process. Also, steam oxidation was carried out to eliminate the mechanical scrubbing process for the removal of SiO deposit. Webs were oxidized in steam at 1100°C for an hour (with ramp-down cooling, at a cooling rate of about 3°C/minute down to 500°C), to recover minority carrier lifetime due to higher temperature heat treatment. The oxidized webs were finally dipped in HF and the surface deposits were completely removed.

NOTE: Solar cells were fabricated from the oxidized blanks and the cell performance is given in Section B, 2.0.

Organic and chemical (standard RCA) solutions were used for the final cleaning of the surface.

Thickness of the webs, as received, ranged from 5.6 mils to 9.6 mils and resistivity by four point probe was measured to be around 20-25 ohm-cm with p-type conductivity. SPV measurement of effective minority carrier

diffusion length indicated values between 90-120 μm. See reference
(8) for detailed description of dendritic web process.

The first batch of solar cells were fabricated using standard processing.
A BSF process was applied for the second batch (see Appendix III
for detailed description of standard and BSF processes).
A space-cell type of fabrication process was used in the third batch process.
This process included a shallow junction ($\sim$0.2 μm) formation (ten minutes
oxidation and ten minutes diffusion) and application of fine front contact
lines using photoresist techniques (retaining about 93% active area). The
fourth batch were standard process solar cells of two types; (a) cells
with front contact bars on the bounding dendrites, and (b) solar cells
processed from steam oxidized blanks.

Mechanical yield (unbroken cells) of the relatively thick web solar cells,
(with thickness between 8 to 10 mils), were generally high (about 90%
yield) for both standard and BSF processes. However, thin web cells,
thickness between 5-6 mils, showed lower yield (less than 50%), mainly
because of breakage in the initial blank shaping stages and in removal of
excess aluminum following the BSF process. Detailed causes of the breakage
are listed in Table 16.

2.0   SOLAR CELL PERFORMANCE AND CHARACTERIZATION

Charactertistics Under Illumination

Solar cell parameters, such as I_{SC}, V_{OC}, CFF and η were measured under an
AMO solar simulator at 25°C. Electrical data sheets in the Second·
Quarterly Report (5) give detailed information on individual cells.
Table 17 and Table 18 summarize the results for the cells

of two process types; standard process and BSF process.

BSF solar cells showed improved performance compared with the cells from standard process, average efficiency 10.4% versus 9.6%, with overall increase in both V_{OC} and I_{SC} (mainly in V_{OC}). However, this improvement by BSF process was not as high as observed for starting silicon of this high resistivity. This possibly indicates that the minority carrier diffusion length of the starting web was not long enough to provide significant improvement in V_{OC} and I_{SC}. It is generally believed that a diffusion length greater than 120 μm* is required to achieve significant improvement in V_{OC} and I_{SC} by the BSF process. The relatively low open circuit voltage of standard cells, (average $V_{OC} \sim 530$ mV), was due to the low doping level of the starting webs (~ 20 ohm-cm bulk resistivity) and the low curve fill factor, about 72% in both cases, seems to be due to the increased series resistance resulting from increased bulk resistance. Maximum efficiencies obtained were 9.8% for the standard cells and 10.9% for the BSF cells. Low-performance of web "B" cells in Table 17, compared with web "A" cells, was suspected to be coming from the difference in lifetime of two webs (Westinghouse lifetime data; 13 μs for web "B" and 41 μs for web "A") and partly the difference in web thickness, 9.6 mils for web "A" versus 5.6 mils for web "B".

*This is an empirical observation. Work is in progress to establish a definite relationship.

Some control cells (first control group) started to show degradation in
curve fill factor, mainly due to shunting problems. This was suspected
to be caused by the diffusion process since the second control group,
which were diffused in a separate furnace, did not indicate any significant
degradation in CFF by shunting. Thus, the diffusion tube was cleaned and
control cells were processed using standard process. Their electrical
parameters showed no degradation in CFF with consistent results.

Dark I-V Characteristics

Dark I-V characteristics (forward and reverse) were obtained from selected
web cells. The plots were made by point-by-point measurement and the
results are plotted in Figure 29 for the standard cells and Figure 30 for
the BSF cells. "A" factors in the simple diode equation ranged from
about 1.7 to 2.0 while control cells showed "A" factor ranges between
1.2 and 1.7. Saturation current (I_0) were found to be around 10^{-7} A/cm^2

for the standard web cells and 10^{-10} A/cm^2 for the control cell in standard
process, and this higher I_0 for the web cells can be partly explained by lower
doping level of the webs ($\sim$20 ohm-cm resistivity) than the control blanks
(1-3 ohm-cm). Generally cells from BSF process showed slightly leaky
characteristics, consequently leading to an increase in "A" factor and
saturation current (I_0). Web solar cells showed relatively good junction
characteristics, especially in low leakage at small forward bias condition
(less than 0.4 volts), showing agreement with the earlier reports from
Westinghouse.

Spectral Response

Absolute spectral response (A/W) was measured using a filter wheel set up [Refer to Appendix V-A for details]. Response versus wavelength for the standard cells and BSF cells are given in Figure 31 and Figure 32, respectively. Web solar cells showed responses very close to those of the control cells (this is more pronounced in the case of BSF process cells) and this was in good agreement with the minority carrier diffusion length measurement of the finished solar cells in the following section.

Minority Carrier Diffusion Length

Minority carrier diffusion length was measured using the surface photovoltage (SPV) method for the bulk webs and a short circuit current method for the finished solar cells [refer to Appendix V-B for details]. The exposed beam (monochromatic) size on the bulk sample in SPV mode was about 3 mm in diameter and diffusion lengths were around 90-120 μm, measured from the number of selected webs.

The finished.cells were illuminated on the whole cell area and on spots (spot size about 3-4 mm in diameter) to see the localized variation of diffusion length, and the results are summarized in Table 19. BSF cells showed higher diffusion length than the standard cells, which agrees well with the spectral response plots (compare Figures 31 and 32) in the previous section. BSF cells also showed significant variation in diffusion length from cell to cell (i.e. 70 μm for the cell RE 24-1.5-3 versus 130 μm for the cell RE 24-1.5-8) and from spot to spot within a cell (i.e. 210 μm versus 110 μm in cell RE 24-1.5-3), which could be due

to inhomogenity of bulk webs or possibly a process induced effect. Diffusion length measurement on spots in standard cells indicated slightly higher values than those of the whole area measurement on the same sample but this could possibly be caused by the measurement error.

Diffusion length was also checked on the cells from space type process (third batch) and both web and control cells showed low diffusion length; about 40-50 μm for the web cells and 80 μm for the control cells. This strongly indicated that these cells were contaminated in the process of fabrication, mostly likely in the diffusion step.

Photoresponse by Small Light Spot Scanning

Localized photoresponse of the solar cells were obtained by light spot scanning [refer to Appendix V-C for details]. The result of a scanning is given in Figure 33. The dendritic web cell indicated close response to that of the control cell and no significant number of active boundaries was noticed.

FIGURE 29

DARK I-V CHARACTERISTICS OF SOLAR CELLS
FROM DENDRITIC WEB (~4 cm², STANDARD PROCESS)
AT ROOM TEMPERATURE

Δ: Control Cell No. 9
x: Cell No. RE12-3.3-1
o: Cell No. J65-3.4-4

— — : Forward Characteristics
– · – : Reverse Characteristics

CURRENT DENSITY, (A/cm²)

VOLTAGE, (VOLTS)

-78-
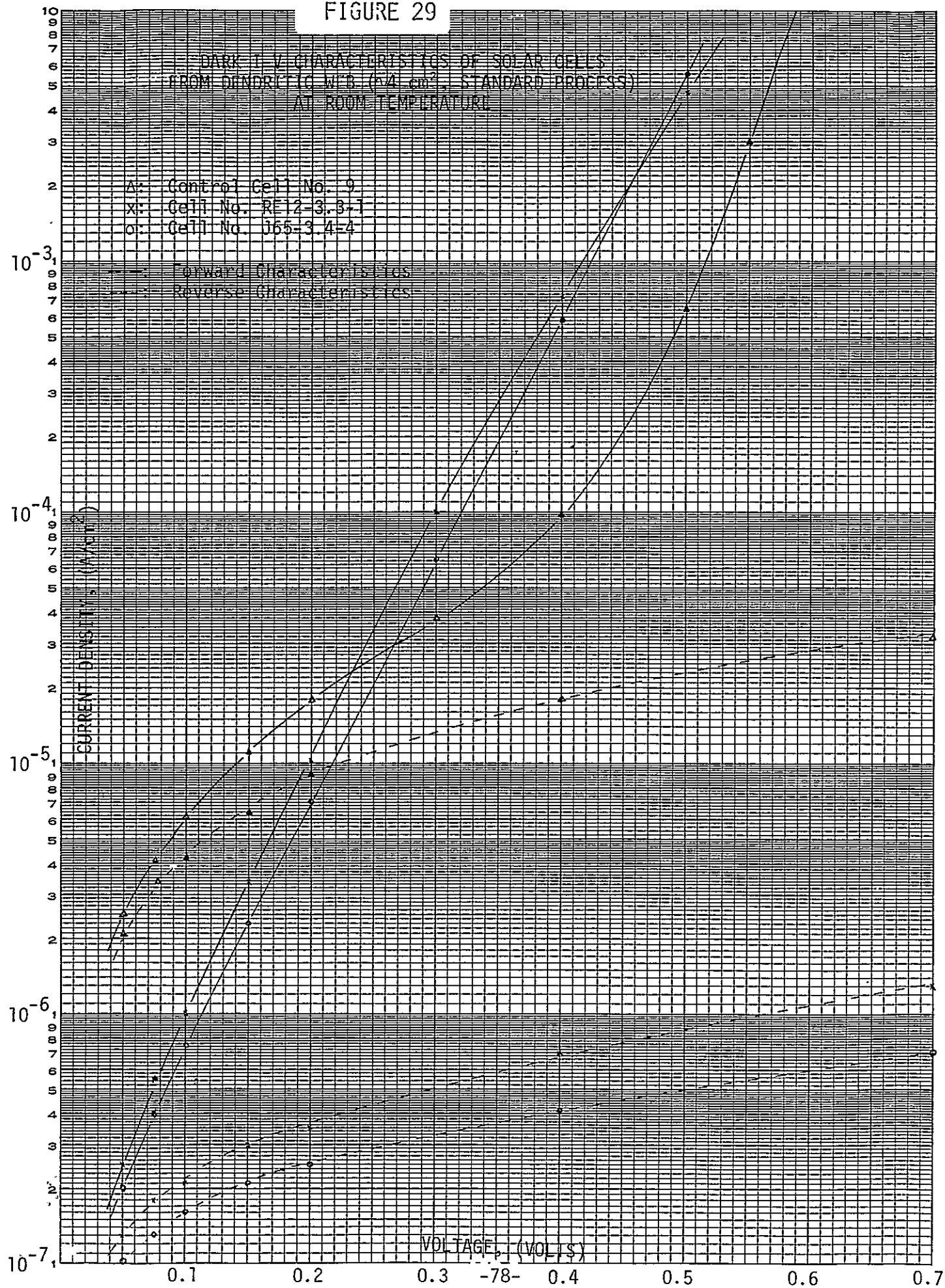
FIGURE 30

DARK I-V CHARACTERISTICS OF SOLAR CELLS
FROM DENDRITIC WEB (≈4 cm²) BSF PROCESS) AT ROOM TEMPERATURE

x: Control Cell No. 12
△: Cell No. RE24-1.5-5
○: Cell No. RE24-1.5-8
□: Cell No. J64-1.6-4

——— Forward Characteristics
- - - Reverse Characteristics

CURRENT DENSITY - (A/10⁴)

VOLTAGE (VOLTS)

-79-
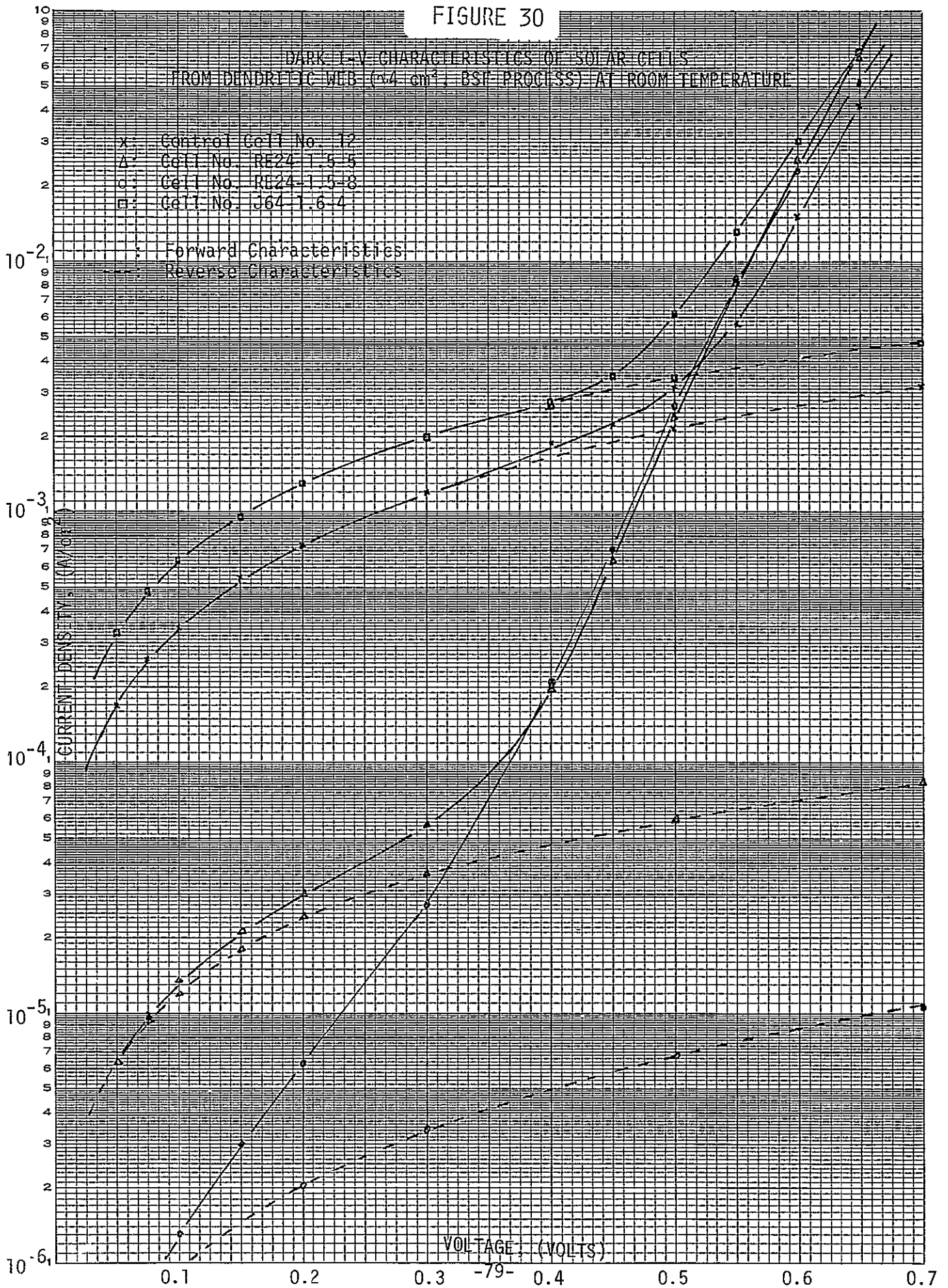
FIGURE 32

SPECTRAL RESPONSE OF SOLAR CELLS FROM DENDRITIC WEB
(BSF PROCESS)

FIGURE 33

SMALL LIGHT SPOT SCANNING OF A DENDRITIC WEB SOLAR CELL

CONTROL CELL

DENDRITIC WEB CELL

GRID LINES

RELATIVE RESPONSE

DISTANCE

← ~.6 mm →
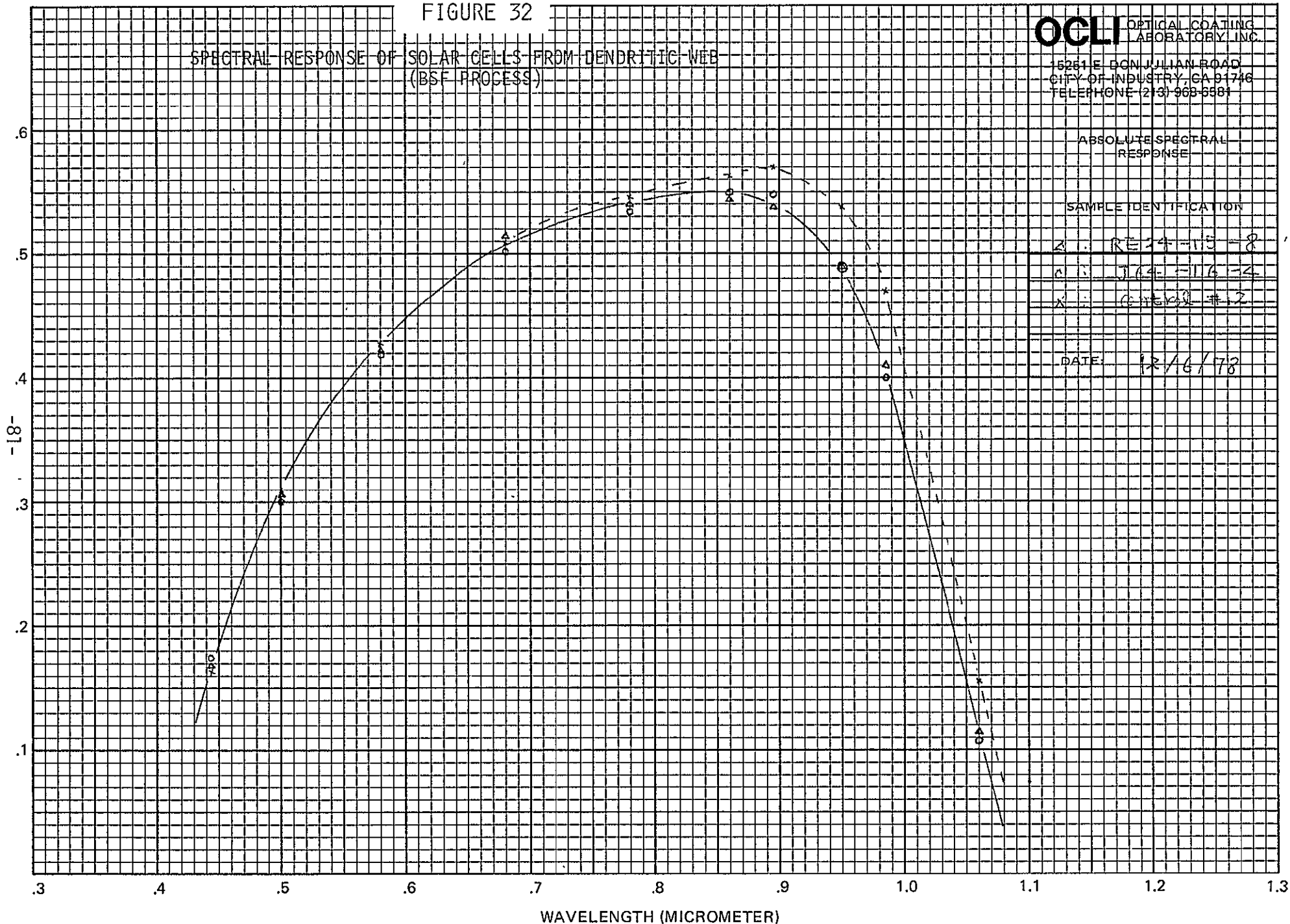
-82-
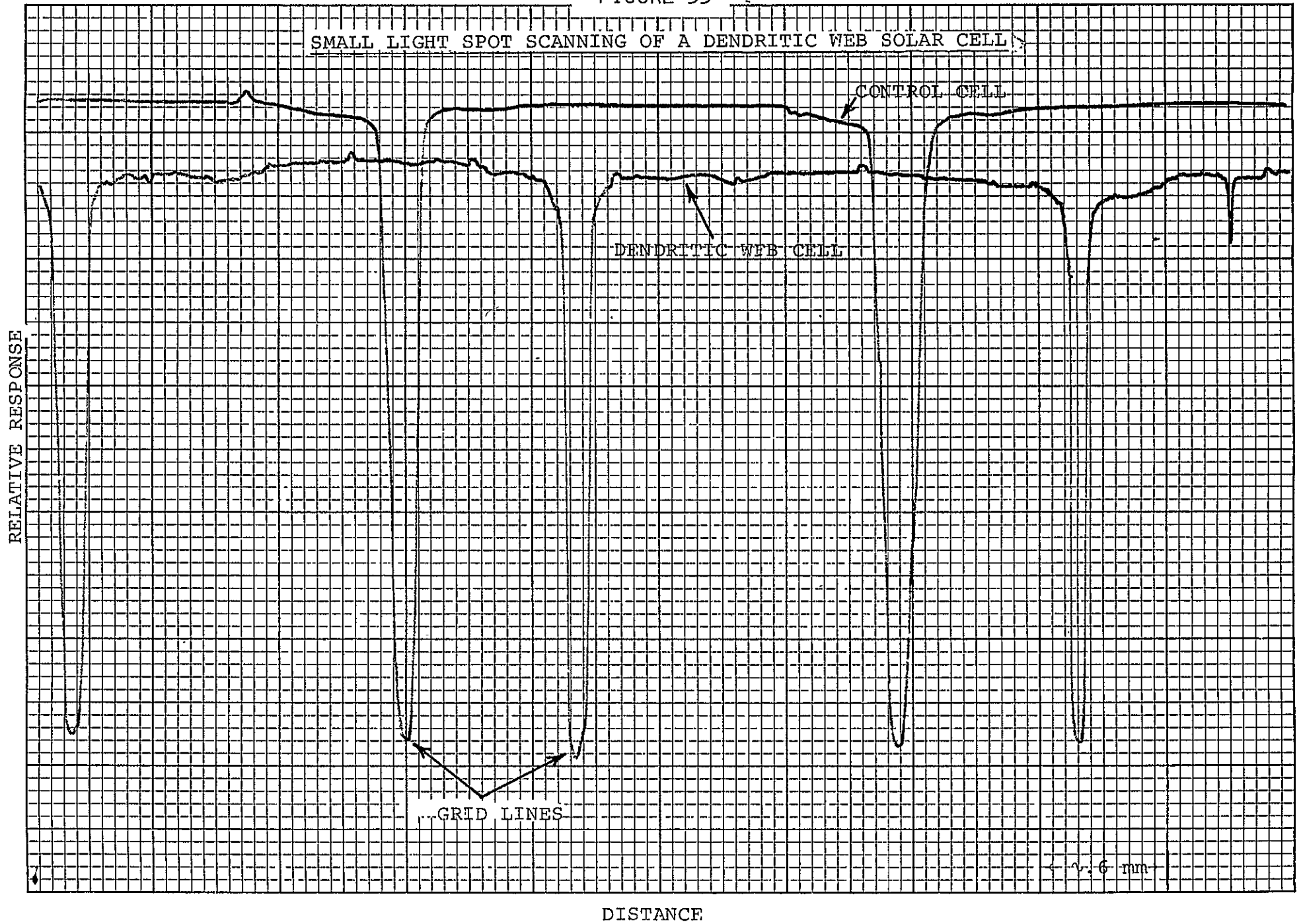
STANDARD PROCESS

CAUSE WEB THICKNESS	9.6 MILS	5.6 MILS
SLICING IN SIZE	---	2
SCRUBBING FOR REMOVAL OF SiO DEPOSIT	1	4
FINAL BLANK CLEANING	---	1
ELECTRICAL TEST	1	---
STARTING NUMBER OF BLANKS	12	10

BSF PROCESS

CAUSE WEB THICKNESS	8.6 MILS	5.6 MILS
REMOVAL OF EXCESS ALUMINUM	---	3
ELECTRICAL TEST	2	---
STARTING NUMBER OF BLANKS	12	4

TABLE 16

MECHANICAL FAILURE OF DENDRITIC WEB
SOLAR CELLS IN THE PROCESS OF FABRICATION

TABLE 17

SUMMARY OF PARAMETERS OF SOLAR CELLS
FABRICATED FROM DENDRITIC WEB; STANDARD PROCESS

WAFERS		WEB "A"	WEB "B"	CONTROL
V_{OC} (mV)	AVERAGE	534 (525)	518 (508)	595 (584)
	STANDARD DEVIATION	3.3 (1.0)	--- ---	3.2 (2.3)
	RANGE	529-537 (523-526)	514-520 (506-510)	589-598 (581-587)
J_{SC} (mA/cm^2)	AVERAGE	33.8 (24.3)	32 (22.8)	33.3 (23.5)
	STANDARD DEVIATION	0.3 (0.2)	--- ---	0.7 (0.4)
	RANGE	33.3-34 (24-24.5)	31.5-32.3 (22.5-23)	32.2-34.3 (23-24.3)
CFF (%)	AVERAGE	72 (72.7)	73 (73)	78 (78)
	STANDARD DEVIATION	0.9 (1.2)	--- ---	0.8 (1.7)
	RANGE	71-73 (71-74)	72-75 (72-75)	77-79 (79-80)
η (%)	AVERAGE	9.6 (6.8)	9.0 (6.3)	11.3 (8.0)
	STANDARD DEVIATION	0.1 (0.1)	--- ---	0.3 (0.3)
	RANGE	9.5-9.8 (6.7-6.9)	8.9-9.1 (6.3-6.4)	10.8-11.8 (7.5-8.3)

NOTE: 1. Measured under AMO condition at 25°C.

2. Cells (2x2 cm) with SiO antireflective (AR) coating, parenthesis numbers are for the parameter before AR coating.

3. Web "A": Six solar cells from Web No. RE12-3.3 (Thickness ∿9.6 mils).
   Web "B": Three solar cells from Web No. J65-3.4 (Thickness ∿5.6 mils).
   Control: Six solar cells.

TABLE 18

SUMMARY OF PARAMETERS OF SOLAR CELLS
FABRICATED FROM DENDRITIC WEB; BSF PROCESS

WAFERS		WEB "C"	WEB "D"	CONTROL
V_{OC} (mV)	AVERAGE	564 (552)	565 (551)	588 (573)
	STANDARD DEVIATION	16.8 (15.9)	--- ---	9.2 (14.1)
	RANGE	521-578 (511-567)	--- ---	575-598 (552-588)
J_{SC} (mA/cm²)	AVERAGE	35.5 (25.4)	34.5 (24.6)	34.3 (25)
	STANDARD DEVIATION	0.8 (0.5)	--- ---	0.3 (0.3)
	RANGE	33.2-35.9 (23.9-25.7)	--- ---	33.8-34.7 (24.5-25.4)
CFF (%)	AVERAGE	71 (74)	67 (67)	66 (63)
	STANDARD DEVIATION	2.7 (1.4)	--- ---	7 (8.7)
	RANGE	65-73 (70-75)	--- ---	56-73 (51-71)
η (%)	AVERAGE	10.4 (7.6)	9.6 (6.7)	9.9 (6.7)
	STANDARD DEVIATION	0.6 (0.4)	--- ---	1.2 (1.1)
	RANGE	9.2-10.9 (6.7-8.1)	--- ---	8.2-11.0 (5.2-7.7)

NOTE: 1. Measured under AMO condition at 25°C.

2. Cells (2x2 cm) with SiO antireflective (AR) coating, parenthesis numbers are for the parameter before AR coating.

3. Web "C": Ten solar cells from Web No. RE24-1.5 (Thickness ∿8.6 mils).
    Web "D": One solar cell from Web No. J64-1.6 (Thickness ∿5.6 mils).
    Control: Six solar cells.

TABLE 19

SUMMARY OF MINORITY CARRIER DIFFUSION LENGTH OF THE DENDRITIC WEB CELLS, MEASURED BY I_{SC} METHOD

CELL NO.	POSITION	1	2	3	4	5	WHOLE AREA
STANDARD CELL	RE 12-3.3-3	---	---	---	---	---	74
	RE 12-3.3-6	90	90	90	90	76	74
	J 65-3.4-4	---	---	---	---	---	62
	J 65-3.4-7	72	72	72	80	80	62
	CONTROL NO. 3	---	---	---	---	---	122
BSF CELL	RE 24-1.5-3	90	60	90	85	60	70
	RE 24-1.5-8	160	160	150	210	110	130
	J 64-1.6-4	---	---	---	---	---	130
	CONTROL NO. 12	---	---	---	---	---	150

NOTE: Unit; μm

IDENTIFICATION OF BEAM SPOT (BEAM SIZE 3-4 MM IN DIAMETER)
FOR DIFFUSION LENGTH MEASUREMENT ON LOCALIZED AREAS OF A 2x2 CM CELL
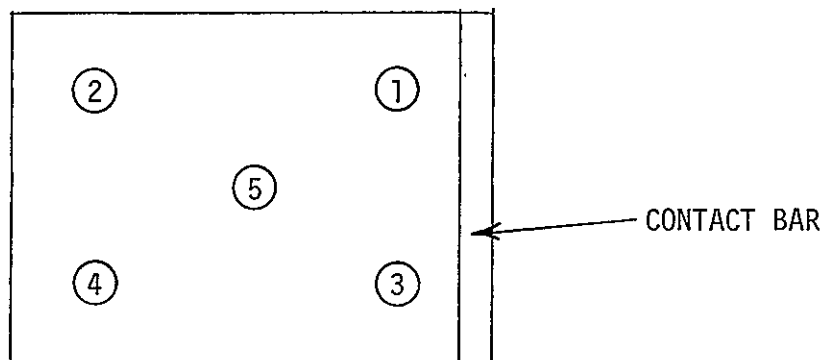
F.   CAST SILICON (HEM) SOLAR CELLS

1.0   SOLAR CELL FABRICATION

Blanks (2x2 cm) were prepared by slicing the cast silicon blocks (2x2 cm cross section) using an ID saw. Silicon blocks were prepared from two casting experiments of different resistivities; nominal 3 ohm-cm and 0.5 ohm-cm. Measured resistivity of the sliced blanks from 3 ohm-cm material showed resistivity variation between 2.6 and 3.3 ohm-cm from end-to-end of the 3" block, while those of 0.5 ohm-cm cast silicon indicated between 0.4-0.8 ohm-cm. Most of the blanks were single crystalline, with a few partly polycrystalline with large crystallites. Some of the blanks were measured for minority carrier diffusion lengths using the SPV method and results indicated a range of 30-60 μm for the low resistivity blanks (0.5 ohm-cm) and 40-70 μm for the 3 ohm-cm blanks.

NOTE: Czochralski control blanks (1-3 ohm-cm) showed diffusion lengths in the range 130-160 μm.

Thickness of the sliced blanks was about 16 mils and the blanks were thinned down to 13 mil using a planar etching solution. Standard and BSF solar cells were fabricated from the blanks with a mechanical yield (ratio of unbroken solar cells to initial starting blanks) above 90%, which is about the same yield as for Czochralski blanks.

[See Appendix III for detailed description of standard and Back Surface Field (BSF) processes. Reference (9) provides technical details of casting techniques by Heat Exchanger Method (HEM).]

FIGURE 31

SPECTRAL RESPONSE OF SOLAR CELLS FROM DENDRITIC WEB
(STANDARD PROCESS)
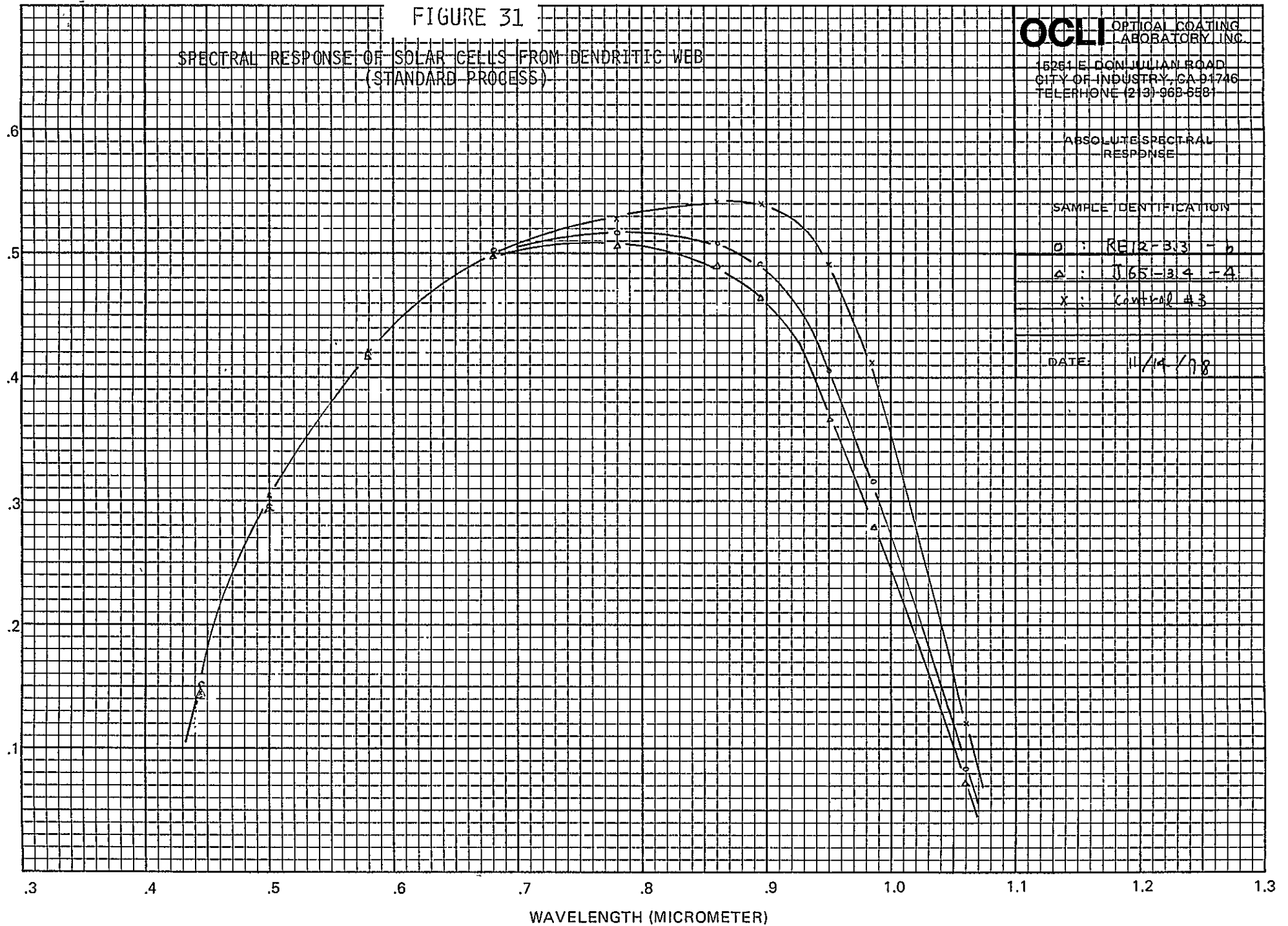
2.0   SOLAR CELL PERFORMANCE AND CHARACTERIZATION

Characteristics Under Illumination

Final finished solar cells had SiO AR coatings and about 90% active area
with Ti-Pd-Ag metallizations. Solar cell parameters, such as I_{SC}, V_{OC},
CFF and η, were measured under an AMO simulator at 25°C block temperature.

NOTE: Detailed information on solar simulator and measurement techniques
        are discussed in Appendix IV. The Third Quarterly Report (6)
        provides the parameters of individual solar cell from HEM
        cast silicon.

Table 20 summarizes the cell parameters from the standard process. Solar
cells from HEM cast silicon showed maximum efficiency of 10.1% for the
3 ohm-cm material and 9.2% for the 0.5 ohm-cm silicon with an average
efficiency of 9.5% and 7.4%, respectively. The average efficiency of
control solar cells was about 11%. Solar cells from the low resistivity
cast silicon generally showed low curve fill factor, in the range of
40-75%, which is suspected to be due to the imperfections in the cast
silicon. This will be discussed in the latter part of this section.
Substrates exhibiting polycrystallinity were also fabricated into solar cells
and the results are summarized in Table 21, indicating no basic difference
in cell performance. Note: Most substrates had large crystallites,
approximately centimeter dimensions.

Solar cells from BSF processes showed lower cell performance than the
standard cells, mainly due to the leaky characteristics of the cells.
A few of the control cells showed the same problem. This BSF process

-88-

showed slight improvement in short circuit current and the results are given in Table 22. However, no improvement in open circuit voltage was observed possibly due to overshadowing effect on reduction of V_{OC} by shunting rather than improvement in V_{OC} by the BSF process. Maximum AMO efficiency of these cells was 9.8% for the 3 ohm-cm material and 7.4% for the 0.5 ohm-cm material, while that of the control cell was 11.4%. Solar cells from low resistivity cast silicon, 0.5 ohm-cm, showed a higher degree of leakage than those of the higher resistivity cast silicon.

Dark I-V Characteristics

Dark I-V characteristics (forward and reverse) at room temperature were obtained from the selected sample cells. The plots were made by point-by-point measurements and a typical results are given in Figure 34 for the solar cells from the standard process and Figure 35 for the BSF solar cells. The "A" factor from the simple diode equation, was derived from the data at the high bias conditions (bias voltage >0.4 volt). A standard HEM solar cell yielded about 1.8 while that of a control cell was about 1.6. Saturation current (I_0) was also obtained from the plots, indicating 4×10^{-8} A/cm^2 for the HEM cast cell and 2×10^{-9} A/cm^2 for the control cell. The characteristics of BSF cells were slightly leakier than the standard cells (this was always the case in the past), showing "A" factors of 2.2 for the HEM cell and 2.0 for the control cell. The increased saturation current (I_0) of about 3×10^{-7} A/cm^2 for the HEM cell and about 8×10^{-8} A/cm^2 for the control; was probably due to the leaky characteristics.

The characteristics indicated that shunting and space charge recombination effects are higher in the cells from the HEM cast silicon than in the control cells. Saturation current of the HEM solar cells seems to be approximately an order of magnitude higher than those of the controls, which might have been caused by the higher degree of shunting and low lifetime effects.

Spectral Response

Absolute spectral response (A/W) was obtained using a filter wheel set-up which is a combination of a set of narrow bandwidth filters and a light source. [See Appendix V-A for the detailed techniques of the measurement procedure.] Responses of the standard HEM cells are plotted in Figure 36, in which the cells from the cast silicon of 3 ohm-cm resistivity, Cell No. 1-852-13, showed relatively good response in overall wavelength. However, the cell from 0.5 ohm-cm resistivity indicated significantly lower response than that of the control, especially at wavelengths above 0.6 µm, suggesting low minority carrier diffuion lengths.

Minority Carrier Diffusion Length

Minority carrier diffusion length (Le) was measured using the surface photovoltage (SPV) method for the bulk cast silicon substrates and a short circuit current method for the finished solar cells. [See Appendix V-B for the detailed description on measurement procedures.] Le by SPV method (spot measurement) showed ranges of about 30-60 µm for the 0.5 ohm-cm cast silicon and 40-70 µm for the 3 ohm-cm cast silicon.

Le measurement of the finished cast cells were slightly higher than those of the bulk silicon, 50-60 μm for the 0.5 ohm-cm material and 100 μm for the 3 ohm-cm material. The cause of the increases is not known at present. There might be a possibility of gettering effects from oxides formed in the diffusion process.

Photoresponse by Small Light Spot Scanning

Localized photoresponse of the solar cells was made using a small light spot scanning technique. [Detailed descriptions on measurement techniques and procedures are given in Appendix V-C.] The light source used was a white light from a tungsten lamp filtered by a thin transparent layer of silicon, generating a beam spot size on a flat sample of around 50-100 μm. Relative photoresponse of both cells from cast silicon and control are given in Figure 37. Generally, the cast solar cell indicated lower response than the control cell everywhere. Also the cast cell from the low resistivity material showed lower response than those of the cells from the high resistivity material. This agrees well with the minority carrier diffusion length measurements of the finished cells. By inspection, the solar cells from the cast silicon in the figure do not seem to possess any grain structure or other defect sites. However, reduction of response in some localized area was noticed. This dip in response is in contrast with the response from the localized area containing microcracks which will be discussed in the following section.

Defect Study

Limited efforts were made in an attempt to identify defects which will influence solar cell performance. The efforts were concentrated on the cast silicon of 0.5 ohm-cm resistivity since those cells showed shunting problems and low cell efficiency. The most common defects, other than grain boundaries existing in some part of the cast ingot, were inclusions and microcracks. Figure 38 shows photographs of defects found in solar cells from the low resistivity cast silicon; (a) An inclusion surrounded by either gross lineage (low angle grain boundary) or microcracks, (b) Microcracks. Photoresponse by small light spot scanning was also carried out on a solar cell showing microcracks. Figure 39 is the scanning result in which sharp drops in response were observed in areas having microcracks.

FIGURE 34

DARK I-V CHARACTERISTICS OF HEM SOLAR CELLS
(2x2 cm² area, standard process) AT ROOM TEMPERATURE

Forward Characteristics
Reverse Characteristics
o   Control Cell No. 1
x   HEM Cell No. 1-852-16
Δ   HEM Cell No. 1-860-18

CURRENT DENSITY, (A/cm²)

VOLTAGE, (VOLTS)

-93-
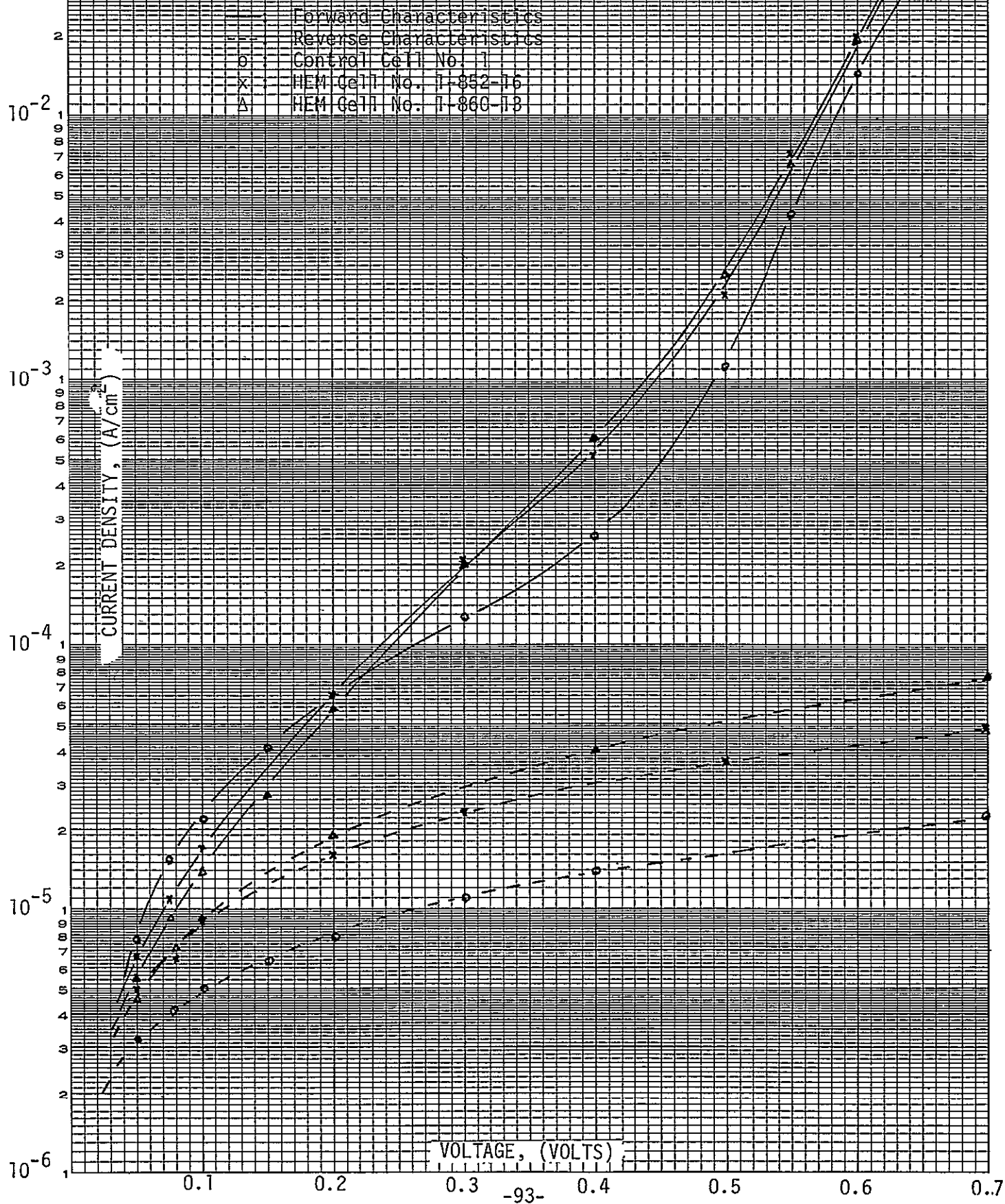
FIGURE 35

DARK I-V CHARACTERISTICS OF HEM SOLAR CELLS
(4x2 cm in area, BSF Process) AT ROOM TEMPERATURE
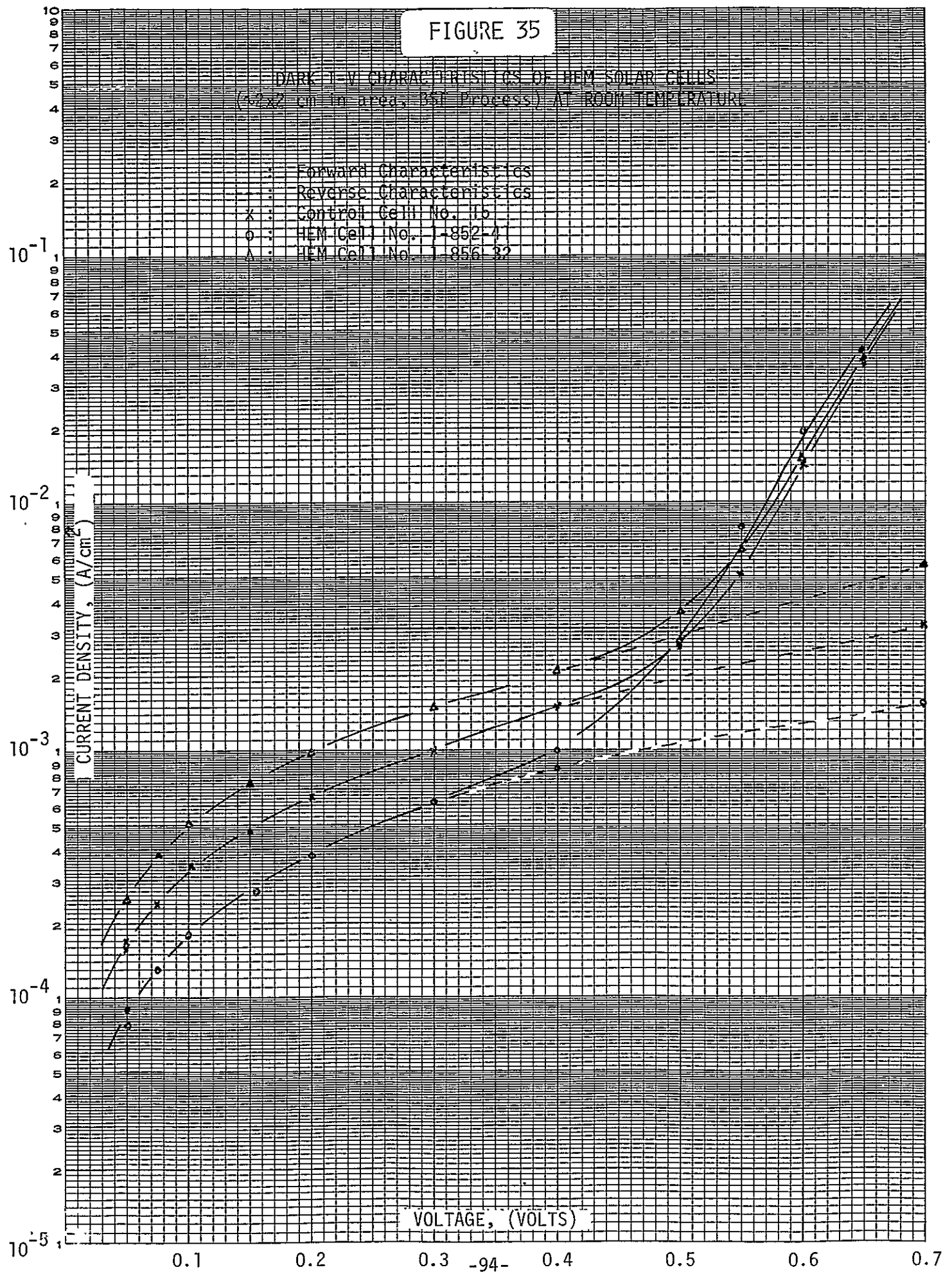
Forward Characteristics
Reverse Characteristics
x : Control Cell No. 15
o : HEM Cell No. 1-852-4
Δ : HEM Cell No. 1-856-32

CURRENT DENSITY, (A/cm²)

VOLTAGE, (VOLTS)

-94-

FIGURE 36

FIGURE 37

SMALL LIGHT SPOT SCANNING OF HEM SOLAR CELLS

Control No. 4

HEM Cell No. 1-852-43

HEM Cell No. 1-860-13

Gridlines

6 mm

RELATIVE PHOTORESPONSE

DISTANCE

-96-

FIGURE 38

(a)

(b)
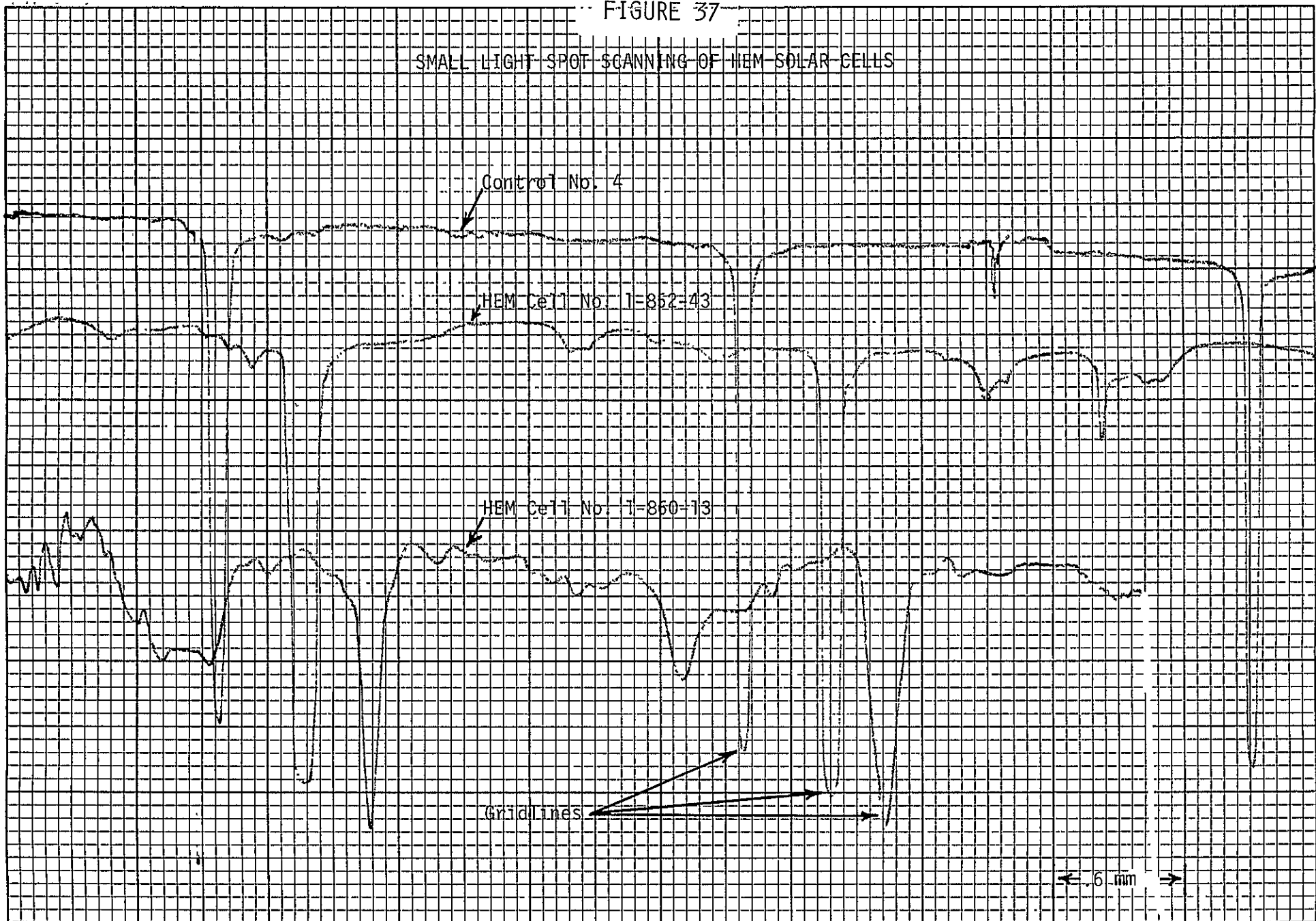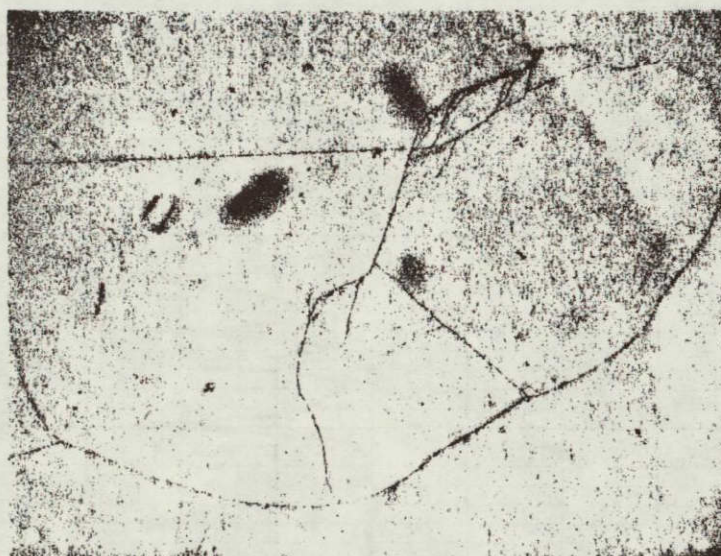
MICROSCOPIC PHOTOGRAPHS OF DEFECTS
FOUND IN HEM CAST SILICON SOLAR CELLS
(200X Magnification)

(a) Inclusion (found in Cell No. 1-860-1)

(b) Microcracks (found in Cell No. 1-860-14)

FIGURE 39

SMALL LIGHT SPOT SCANNING OF A HEM SOLAR CELL CONTAINING MICROCRACKS

CELL NO. 1-860-43

RELATIVE PHOTORESPONSE

-86-

MICROCRACKS

GRIDLINES

.6 mm

DISTANCE
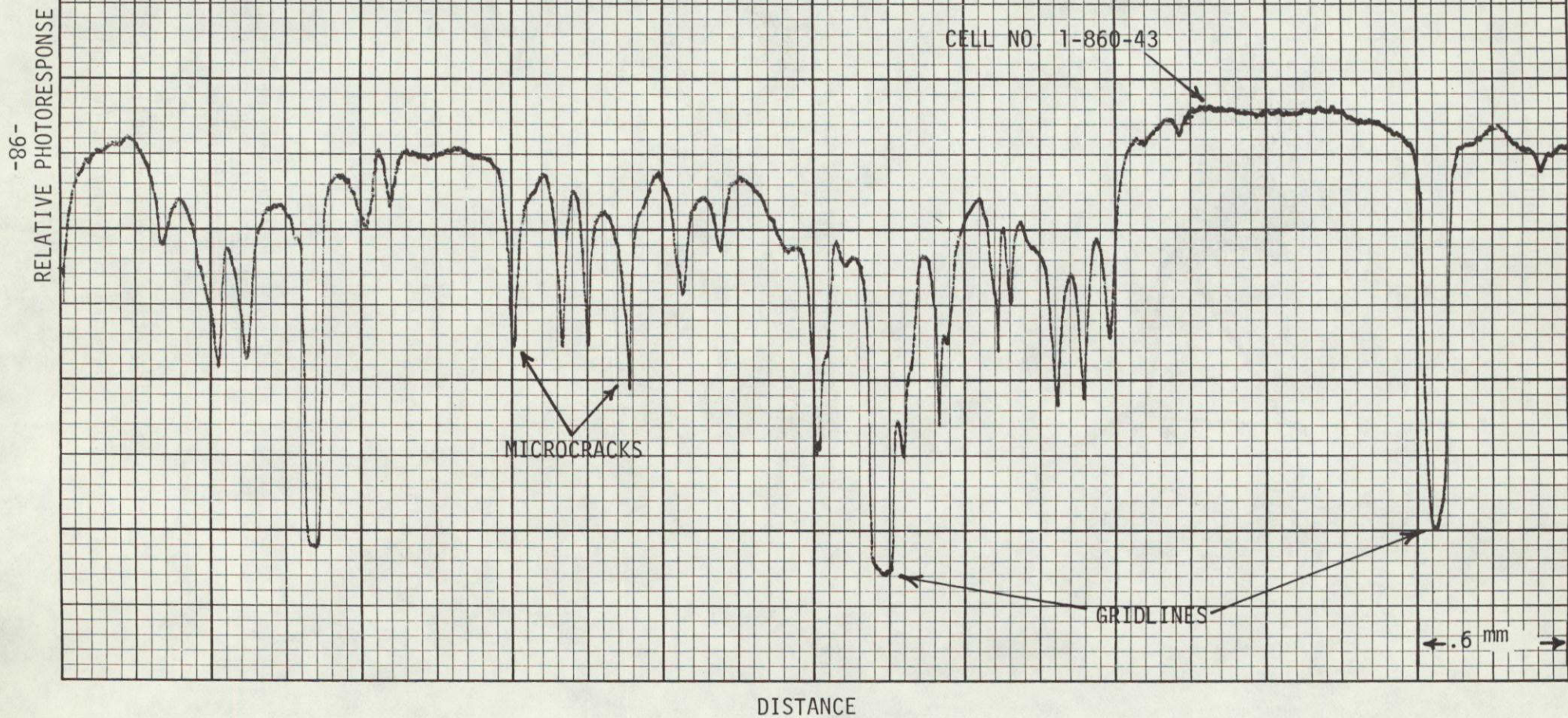
TABLE 20

SUMMARY OF PARAMETERS OF SOLAR CELLS FABRICATED FROM CAST SILICON BY HEM; STANDARD PROCESS

		CAST SILICON "A"	CAST SILICON "B"	CONTROL
V_{OC} (mV)	Average	568	571	591
	Standard Deviation	4	18	3
	Range	557-574	535-588	588-595
J_{SC} (mA/cm^2)	Average	30.8	28.4	33.4
	Standard Deviation	0.6	0.8	0.2
	Range	29.5-31.5	27.2-28.9	33-33.6
CFF (%)	Average	73	61	75
	Standard Deviation	2	11	2
	Range	67-75	46-75	73-77
η (%)	Average	9.5	7.4	10.9
	Standard Deviation	0.4	1.4	0.2
	Range	8.4-10.1	5.3-9.2	10.7-11.2

NOTE: 1. Measured at 25°C under AMO conditons (with SiO AR)

2. Cast Silicon "A": 3 ohm-cm
   Cast Silicon "B": 0.5 ohm-cm

3. Number of Samples: Cast Silicon "A" - 18
   Cast Silicon "B" - 12
   Control Cells - 6

TABLE 21

Summary of Parameters of Standard HEM Solar
Cells Having Some Degree of Polycrystallinity

		SILICON	
		"A"	"B"
V_{OC} (mV)	Average	565	557
	Standard Deviation	4	23
	Range	558-571	527-589
J_{SC} (mA/cm^2)	Average	30.9	27.3
	Standard Deviation	0.6	1.3
	Range	29.8-32	25-28.4
CFF (%)	Average	74	55
	Standard Deviation	2.4	12
	Range	68-76	44-73
η (%)	Average	9.5	6.3
	Standard Deviation	0.4	1.6
	Range	8.7-10.1	4.3-8.6

NOTES: 1. Measured at 25°C under AMO Conditions.

2. Cast Silicon "A": 3 ohm-cm
   Cast Silicon "B": 0.5 ohm-cm

3. Number of Samples: "A" - 10
   "B" - 5

TABLE 22

SHORT CIRCUIT CURRENT DENSITY OF
HEM CAST SOLAR-CELLS FROM BSF PROCESS

	CAST SILICON "A"	CAST SILICON "B"	CAST SILICON "C"	CONTROL
·AVERAGE	32.7 (32.1)	29.3 (29.3)	30.9	35.1
STANDARD DEVIATION	0.4 (0.7)	0.7 (0.4)	0.7	0.5
RANGE	32.2-33.5 (30.6-32.8)	28.3-30.4 (28.9-29.8)	29.6-31.5	34.5-35.7

NOTE: 1. Measured at 25°C under AMO conditions.

     2. Cast Silicon "A":   3   ohm-cm   1-852 Series (18 cells)
                    "B":   0.5 ohm-cm   1-860 Series (10 cells)
                    "C":   0.5 ohm-cm   1-856 Series (5 cells)

     3. Parenthesis numbers for the cells containing polycrystallinity.

     4. Units: mA

G. SILICON ON CERAMIC (SOC) SOLAR CELLS

1.0 SOLAR CELL FABRICATION

The SOC substrates were cleaned first in organic solvents and baked in a oven (set at 120°C in N_2 atmosphere) overnight. Immediately after removing from the oven, a standard diffusion procedure was applied to form a junction. After removal of the diffused oxide, a back contact metallization was applied by evaporation of metals (Ti-Pd-Ag in sequence) on the whole back area, followed by heat treatment at 600°C for about 10 minutes to form the proper ohmic back contact. Several attempts were tried to fill the opening of the slots in the substrates; by

(1) Solder dipping

(2) Squeeze-in of silver paste, followed by baking, and

(3) Filling with indium solder.

First method was not successful since difficulty in wetting of the solder inside the slots was experienced. Second method was also not promising because discontinuity of the silver was observed after baking typically in a furnace set at 300°C. Finally, indium solder (indium; tin = 1:1) was successfully filled in the slots by applying the solder to the back while heating the cells on a hot plate. Observation of a cross-section of the slots indicated that the slots were well filled with the solder, assuring a good contact to the back side of silicon. Front contact metallization was done by conventional metal shadow masking techniques. Bowing of the substrates caused a problem of metallization smearing and made it

difficult to get cells of good active areas (>90%). Measured active areas were in the range between 80-85% depending on the degree of warpage of the substrates.

Finally, the periphery of the cells were defined by using waxing and etching methods. Mesa solar cells were made as large as possible, resulting in an average area of about 15 cm^2. Mechanical yield of the solar cells is expected to be good if proper front contact metallization techniques are developed. It was difficult to apply metal shadow metal masking techniques since breakage happened during the tightening step. NOTE: In one batch three out of eight starting substrates were broken in this step and no breakage occurred after that, indicating about 60% yield.

An effort to reduce series resistance was carried out by forming a P+ layer on the back side of the SOC substrate. A thin layer of aluminum (about 8000Å) was evaporated first on the back and a P+ layer was formed by alloying in the diffusion step. Diffusion mask on the back was not necessary since aluminum layer will provide heavily doped P-layer on the back. Following the standard diffusion process, diffusion oxides from back and front were removed by dipping in dilute HF and standard metallization and AR coating process, was followed thereafter.

Four-point probe measurement showed resistivity of about 1 ohm-cm with P-type conductivity. Minority carrier diffusion lengths of the bulk SOC by SPV method were in the range between 20-40 μm. [See reference (10) for the detailed description on SOC process.]

2.0 SOLAR CELL PERFORMANCE AND CHARACTERIZATION

Characteristics Under Illumination

First batch of standard cells was a trial run in which most of the cells were wasted, except for a few in establishing a reliable process adaptable to these substrates.

The second batch was successfully carried out to provide reliable cell performance data. Solar cell parameters from the first two batches were measured under AMO conditions at 25°C, with individual cell data appearing in the Third Quarterly Report (6). Good performance of the control cells from both batches strongly indicates that there is no cross contamination of the impurities. Table 23 is the summary table of the SOC cells (second batch) performance. An average efficiency of about 6% was obtained in the relatively large area cells (15 cm² average). If the improved active area was achieved by using other metallization techniques, such as photoresist method, the average efficiency would have increased. SOC solar cells generally showed slightly low curve fill factor, an average of 60%, which seems to be due to the combination of both shunting and series resistance problems. Work has been in progress to improve the series resistance problems by forming P-layer in the back and this process is described in the previous section. Five (5) solar cells were fabricated from this process and their individual electrical data is shown in reference (13). Summary of the cell parameters are given in Table 24 and slight improvement in curve fill factor was noticed. An average CFF was about 66%, with

a range between 64-69%. However, there was no significant improvement in open circuit voltage. The CFF of the SOC cells is still considerably low compared with the controls and this seems to be due to high series resistance; an average series resistance was approximately 3.0 ohm-cm^2.

Effect of Back Metallization Coverage on Series Resistance and CFF

High series resistance could be due to the small opening of the slots in the back of the SOC substrate (around 30-40% of the total area). Thus an experiment was performed to see the effect of back metal coverage on series resistance (or curve fill factor) using single crystalline silicon. Back contact metals (Ti-Pd-Ag) were evaporated using metal show mask of various openings; 35, 50, 70, 85 and 100%. Individual cell performance data is given in reference (13) and summary of curve fill factor and series resistance is given in Table 25. The curve fill factor did not clearly indicate the effect of series resistance since shunting effects were combined in CFF. However, there is a tendency to decrease CFF as the back metal coverage is decreased. Separate measurement also indicates that series resistance increases as the metal coverage decreases. The series resistance was measured by using the method described by Handy (11), in which the current-voltage characteristics of a solar cell are measured at three different light intensities.

Dark I-V Characteristics

The characteristics of all the cells were measured using the dark I-V plotter. A typical good cell was selected for point-by-point measurement and results are plotted in Figure 40. The saturation current (I_o) and "A" factor of the SOC cell were about 10^{-7} A/cm^2 and 2, while those

of the controls were 2×10^{-9} A/cm^2 and 1.6, respectively. Since a cell
of larger area generally shows a higher degree of shunting this might
not be the proper way to make a direct comparison of both SOC and the
control cells. Series resistance problem of the SOC cell was also
noticed from the characteristics at high bias conditions (forward
V_B >0.6 volt).

Spectral Response

Absolute spectral responses (A/W) of SOC solar cells were measured
using a filter wheel set-up described in Appendix V-A. A typical
response curve is given in Figure 41. Effect of low lifetime of
the minority carriers is indicated at long wavelength response.

Minority Carrier Diffusion Length

Minority carrier diffusion lengths were measured using the SPV method
for the bulk and the short circuit current method for the finished
solar cells. Detail measurement techniques are discussed in Appendix
V-B. The exposed beam size (monochromatic) on the bulk sample was about
3 mm in diameter yielding diffusion length calculated to be in the range
between 20-40 μm. Short circuit current method also indicated similar
results.

Photoresponse by Small Light Spot Scanning

Nonflat surface feature of SOC substrate and noise problem prevented these
cells from obtaining reliable data at present.

Defect Study

The SOC substrates were sectioned and potted to see the crystallographic details at the cross-section of the substrates. After the final polishing using 0.2 μm alumina powder the polished surface was etched in Sirtl etch or a planar etch for about a minute. (Note: Original polished surface was not free from scratches). Planar etched surface seems to reveal better structural details than those with the Sirtl etch. Thus, the discussion is based on the results from the planar etch. Figure 42 is the microscopic pictures of the cross-section, silicon bridging ceramic slots in (a) and showing parallel twins in (b).

The main purpose for the sectioning of the substrate was to see if any grain boundaries existed parallel to the surface of the substrate, which might introduce the high series resistance problem. However, no such grain boundaries have been found so far. A number of parallel twin boundaries were observed, in Figure 42 (b), extending from the bottom to the top surface. A surface inclusion was also detected in Figure 43, whose identity is not clear at present.

FIGURE 40

DARK I-V CHARACTERISTICS OF A SOC SOLAR CELL
(Standard Process) AT R.T.

x: Control No. 15 (area 4 cm²)
o: SOC Cell No. 161-9 (area 12.5 cm²)
—:   Forward Characteristics
---: Reverse Characteristics

CURRENT DENSITY, (A/cm²)

VOLTAGE, (VOLTS)

-108-
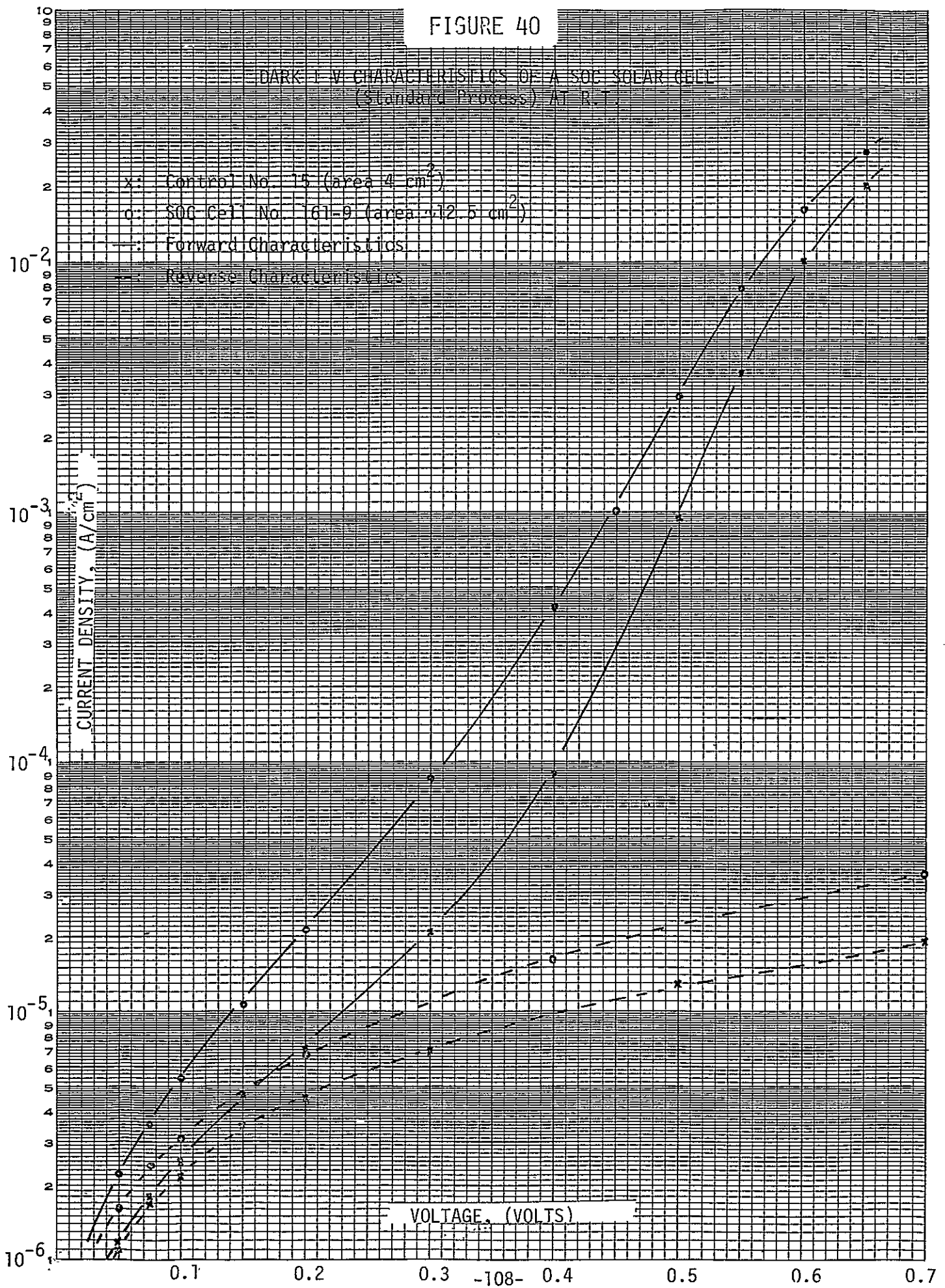
FIGURE 41

SPECTRAL RESPONSE OF A SOC SOLAR CELL
(Standard Process)

OCLI OPTICAL COATING LABORATORY, INC.

15251 E. DON JULIAN ROAD
CITY OF INDUSTRY, CA 91746
TELEPHONE (213) 968-6581

ABSOLUTE SPECTRAL
RESPONSE

SAMPLE IDENTIFICATION

x: Control
o: Cell No. 159-7

DATE:

SPECTRAL RESPONSE (A/W)

WAVELENGTH (MICROMETER)

FIGURE 42

CERAMIC
SUBSTRATE
(a)
CERAMIC
SUBSTRATE

CERAMIC
SUBSTRATE

(b)
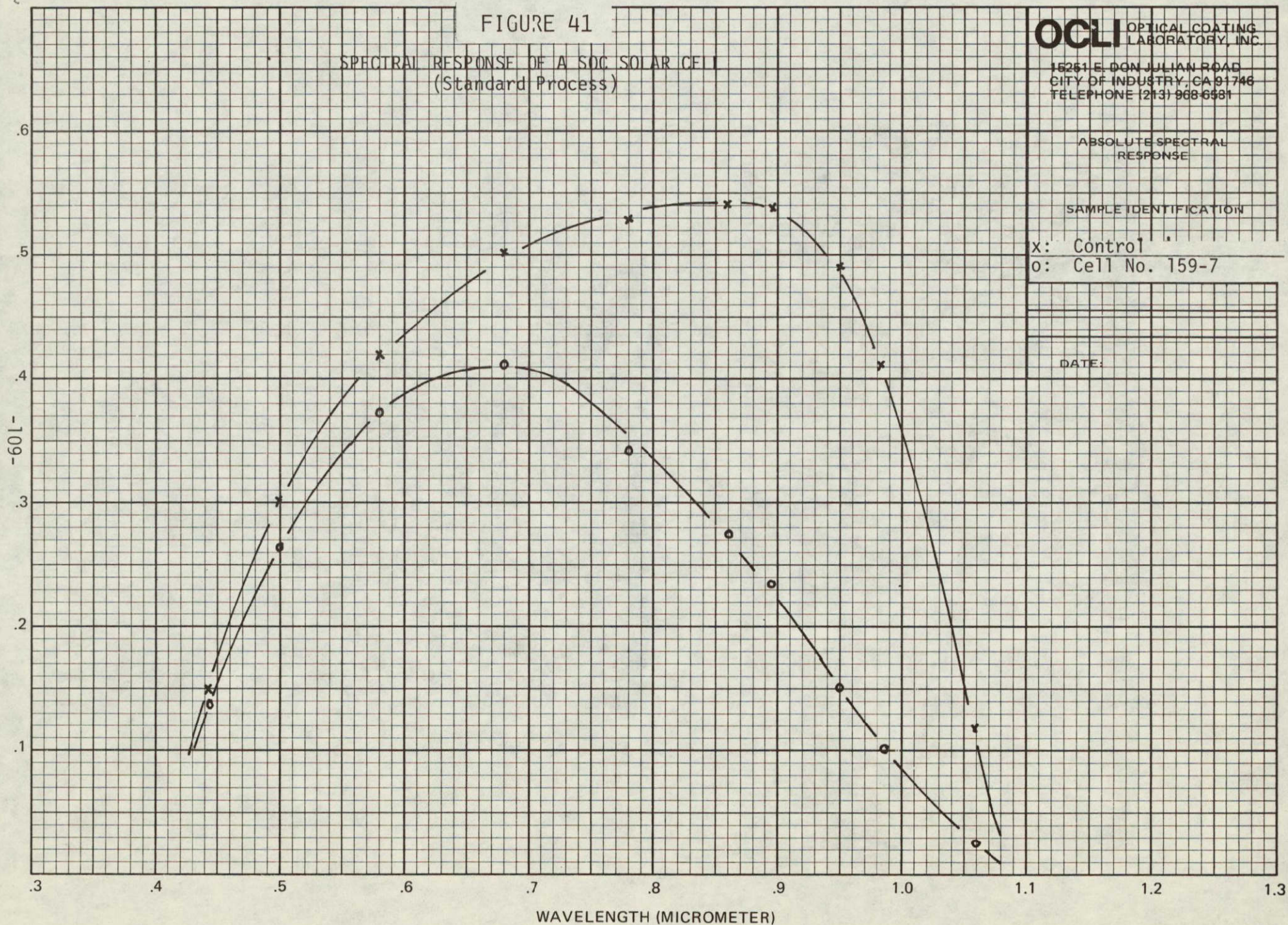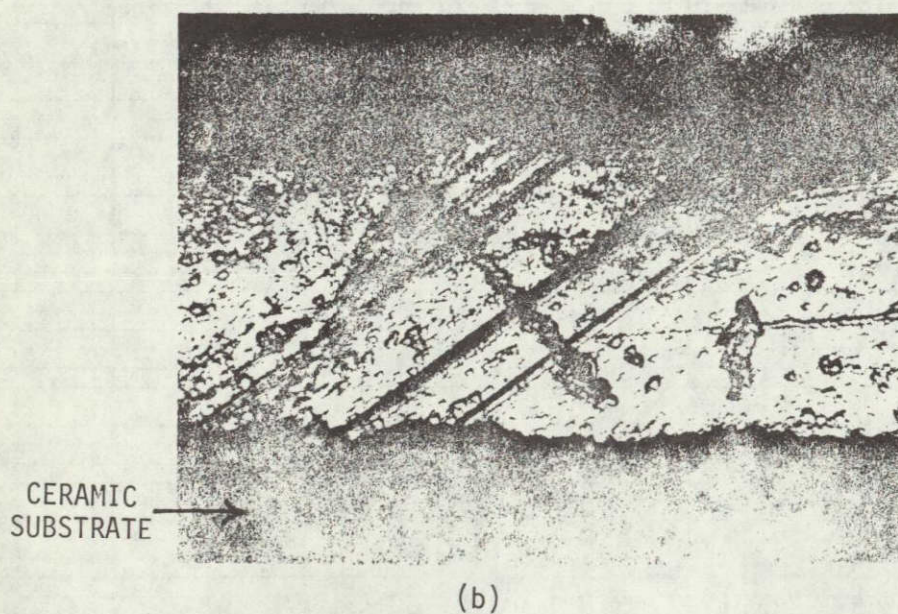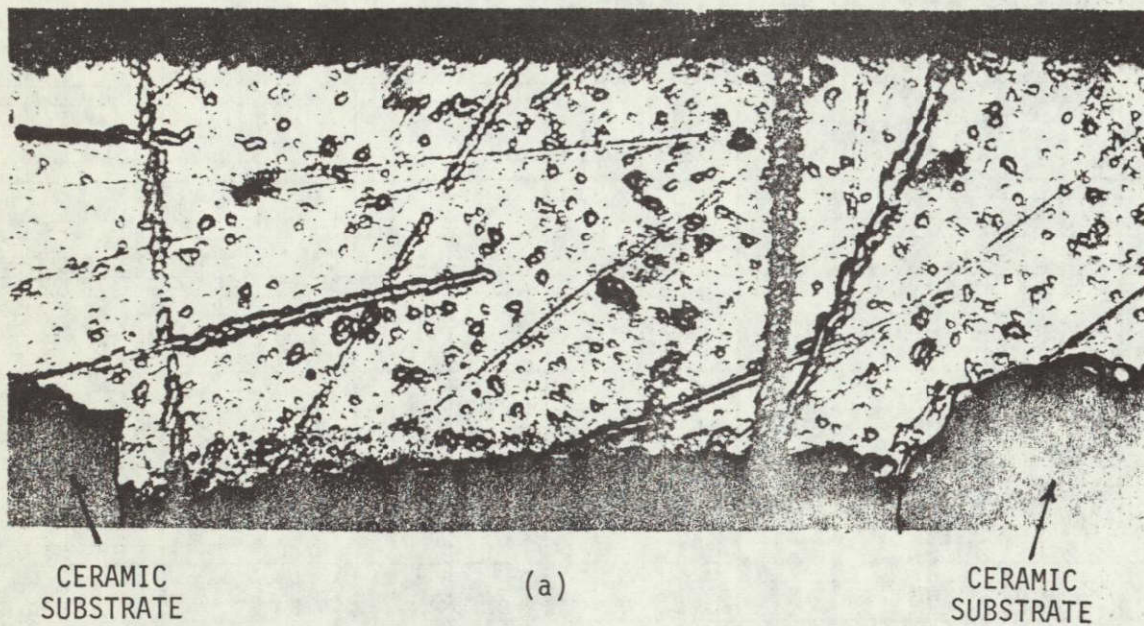
MICROSCOPIC PICTURES OF CROSS-SECTIONS OF SILICON ON CERAMIC
FOLLOWING MECHANICAL POLISHING AND CHEMICAL ETCHING
(200X Magnification)

(a) A cross-section bridging ceramic

(b) A cross-section showing parallel twins

-110-

FIGURE 43

A SURFACE DEFECT FOUND IN A SOC SUBSTRATE
(200X Magnification)

-111-

TABLE 23

SUMMARY OF PARAMETERS OF SOLAR CELLS
FABRICATED FROM SOC; STANDARD PROCESS

		SOC	CONTROL
V_{OC} (mV)	Average	547	589
	Standard Deviation	3.7	4
	Range	541-553	581-592
J_{SC} (mA/cm^2)	Average	24.1	33.8
	Standard Deviation	1.4	0.8
	Range	22-26.3	32.4-34.8
CFF (%)	Average	60	72
	Standard Deviation	6	3
	Range	52-69	67-77
η (%)	Average	5.9	10.6
	Standard Deviation	0.6	0.5
	Range	5.1-6.8	10-11.3

NOTE: 1. Measured Under AMO Condition.

        2. SOC Solar Cells:

            Average Cell Size: 15.1 cm^2

            Number of Cells Evaluated:. 7

            Active Area: 80-85%

            AR Coating: SiO

TABLE 24

SUMMARY OF PARAMETERS OF SOLAR CELLS
FABRICATED FROM SOC: BACK P+ PROCESS

PARAMETERS	AVERAGE	STANDARD DEVIATION	RANGE
V_{OC}, mV	537	5.4	531-544
J_{SC}, mA/cm^2	23	2.1	20.5-26.3
CFF, %	66	2.4	64-69
n, %	6	0.6	5.5-6.9
R_s, ohm-cm^2	3.3	0.4	2.7-3.8

NOTES: 1. R_s; series resistance

2. Wide variation in J_{SC} is partly due to the variation in front contact coverage

3. Measured under AMO condition

4. SOC Solar Cells:

   Average Cell Size: 13.6 cm^2
   No. of Cells Evaluated: 5
   Active Area: $\sim$80-85%
   AR Coating: SiO

TABLE 25

Effect of Back Metallization Coverage in Single Crystalline
Solar Cell on Curve Fill Factor and Series Resistance

PERCENTAGE BACK METAL COVERAGE		CFF, %	R_S, OHM-CM^2	NO. OF SAMPLES
100	Average	74	0.8	2
	Range	70-77	0.7-0.8	
85	Average	74	1.0	3
	Range	74-75	0.8-1.2	
70	Average	71	1.6	2
	Range	71	1.2-2.0	
55	Average	75	1.2	4
	Range	73-77	0.9-1.3	
35	Average	72	1.8	3
	Range	71-72	1.3-2.1	

NOTE: Metallization Ti-Pd-Ag

R_S: Series Resistance

-114-

H.   CONTINUOUS CZOCHRALSKI GROWTH (HAMCO)* SOLAR CELLS

1.0   SOLAR CELL FABRICATION

Six ingots, 4 inches in diameter, were grown from the first 100 Kg
throughput run at HAMCO. The ingots are identified in numerals.
1 through 6 in order of growth sequence and the second identification,
the letters (T,M,B), following the numerals, refer to the relative
position in each ingot from which the sample was taken; top, middle,
and bottom, respectively. The samples were quadrant silicon sections of
about 1-1 1/2" in length and they were sliced to wafers (18 mils in
thickness) using an ID saw. Wafers were cut to 2x2 cm blanks and the
blanks were thinned down to about 12-13 mils using chemical etching in
planar etch solution.

Of the twelve sections delivered to OCLI, five sample sections, 2-M,
2-B, 3-B, 4-B, and 6-M, consisted of polycrystalline silicon. Resistivity
was measured using four point probe, indicating 1-3 ohm-cm, with
P-type conductivity. Minority carrier diffusion length of the single
crystalline wafers (1-T, 1-M, 2-T, 3-T, 4-T, 5-T, and 6-T) was in the
range between 100-200 µm from SPV measurement, showing a tendency
for decreased diffusion length as the number of ingot growth increased.
Polycrystalline wafers showed diffusion lengths in the 20-50 µm range.
*[See reference (12) for the details of Hamco's continuous Czochralski
process.]

The first group of the blanks (2x2 cm) were processed by a standard

sequence, which is described in Appendix III-A. The mechanical yield

obtained was similar to that for conventional Czochralski silicon

(over 90%). After evaluation of these standard solar cells, blanks

were selected from the best section and worst section to fabricate

BSF solar cells using the procedure described in Appendix III-B.

The electrical performance of these cells are discussed in the following

section.

2.0   SOLAR CELL PERFORMANCE

Characteristics Under Illumination (AMO)

Solar cell parameters from the two batches, standard and BSF process,
were measured under AMO conditions at 25°C. [See Appendix IV for AMO
solar simulator and measurement description.] Individual cell parameters
are given in reference (13) and Table 26 summarizes the parameters of
standard solar cells from various ingot sections. Figure 44 is a
plot of efficiency versus ingot sections, indicating an average
efficiency of the top section of the ingots (single crystalline)
decreases approximately one percent by increasing ingot number
from one to six (range 10-11.2%). Solar cells from polycrystalline
sections showed considerably lower efficiency than those of the single
crystalline cells, showing a range of average efficiency between 7.5%
and 9.2%.

Solar cells from the BSF processes showed lower performance than the
standard cells, mainly due to the shunting problems from the BSF process.
Note; Most of the control cells showed the same problem. No reliable
data are available from these cells at present.

Dark I-V Characteristics

The forward characteristics of all the standard solar cells were obtained using a dark I-V plotter. A typical good cell was selected for point-by-point measurement and results are plotted in Figure 45. The saturation current (I_o) and "A" factor of the single crystalline Hamco cells were about 10^{-8} A/cm^2 and 1.7, while those of the poly-crystalline Hamco cell were 10^{-7} A/cm^2 and 1.7, respectively. Higher I_o of the polycrystalline cell is mainly due to the lower minority carrier lifetime of the cell. Control cells showed lower I_o and "A" factor values than Hamco cells, giving about 5×10^{-10} A/cm^2 and 1.4, respectively.

Spectral Response

Absolute spectral response (A/W) of the Hamco solar cells (standard process) were measured using a filter wheel set-up described in Appendix V-A. Typical response curves are given in Figure 46. A single crystalline Hamco solar cell (IT 11-1) showed higher response in overall wavelength range than the control cell. However, a polycrystalline cell (No. 3B6) indicated strongly the effect of low lifetime by showing poor response at long wavelength region. It is also interesting to point out that a Hamco cell from the top section of the last grown ingot (Cell No. 6T22) showed considerably lower response than the control, which could possibly be due to the impurity contamination in crystal growth process. Results of diffusion length measurement of these cells are given in the next section.

Minority Carrier Diffusion Length

Minority carrier diffusion lengths were measured using the SPV method for the bulk and short circuit current method for the finished solar cells. Detailed measurement techniques are discussed in Appendix V-B. Single crystalline Hamco solar cells showed ranges of the diffusion length between 80 and 200 μm and 20-30 μm for the polycrystalline solar cells. This is similar to the bulk SPV results in section 1.0 and the diffusion length of the single crystalline cell showed again a tendency to decrease as the number of grown ingot increases. A solar cell from the top section of the first grown ingot (Cell No. IT11-1) showed Le of about 200 μm, while Le of a solar cell from the last grown ingot (Cell No. 6T22) indicating about 80 μm. Le of the control cells (C-2 and C-4) were about 170 μm.

Photoresponse by Small Light Spot Scanning

Localized photoresponse of the solar cells were obtained using a small light spot scanning technique. Detailed descriptions on measurement techniques and procedures are given in Appendix V-C. Typical results of scanning Hamco solar cells, a single crystalline cell (Cell No. IT11-1) and a polycrystalline cell (No. 6M22), is given in Figure 47. The single crystalline cell, which is the same cell used for spectral response measurement, showed higher response than a control cell. The polycrystalline cell revealed a number of electrically active boundaries.

FIGURE 44

Efficiency Versus Ingot Growth Sequence (Standard Process)

-120-
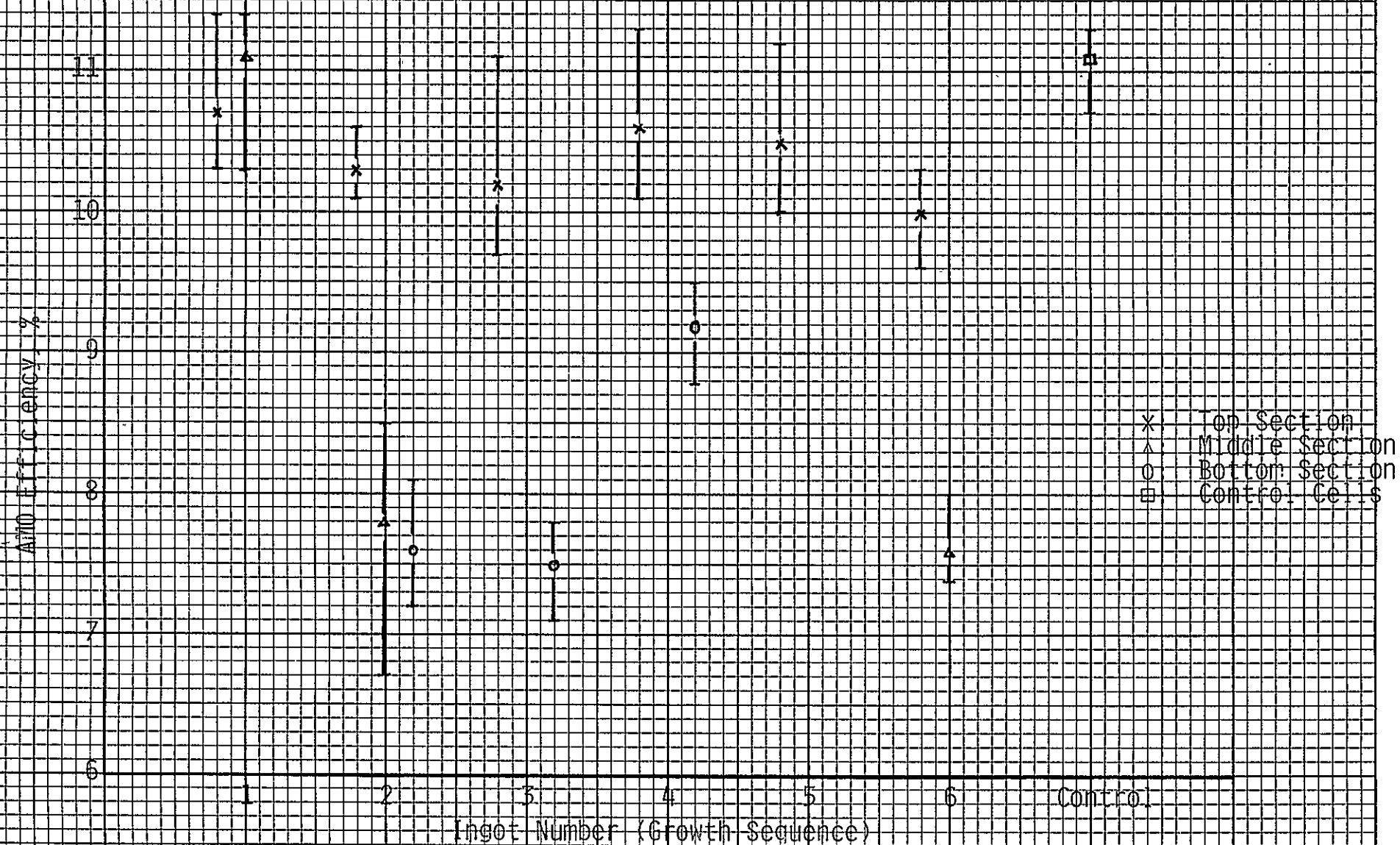
FIGURE 45

Dark I-V Characteristics of Lidrco
Solar Cells (Standard Process) at R.T.

Forward Characteristics
Reverse Characteristics
x: Control Cell No. C-5
o: Cell No. 1M1 (Single Crystalline)
△: Cell No. 6M22 (Polycrystalline)

Current Density, (A/cm²)

Voltage, (Volts)
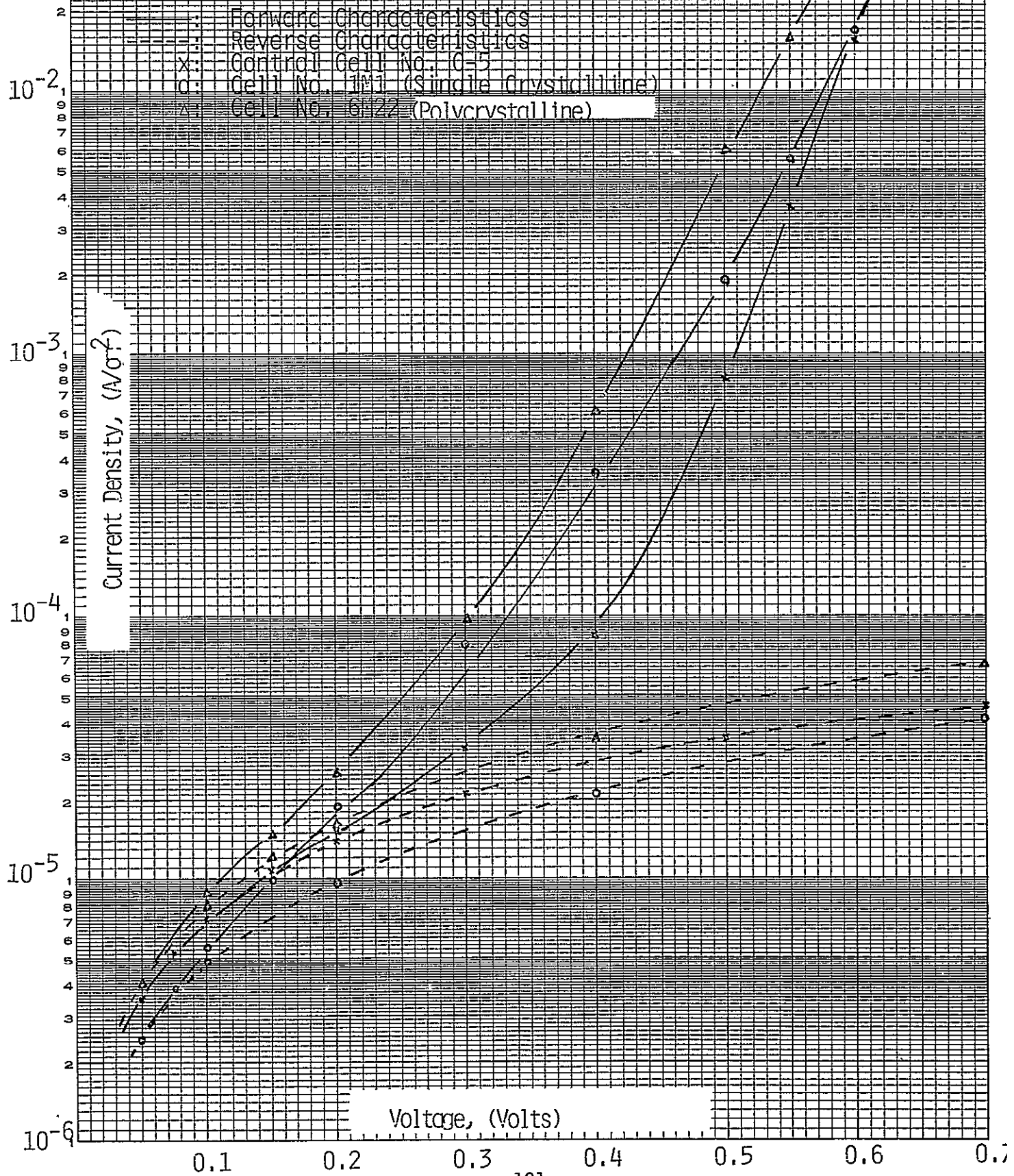
FIGURE 46

Spectral Response of Hamco Solar Cells
(Standard Process)

FIGURE 47

Small Light Spot Scanning of Hamco Solar Cells
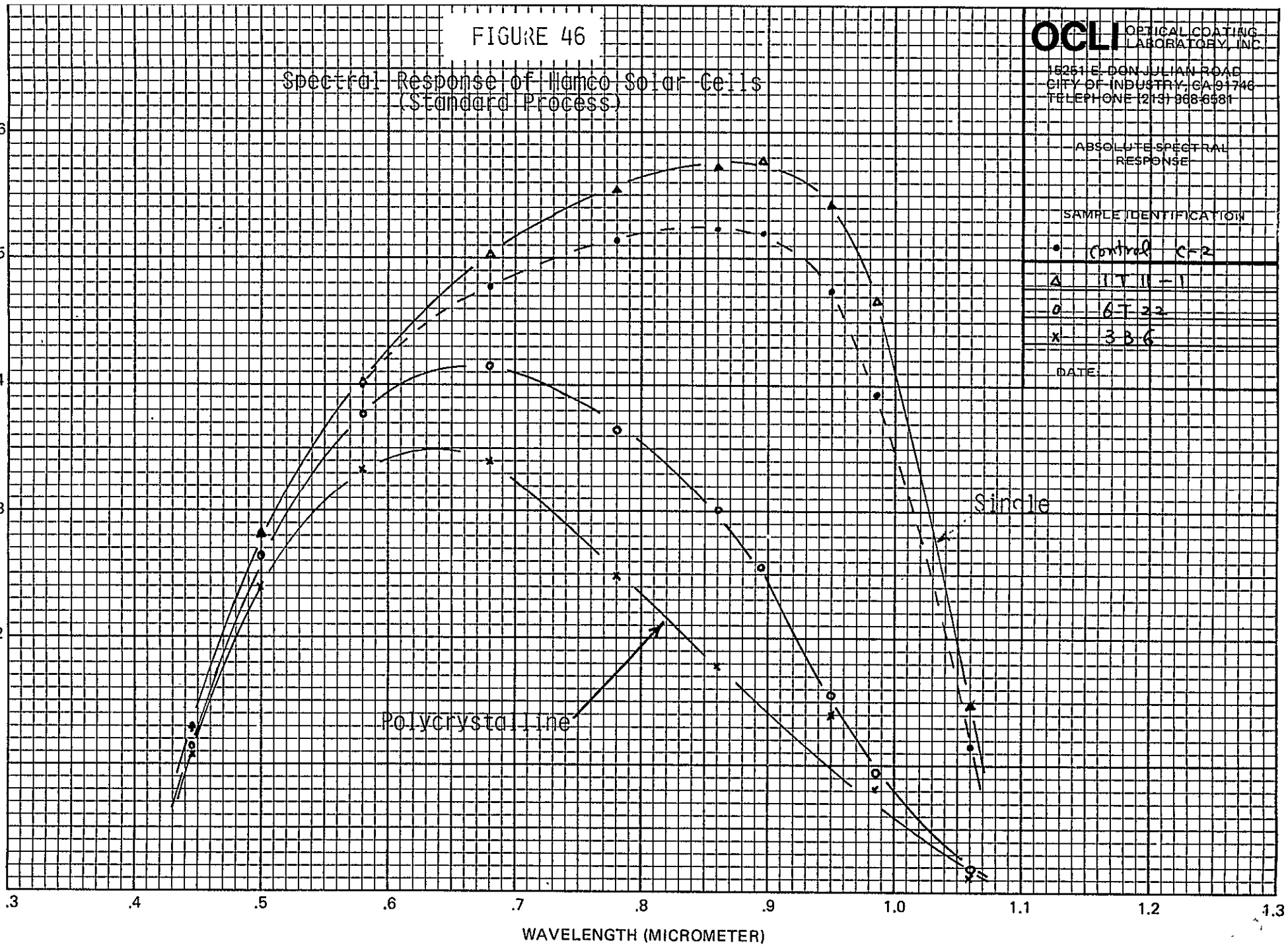
Cell No. 1-11-1

Control Cell No. C-4

Cell No. 6M22 (Poly)

Gridlines

|← 6 mm →|

Relative Photoresponse

Distance

-123-
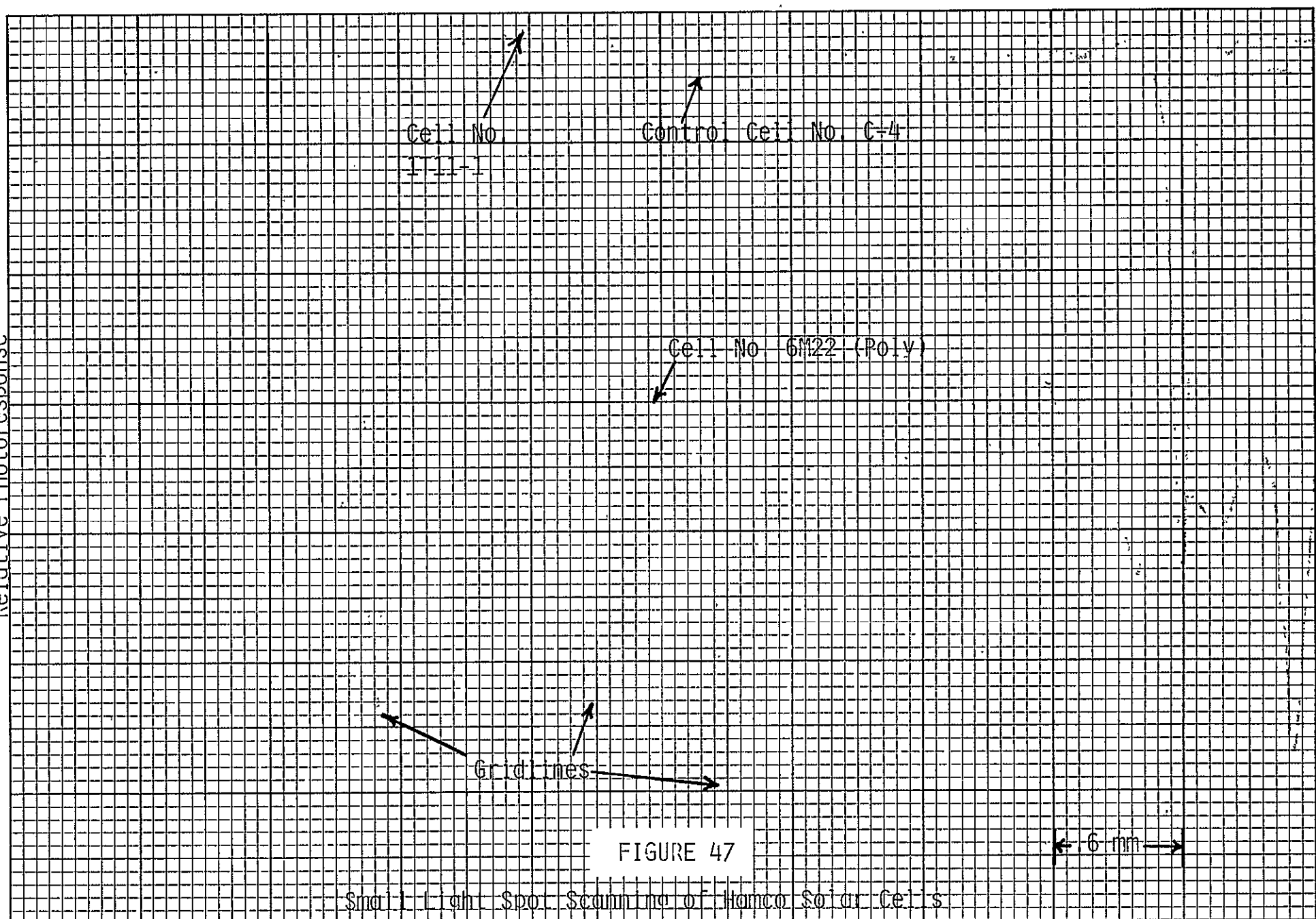
TABLE 26

SUMMARY OF PARAMETERS OF SOLAR CELLS FABRICATED FROM HAMCO CONTINUOUS CZOCHRALSKI WAFERS; STANDARD PROCESS

PARAMETERS		INGOT IDENTIFICATION						
		1T	1M	2T	2M*	2B*	3T	3B*
V_{OC}, mV	Average	586	590	582	538	540	573	534
	Standard Deviation	5	2	2	3	6	2	4
	Range	579-594	587-592	580-585	534-542	532-546	570-575	528-538
J_{SC}, mA/cm^2	Average	33.9	34.0	33.6	27.7	26.7	32.8	26.6
	Standard Deviation	0.9	0.4	1.3	3.4	3.9	0.9	0.5
	Range	32.5-35.3	33.5-34.5	31.5-34.8	27-29	25-27.8	31.5-34.3	26-27.3
CFF, %	Average	72.7	74.5	71	70.5	71.5	72.8	71.2
	Standard Deviation	2.5	4	2.9	4	2.2	2	0.8
	Range	70-77	67-78	67-76	63-74	68-74	70-76	70-72
η, %	Average	10.7	11.1	10.3	7.8	7.6	10.2	7.5
	Standard Deviation	0.4	0.4	0.2	0.7	0.4	0.5	0.3
	Range	10.3-11.4	10.3-11.4	10.1-10.6	6.7-8.5	7.2-8.1	9.7-11.1	7.1-7.8
		4T	4B*	5T	6T	6M*		Control
V_{OC}, mV	Average	585	561	583	579	531		593
	Standard Deviation	4	3	3	3	4		3
	Range	580-589	558-565	578-586	576-583	526-537		590-596
J_{SC}, mA/cm^2	Average	33.5	29.7	32.9	32.2	26.9		33
	Standard Deviation	0.5	0.6	0.8	1.3	0.8		0.4
	Range	32.8-34.3	28.8-30.5	31.8-34	30.8-34	25.5-27.8		32.5-33.5
CFF, %	Average	73.2	74.2	74.2	72.3	71.8		77.6
	Standard Deviation	3	1.2	2.6	2.4	1.5		2.3
	Range	70-77	72-75	71-78	70-77	70-74		75-80
η, %	Average	10.6	9.2	10.5	10	7.6		11.1
	Standard Deviation	0.5	0.2	0.4	0.3	0.2		0.2
	Range	10.1-11.3	8.8-9.5	10-11.2	9.6-10.3	7.4-8.0		10.8-11.3

Notes: 1. Measured under AMO condition at 25°C.
2. Standard solar cells (2x2cm) with SiO AR coating.
3. *Polycrystalline Cells: 2M, 2B, 3B, 4B and 6M.

I.   SUMMARY OF FABRICATION AND PERFORMANCE OF STANDARD SOLAR CELLS

1.0   SOLAR CELL FABRICATION

Eight (8) unconventional silicon sheets of various growing techniques, namely EFG (RH), EFG (RF), RTR, Dendritic Web, Silso, HEM, SOC and Continuous CZ (Hamco), were processed to make solar cells using a standard process and other process modifications such as BSF etc.. The performance is summarized in the next section. First we will discuss the processing aspects. Three major areas of difficulties were experienced using conventional processing and measurement methods;

(1) Breakage of the silicon sheets at initial blank shaping step - (slicing), especially of thin and highly stressed sheets.

(2) In metallization, difficulties arose from non-flat and non-uniform thickness of the sheets. It was more difficult than usual to use either metal shadow masks or to apply photoresist by spinning. However, photoresist by spraying techniques could possibly adapt successfully to most of the sheet substrates.

(3) Measurement difficulties were mainly in control of cell temperature while measuring illumination characteristics, again because of mechanical irregularities in the sheets.

Besides these, there are some other areas of difficulties unique to a specific type of a sheet, i.e., removal of surface deposit (SiO) from dendritic web and keeping the ceramic substrates (for SOC) free from

moisture before high temperature treatment (absorbed moisture chipped silicon from the ceramic substrate at high temperatures, such as in diffusion etc.). Table 27 summarizes these processing difficulties experienced in solar cell fabrication and shows the mechanical yield (unbroken cells over initial starting blanks) obtained in the right hand column.

2.0   SOLAR CELL PERFORMANCE

Characteristics Under Illumination [Refer to Appendix IV for AMO
Simulator and Other Measurement Techniques]

Figure 48 is a summary of illumination characteristics (AMO at 25°C)
of solar cells made by standard processing. Parameters of interest
are J_{SC}, V_{OC}, CFF and η. Their average values (indicated by circles)
and ranges are shown in the figures for the various forms of silicon
sheets. The figure shows that cells from some sheets, such as Web, Silso
and HEM, showed cell efficiency close to that of the Czochralski controls
(an average efficiency of about 9-10% versus 11%). The sheet cells
generally gave wider ranges in efficiency than the controls, mainly because
of the wide range of CFF. The cells of low efficiency, such as RTR*, were
due to low values of the three other parameters. The low V_{OC} of the Web
cells was mainly due to the low doping level of the web substrates (about
20 ohm-cm).

Dark I-V Characteristics

Figure 49 shows a summary of dark I-V characteristics (room temperature)
measured by point-by-point from each type of the sheet cells. Dark I-V
characteristics of a solar cell can be expressed in a simple diode
equation (in top of the figure), where, "A" value indicates the degree
of deviation from the ideal diode charateristics.. The higher the "A"
value, the more significant the effect of shunting, space charge

*These RTR samples were supplied at a time when the ribbon processing
was well below the levels presently available.

recombination and series resistance. Ranges of the measured "A" values (measured at forward bias >0.4 volt) are given in the top of the figure; some ribbon cells give "A" values higher than three, suggesting severe shunting problems.

Ranges of saturation current (I_0 in the equation) is also given in the bottom figure. Roughly about two orders of magnitude difference between the sheets and CZ control was noticed and this is the main reason why V_{OC} of the unconventional sheets is considerably lower than those of the control (approximately 50 mV lower in average).

Spectral Response [Refer Appendix V-A for the description of the measurement techniques]

Figure 50 is a summary of plots of absolute spectral response; the dotted line for a CZ control and the remainder for the sheet cells. Solar cells from the sheets showed lower response than the control, especially in the long wavelength region (λ >0.6 μm), indicating shorter minority carrier diffusion length of the sheets compared with the control. However, some sheet cells, such as dendritic webs and cast silicon by HEM, showed the response comparable to that of the control.

Minority Carrier Diffusion Length [Refer to Appendix V-B for the
Detailed Description of the Measurement Techniques]

Figure 51 is a summary of the measurement of minority carrier

diffusion length of the various sheet forms; SPV method for the bulk

silicon and I_{SC} method for the finished solar cells. Average values

and ranges are given in the figure; dotted lines for the SPV method

(bulk) and solid lines for the I_{SC} method (finished cells). Most

of the unconventional sheets indicated diffusion lengths less than

80 µm, an exception being dendritic web. Generally the I_{SC} method

showed slightly lower average values than the SPV method. However,

it is difficult to determine at present whether the difference comes from

the process induced damage or difference in measurement techniques.

Figure 52 is the plots of AMO efficiency (dotted line) and short circuit

current density (solid line) versus minority carrier diffusion length.

Both J_{SC} and η drop fast at diffusion lengths below 50 µm. Some sheet

cells have two data points in the efficiency curve in which the lower

points represent efficiencies actually obtained and upper points indicate

potential efficiencies assuming that CFF can be improved to about

77-78%.

Defects and Their Influence on Cell Performance

The most common defects found in unconventional sheets are grain

boundaries (G.B.), twins and inclusions. Electrically active defect

sites, such as G.B., are expected to decrease I_{SC} and V_{OC} by reduction

in minority carrier lifetime, and inclusions, especially surface inclusions,

are likely to cause shunting problems, resulting in low V_{OC} and low maximum power available from the cells by reduction in CFF. Table 28 summarizes defects found in each type of unconventional silicon sheets. Their effect on solar cell parameters are given in the right hand column of the table.

FIGURE 48

A Summary of Illumination Characteristics of
the Solar Cells From the Unconventional Silicon Sheets

-131-
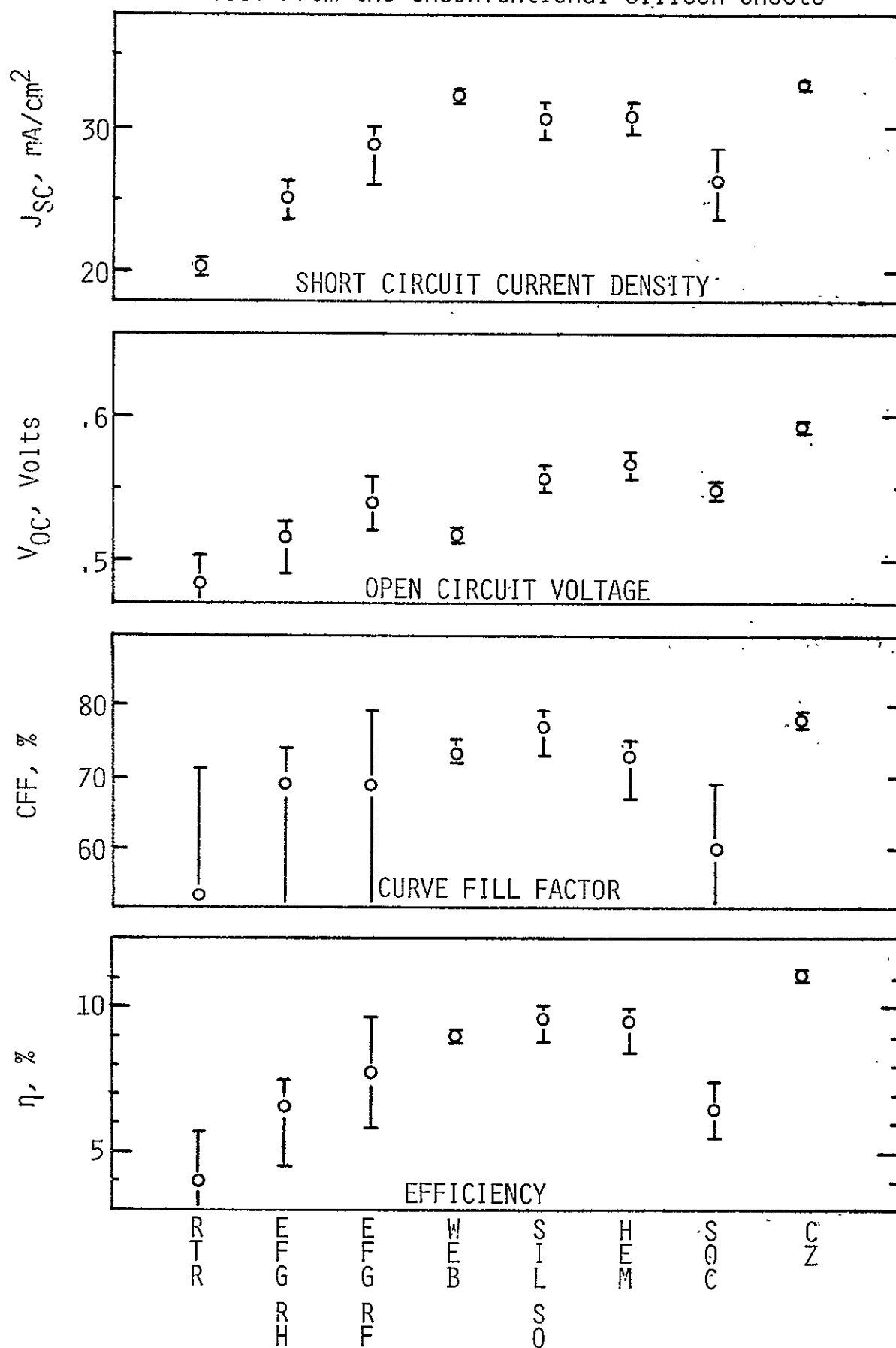
FIGURE 49

A Summary of Forward Dark I-V Characteristic
Parameters of Solar Cells From the Unconventional Silicon Sheets

$$I_D = I_0 \left(\text{Exp } \frac{qV}{AKT} - 1\right)$$
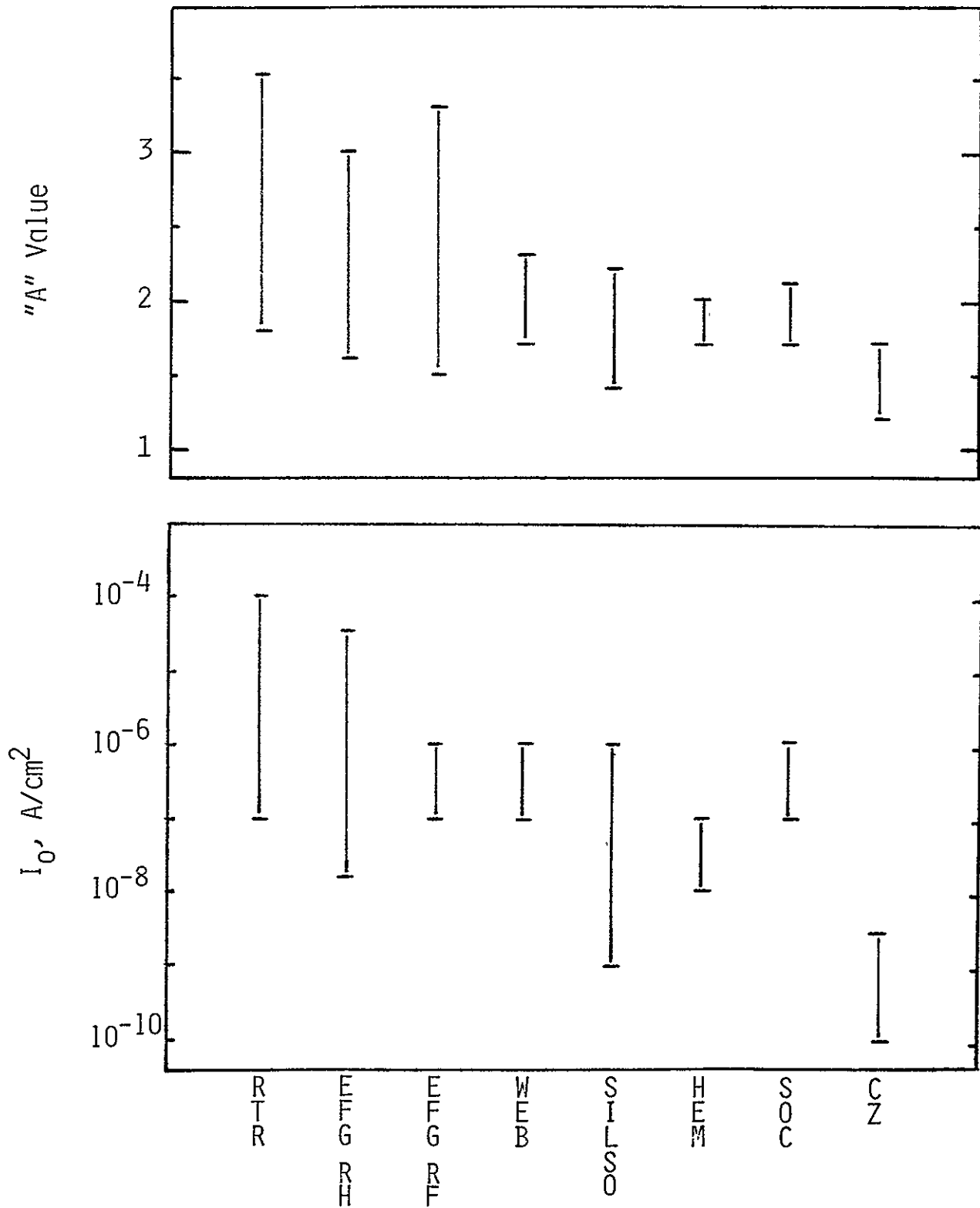
FIGURE 50

SPECTRAL RESPONSE OF SOLAR CELLS FROM UNCONVENTIONAL SHEETS

-133-
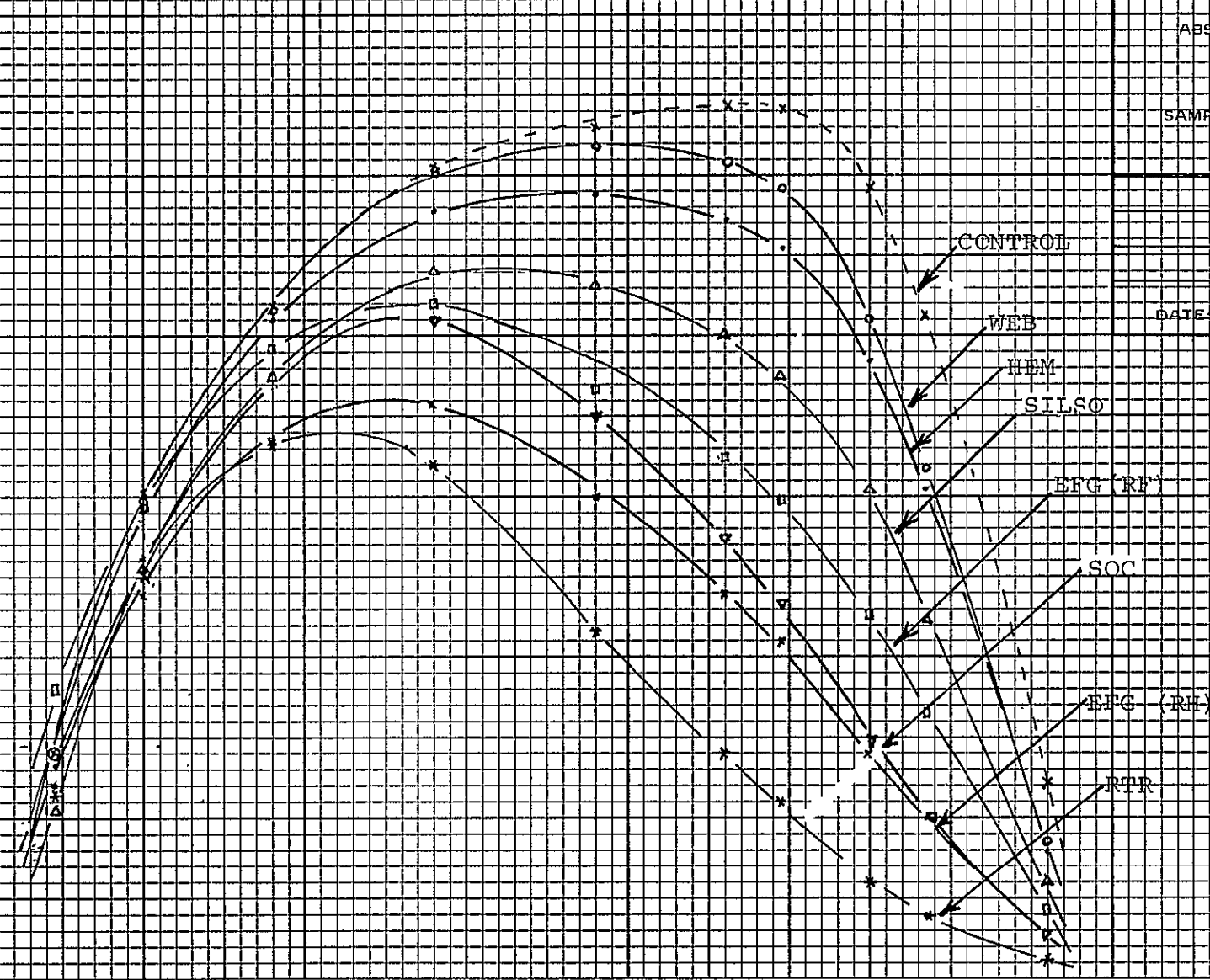
FIGURE 51

Minority Carrier Diffusion Length
of the Unconventional Silicon Sheets
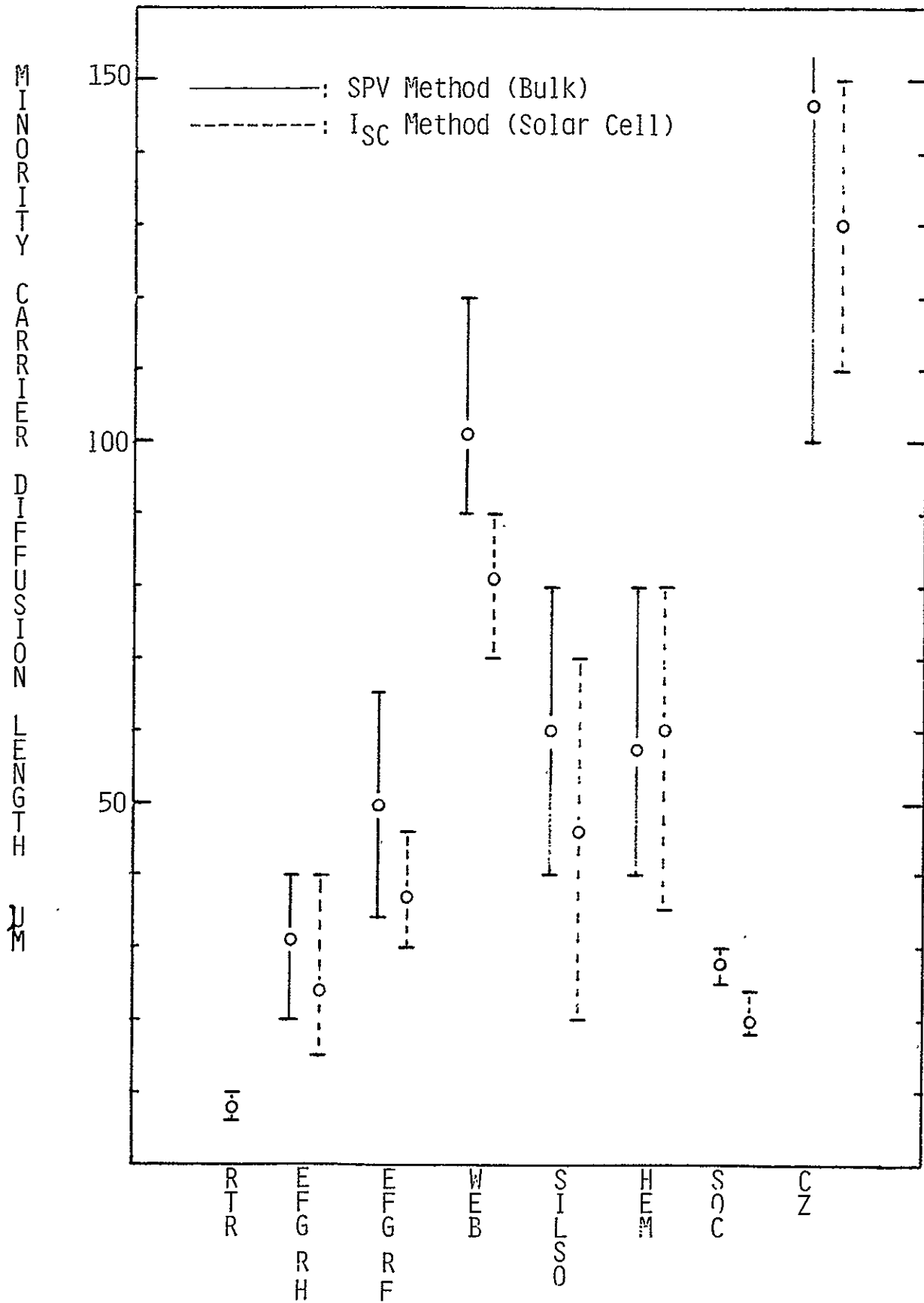
FIGURE 52

Efficiency and Short Circuit Current Density Versus Minority Carrier
Diffusion Length of the Unconventional Silicon Sheets
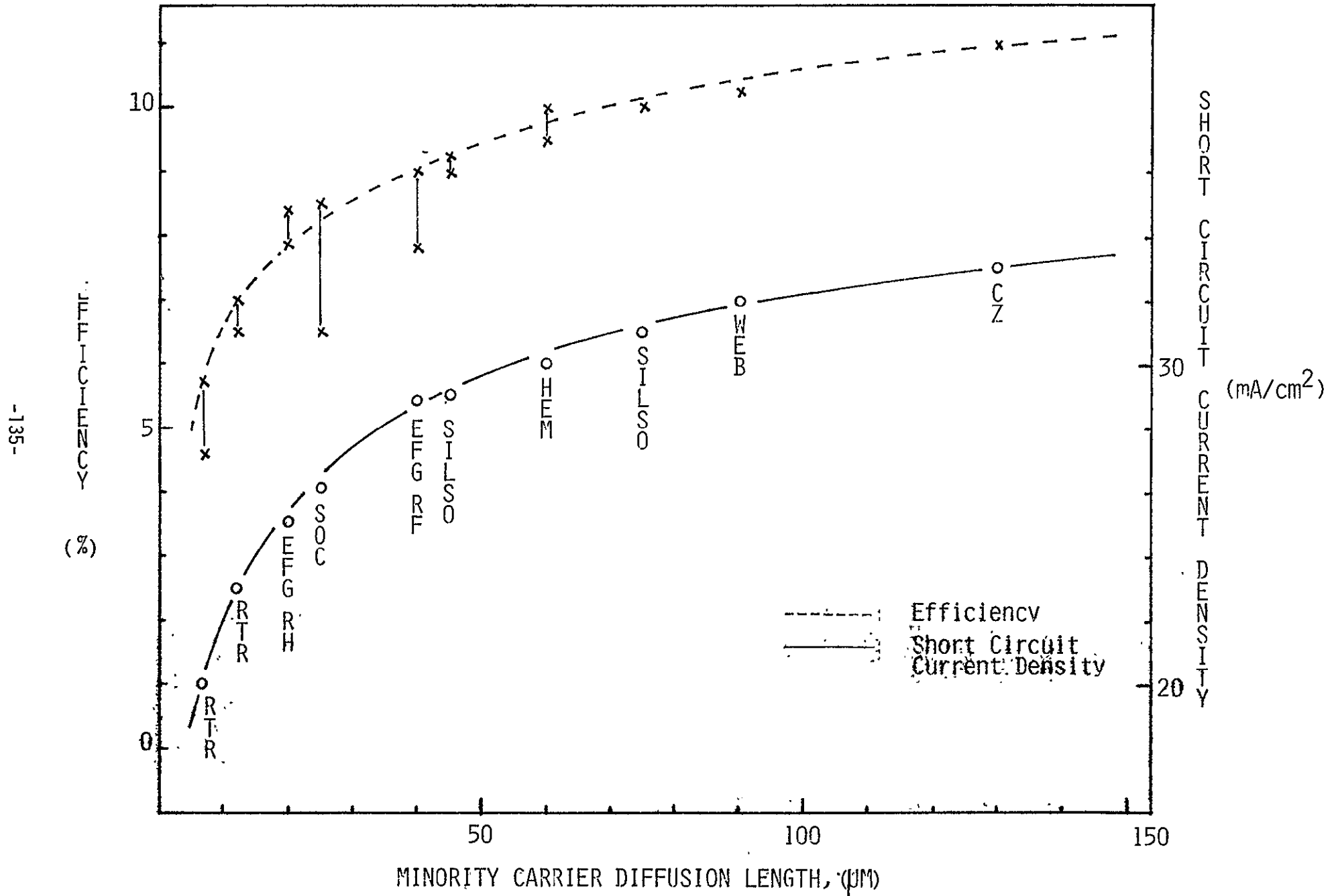
TABLE 27

PROBLEM AREAS RELATED TO STANDARD PROCESS

SHEETS	PROCESS	MECHANICAL YIELD (%)
EFG (RF and RH)	Metallization & Measurement; Non-Flat & Non-Uniform Thickness	55 (RF) 80 (RH)
RTR	Metallization & Measurement; Wavy Surface Handling; Fragile	50
DENDRITIC WEB	Removal of Surface Deposit (SiO) Handling; Fragile (Thin Web)	50* 90**
SILSO (WACKER) WAFER	No Major Problem	94
CAST SILICON BY HEM	No Major Problem	>90 .
SOC	Metallization & Measurement; Warpage & Back Slot Keep the Substrate Free From Moisture Before High Temperature Treatment	60
CONTINUOUS CZ (HAMCO)	No Major Problem	>90

* Thin webs, 5-6 mils
**Thick webs, 8-10 mils

TABLE 28

DEFECTS AND THEIR INFLUENCE ON CELL PERFORMANCE

	SHEETS	DEFECTS	CELL PERFORMANCE

R I B B O N S	RTR	G.B.
		Twins
		Stress Induced
		     Defects
			Low I_{SC};
			   + Contamination
			Low V_{OC}
			Low CFF

	EFG (RH & RF)	G.B. Twins Inclusions (SiC)	Low I_{SC} (EFG RH); + Contamination Low V_{OC} Low CFF
	DENDRITIC WEB	Twins	Low V_{OC}; Low Doping Level
C A S T	SILSO	G.B. Inclusions	Low CFF
	HEM	G.B. Inclusions Microcracks	Low CFF

C O A T E D	SOC	G.B.
		Twins
		Inclusions
			Low I_{SC};
			   + Contamination
			Low CFF; + High
			   Series Resistance

III. CONCLUSIONS AND RECOMMENDATIONS

Conclusions

The conclusions reached after analyzing the cell performance and other related physical measurements are as follows:

- Minority carrier diffusion length (Le) is the parameter limiting the solar cell efficiency. Figure 52 (in II-I) shows the measured cell efficiency, plotted as a function of the measured diffusion length .(Le) of various sheet forms. The lower Le-values led to the major losses (from reduced short circuit current), and were confirmed by corresponding decrease in long wavelength response in the spectral response measurement (see Figure 50).

- The causes of the reduced Le-values were grain boundaries, impurities (contaminants) and stress induced defects.

- Secondary losses resulted from lower V_{OC} or CFF, caused by shunting of the voltage barrier. These shunt paths were mainly due to surface inclusions from die material, crucible and growing atmosphere, etc.

- Some sheets have demonstrated their potential as future solar cell materials while others need improvement in sheet quality. Figure 48 compares the cell performances of various sheets.

- The low diffusion length, possibly combined with low resistivity (3 ohm-cm) values, prevented the BSF process used from having an effect.

- Some sheet samples gave difficulty in processing because of increased breakage caused by warpage and thickness variation; or from apparent high stresses in the sheets.

- The evaluation techniques used provided accurate and reliable information on sheet performance, and self-consistent results were obtained from the various measurement techniques used.

- Considering the variety of silicon material forms investigated, the evaluation method described in this report appears to be the most effective way to characterize the sheets. Any method not giving photovoltaic behavior directly, must rely on a combination of some physical measurements and their combination with a theoretical device model for which the pertinent material parameters are known and can be included in the model with confidence.

Recommendations

Evaluation of the sheets suggested the following:

- Improvements of sheet quality from sheet producer are required to improve solar cell efficiency. Areas of interest are:

  1. Better control of inclusions and geometry of the sheets,
  2. Reduction in impurity contaminations and mechanical stresses in the sheets, and
  3. Increase in grain size for poly sheets.

NOTE: Specific suggestions for improvement of particular sheet forms. can be obtained by study of the report details.

- Efforts to improve solar cell efficiency are suggested in the area of solar cell processing. Areas of interests are:

    1. Grain boundary passivation by preferential diffusion-down grain boundaries, hydrogenation of grain boundaries, etc.

    2. Optimization of diffusion process in consideration of front contact design and grain size, etc.

    3. Development of process and evaluation techniques pertinent to a specific type of sheet material.

- Two-way cooperation between sheet producers and solar cell processors is required to achieve the overall goal of the LSA project.

IV.   <u>WORK PLAN STATUS</u>

Phase II of the program will extend Phase I with an

increase emphasis on improvement of solar cell efficiency

by process optimization and development of new process techniques

tailored to suit the specific sheet form.

V. REFERENCES

1. B. Authier, *"Novel Silicon Crystals and Method for Their Preparation"*, Patent File No. P2508803,3-43, Wacker-Chemitronic, Germany, September, 1976.

2. T.H. Distefano, et.al., *"Enhancement of Carrier Lifetime in Polycrystalline Silicon"*, Proceeding Workshop on Low Cost Polycrystalline Silicon Solar Cells, Southern Methodist University, Texas, May, 1976.

3. H.I. Yoo, et.al, *"Silicon Solar Cell Process Development, Fabrication and Analysis"*, JPL Contract No. 955089, First Quarterly Report, 1978, Optical Coating Laboratory, Inc.

4. F.V. Wald, et.al., *"Large Area Silicon Sheet by EFG"* JPL Contract No. 954355, Technical Report, Mobil Tyco.

5. H.I. Yoo, et.al., *"Silicon Solar Cell Process Development, Fabrication and Analysis"*, JPL Contract No. 955089, Second Quarterly Report, 1978, Optical Coating Laboratory, Inc.

6. H.I. Yoo, et.al., *"Silicon Solar Cell Process Development, Fabrication and Analysis"*, JPL Contract No. 955089, Third Quarterly Report, 1979, Optical Coating Laboratory, Inc.

7. A. Baghadi, et.al., *"Laser-Zone Growth in a Ribbon-to-Ribbon (RTR) Process"*, Technical Reports for the Large Area Silicon Sheet Task of the LSA Project, JPL Contract No. 954376, Motorola.

8. C.S. Duncan, et.al., *"Silicon Web Process"*, Technical Reports for the Large Area Silicon Sheet Task of the LSA Project, JPL Contract No. 954654, Westinghouse.

9. F. Schmid, et.al., *"Silicon Ingot Casting - Heat Exchanger Method Multi-Wire Slicing - Fixed Abrasive Slicing Technique"*, JPL Contract No. 954373, Technical Reports, Crystal Systems.

10. P.W. Chapman, et.al., *"Silicon on Ceramic Process"*, JPL Contract No. 954356, Technical Reports, Honeywell.

11. R.J. Handy, *"Theoretical Analysis of the Series Resistance of a Solar Cell"*, Solid State Electronics, 10, 765, 1967.

12. R.L. Lane, et.al., *"Continuous Czochralski Growth"*, Technical Reports for the Large Area Silicon Sheet Task of the LSA Project, JPL Contract No. 954888, Kayex Corporation, Hamco Division.

13. H.I. Yoo, et.al., *"Electrical Data Sheets for SOC and Hamco Solar Cells"*, These data sheets are available through the Large Area Silicon Sheet Task of the LSA Project, JPL Contract No. 955089. June , 1979.

APPENDIX I

Time Schedule

TIME SCHEDULE

TASK	MONTH												
	JUN	JUL	AUG	SEP	OCT	NOV	DEC	JAN	FEB	MAR	APR	MAY	JUN
1. PROCESS SHEET SAMPLES													
(a) 1/2 Samples → Cells													
(b) Analysis													
(c) Back Up Measurements													
(d) Test Alternate Process													
2. REPORTS													
(a) Monthly			▲	▲		▲	▲		▲	▲		▲	
(b) Quarterly					▲						▲		
(c) Semi-Annual								▲					
(d) Final													▲
3. INTEGRATION MEETING													

NOTE: The final reporting period has been incorrectly stated previously, please note revisions.

APPENDIX II

Abbreviations

ABBREVIATIONS

V_{OC}: Open Circuit Voltage

I_{SC}: Short Circuit Current

J_{SC}: Short Circuit Current Density

I_{SCR}: Short Circuit Current (Red Response) at Wavelength Above $\sim$.6 μm

I_{SCB}: Short Circuit Current (Blue Response) at Wavelength Below $\sim$.6 μm

CFF: Curve Fill Factor

η: Solar Cell Conversion Efficiency

Le: Minority Carrier Diffusion Length (D.L.)

I_{MAX}: Current at Maximum Power Point

V_{MAX}: Voltage at Maximum Power Point

P_{MAX}: Maximum Power Point

BSF: Back Surface Field

V_B: Bias Voltage

I_o: Diode Saturation Current

HEM: Heat Exchanger Method

EFG: Edge Defined Film-Fed Growth

SOC: Silicon on Ceramic

RTR: Ribbon-to-Ribbon

SPV: Surface Photovoltage

MLAR: Multi-Layer Anti-Reflective

R_s: Series Resistance

APPENDIX III

Description of Solar Cell Fabrication

A. Standard Process

B. Back Surface Field (BSF) Process

A.   STANDARD PROCESS

The first group of tests samples is subjected to a "standard process",
(which will be described in this section) to allow uniform evaluation
of all the different sheet forms.

After applying a diffusion mask on the back surface, the silicon blanks,
both the sheets and the controls, were loaded in a furnace, with 12"
temperature zone at 875° $\pm$ 1°C and oxidation was carried out in a dry
oxygen atmosphere for five minutes. Following the oxidation step,
(in the same furnace) slices were diffused for 20 minutes by passing
$POCl_3$-saturated oxygen gas and dry nitrogen gas (carrier gas) over
the blanks. Finally the boat loaded with these diffused blanks was
slowly pulled out of the furnace (manually within 10 minutes). After
removing the glassy-layers formed during the diffusion process, sheet
resistance was measured from selected samples, showing about 25 ohm/
square for single crystalline controls (1-3 ohm-cm, P-type).

Front and back contacts were applied by successive evaporation of
Ti, Pd and Ag in a vacuum chamber (pressure around 10^{-6} Torr) using
resistively heated coils as sources. Back contacts were applied first
using a metal shadow mask and a sintering step, (10-15 minutes at 600°C
in H_2 atmosphere) was followed to minimize the contact resistance at
the back metal-silicon interface. Front contacts were applied by
evaporation of metals through a metal shadow mask which had grid finger
density of four lines per centimeter. About 90% active area of the

solar cells was obtained after evaporation. The thickness of the evaporated front metals was 1000$\overset{\circ}{A}$ for Ti, 250$\overset{\circ}{A}$ for Pd and 4-6 μm for Ag, while the thickness of Ag in the back contact was around 2-3 μm. To minimize peeling of metal contacts during preliminary measurement of solar cell parameters (measurement without anti-reflective coating) a post metallization heat treatment was carried out at 400°C for 10 minutes in hydrogen atmosphere.

An anti-reflective coating was applied on the finished solar cells by evaporation of silicon monoxide in a vacuum chamber with pressure maintained at around 10^{-6} Torr. The thickness of the evaporated SiO_x layer was around 750°C with stoichiometric factor x close to one. Finally the solar cells with anti-reflective coating were sintered again at 500°C for five minutes in hydrogen atmosphere. A block diagram of this process is given in Figure III-1.

B. BACK SURFACE FIELD (BSF) PROCESS

Back surface field was provided by evaporation of a thin Al layer followed by screen printing of Al paste, and an alloying step at an elevated temperature ($\sim$800°C). This process step was added after removal of diffused oxides in the standard process. Back and front contacts (Ti, Pd and Ag) were evaporated after the alloying step. A sintering step (at 600°C) after metallization of back contact was not necessary in the BSF process since the alloyed layer in the back provided good ohmic contacts.

SOLAR CELL STANDARD PROCESS

Si Blank	Cut to size and clean
↓ ↓	
Surface Preparation	Chemical polishing in planar etch (remove $\sim$ 1.5 mils from each face)
↓ ↓	
Diffusion	875°C, $POCl_3$ - 5 Minutes Oxidation 20 Minutes Diffusion
↓ ↓	
Diffusion Glass Removal	
↓ ↓	
Contacts By Evaporation	Metal Shadow Mask - Ti / Pd / Ag
↓ ↓	
AR Coating By Evaporation	$SiO_x \sim 750\text{Å}$ ($x \sim 1$)
↓ ↓	
Sintering	500°C in H_2 - 5 Minutes
↓ ↓	
Solar Cell	

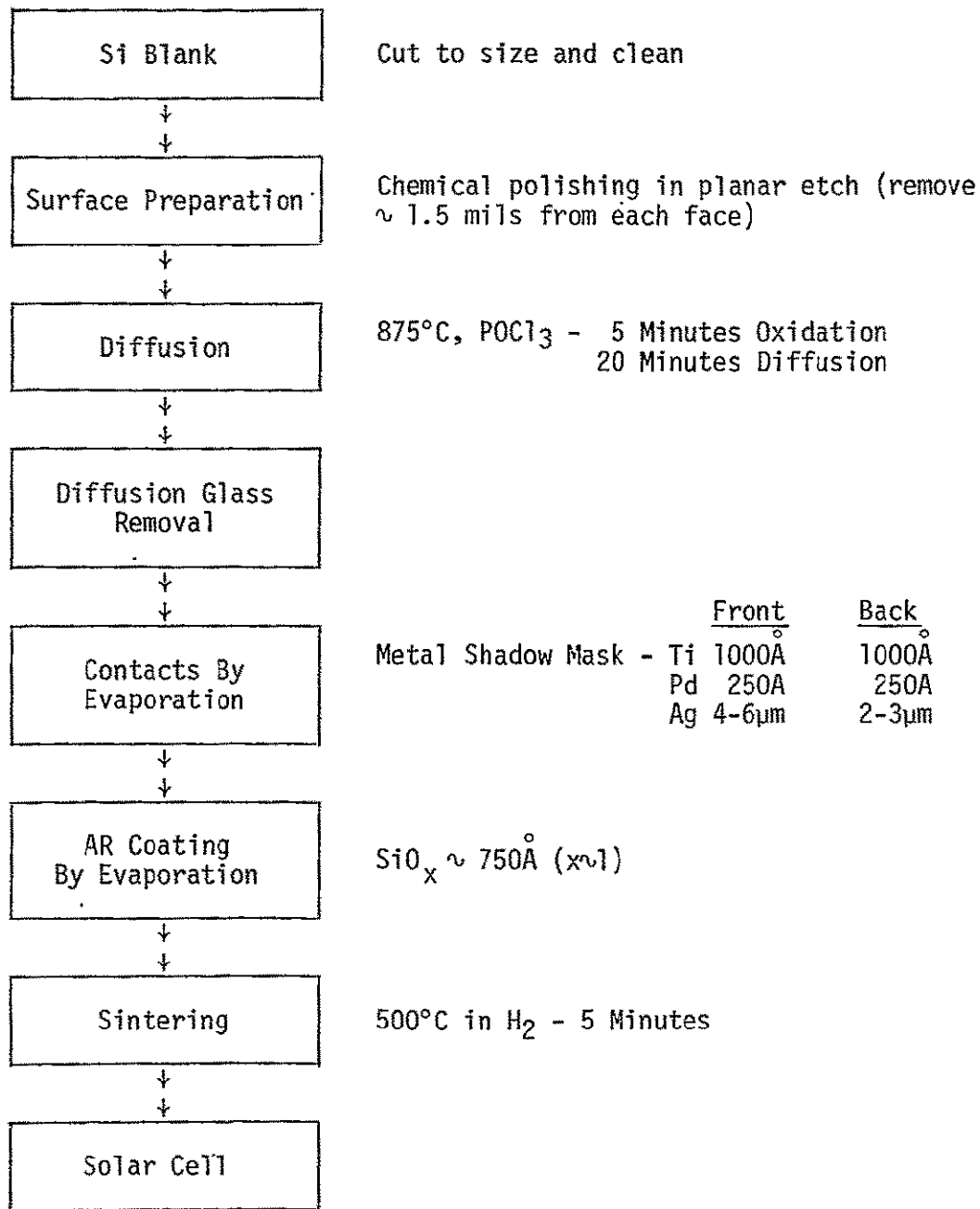|	Front	Back
Ti	1000Å	1000Å
Pd	250Å	250Å
Ag	4-6µm	2-3µm

FIGURE III-1

APPENDIX IV

OCLI AMO Solar Simulator

The OCLI AMO Simulator is described under three headings; the light sources and calibration, the cell holding fixtures and the readout equipment.

(a) Light Sources and Calibration

The AMO spectrum is simulated by two separate sources.

o The blue portion of the spectrum is obtained from a xenon arc lamp with an absorption filter which attenuates the large energy spikes in the near IR region.

o The red portion of the spectrum is due to a tungsten lamp set at 2800°K color temperature with suitable filters to blend with the blue portion of the spectrum, resulting in close approximation to the AMO spectrum. Figure IV-1 shows the Johnson AMO spectrum (approximates closely to the Thekaekara spectrum) and also the output of the OCLI Simulator. Also shown are the separate xenon (blue) and tungsten (red) contributions.

The two light sources do not provide collimated light, the cell test plane is placed at the plane of correct convergence; the uniformity across this plane is ±2% for areas up to 8 cm². The deviation of the centerline of each light source from perpendicular is around 11°.

In addition to allowing cell characterization under the AMO spectrum, this simulator has an added advantage for cell evaluation. By use of suitable blocking shields, either the blue or the red spectral output shown in Figure IV-1 can be used to illuminate the cell. Analysis of the absolute output under

these two filters can provide a rapid indication of the process control achieved on the cell. Experience has provided guidelines for "typical" readings in these two broadband regions for a variety of cells [including intentional variations in the silicon resistivity, diffusion conditions, surface finish, contact area coverage and whether or not the cell surface has an AR coating]. Thus evaluation of the blue response can indicate the performance of a given diffusion schedule with a given resistivity silicon, and can also check the effectiveness of an AR coating. The red response can also indicate whether the final bulk output is as expected, and can thus be used to assess the minority carrier diffusion length (D.L.) achieved. Although separate methods (surface or bulk photovoltage) are used for diffusion length measurement, this broadband check is most valuable to indicate the possible range of the diffusion length. For low diffusion length values, the red response decreases and crosses over the blue response for D.L. ∿10 μm. Thus the red response data are most useful for scanning a larger number of samples, and can then be related to more precise D.L.-values obtained by more detailed (separate) measurements.

Calibration

When first constructed the AMO·Simulators were calibrated by a set of standard cells which were calibrated regularly on Table Mountain by measuring the solar spectrum incident there, and by adjusting for the measured absorption band in the spectrum, extrapolating to AMO readings. Since then, it has become common

practice to use balloon-flown and recovered standard cells to set the AMO simulator intensity, and OCLI follows this practice using either OCLI-BF cells or those supplied by customers.

(b) Cell Holding Fixture

A variety of fixtures are used, depending on the size of the cell; if the cells are very fragile (thin or stressed slices) or the contacts are wraparound, a special fixture is used.

All these fixtures include a block which is controlled at preset temperatures by water pumped by a thermostatically controlled water bath, with feedback from a thermocouple embedded in the test block. These blocks also have vacuum hold-down facility, and contain voltage and current probes for measurement of cell electrical output.

(c) Read-Out Equipment

The simulator has a digital meter, reading selected parameters V_{oc}, I_{sc} and the current at pre-set voltage levels. In addition, digital print out of these values plus up to three other load voltage readings are available.

Finally for development purposes, the I-V curves can be traced and from these maximum power, CFF and efficiency values can be estimated.
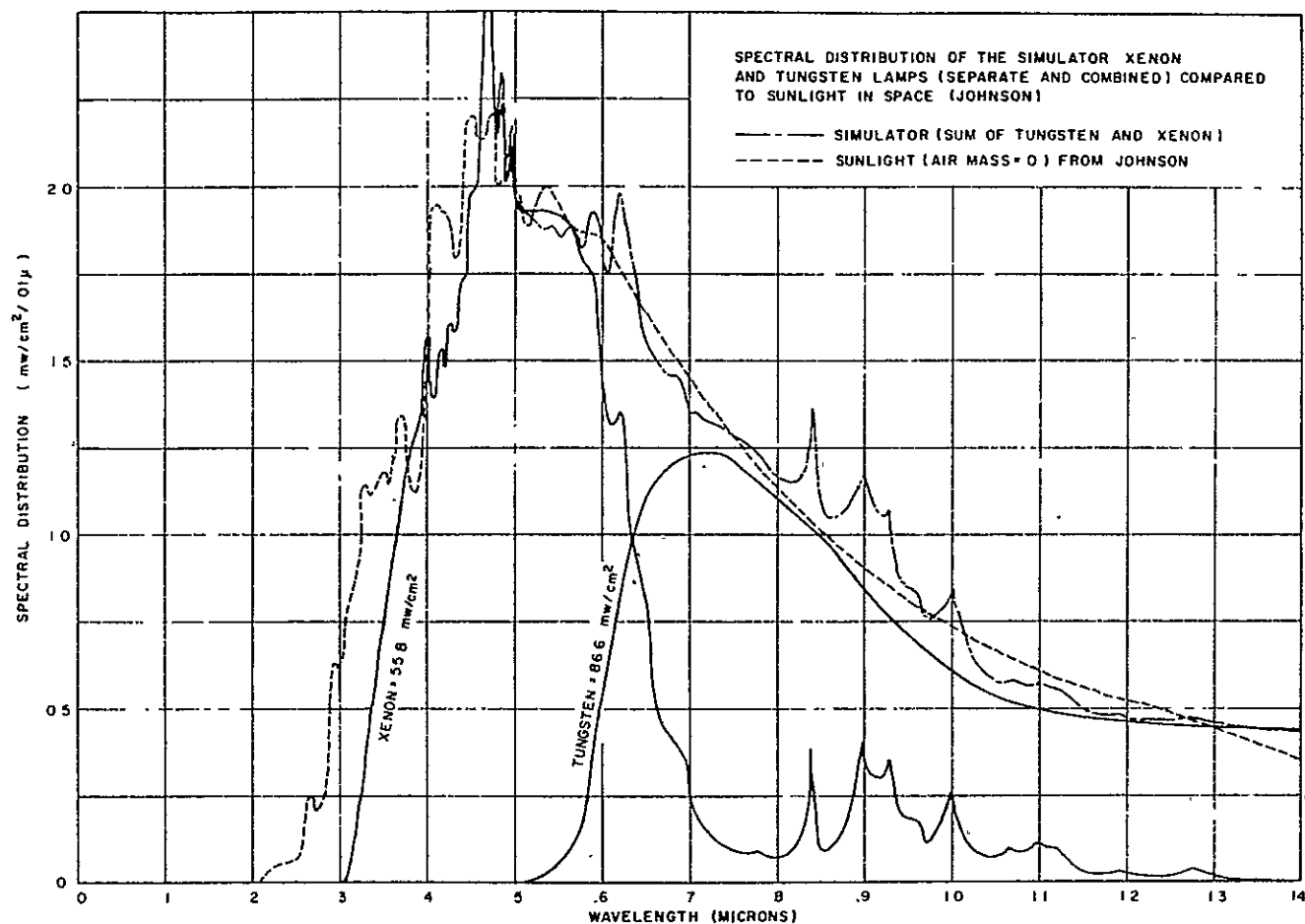
FIGURE IV-1

Spectral Distribution of the Simulator Xenon and
Tungsten Lamps (Separate and Combined) Compared
to Sunlight in Space (Johnson)

APPENDIX V

Description of Measurement Techniques

A. Spectral Response
B. Minority Carrier Diffusion Length
C. Photoresponse by Small Light Spot
   Scanning

A. SPECTRAL RESPONSE

Absolute spectral response (A/W) was measured using a filter wheel
which is a combination of a set of narrow bandwidth filters and a
light source (tungsten lamp operated at color temperature of 2800°C).
Spectral response of the solar cells was obtained by reading the
current (short circuit) of the cells (to be measured) at known wavelength:
and by calibrating this current to the current of a cell of known
spectral response (standard cell of known spectral response) from
the following relation:

$$S.R\ (\lambda) = S.R_{s.c}\ (\lambda) \cdot \frac{I\ (\lambda)}{I_{s.c}\ (\lambda)} \cdot N$$

where   S.R (λ):   Spectral response of a solar cell to be measured

   $S.R_{s.c}\ (\lambda)$:   Spectral response of a standard cell

   I (λ):   Short circuit current of a solar cell to be measured

   $I_{s.c.}(\lambda)$:   Short circuit current of a standard solar cell

   N: Normalization factor

$$N = \frac{A_{s.c}}{A}$$

where $A_{s.c}$:   Active area of a standard solar cell

   A: Active area of a solar cell to be measured

B. MINORITY CARRIER DIFFUSION LENGTH

Minority carrier diffusion length (D.L.) was measured using the surface photovoltage (SPV) method(on both bulk "Silso" wafers and diffused wafers. The exposed filtered beam size was about 3 mm in diameter.

Diffusion length measurement was also carried out using a short circuit current method** for the finished solar cells. The whole area of a solar cell was illuminated by a light source through a filter wheel and the effective minority carrier diffusion length of a solar cell was obtained from light intensity values at selected wavelengths. Wavelengths used for this measurement were 0.78, 0.86, 0.895, 0.95 and 0.98 μm. The wavelength dependence of reflection and absorption in anti-reflective coating layer was not considered for simplicity (generally, a straight line plot could be achieved).

*"Minority Carrier Diffusion Length in Silicon by Measurement of Steady State Surfaces Photovoltage", F391-73T ASTM, February, 1974.

**"Diffusion Lengths in Solar Cells From Short-Circuit Current Measurement", E.D. Stokes and T.L. Chu, Applied Physics Letters, 30, 425, 1977.

C. <u>PHOTORESPONSE BY SMALL LIGHT SPOT SCANNING</u>

<u>Description of Measurement</u>

A useful addition to analytical methods used to evaluate silicon sheet material for solar cell use is the small light spot scanner. This provides readout of the photosensitivity in small regions across the sheet (usually by moving a spot across a line near the center of a cell made from the sheet). In this way, the following information can be provided.

(i) Direct comparison of the output from different regions, can show the relative values of minority carrier diffusion lengths in those regions. In this way, spatial inhomogeneities can be seen and attempts made to correlate the different response with visual features, either present in the processed sheet silicon, or developed after additional chemical etching.

(ii) A particular case of interest is when crystalline grains are present, where the response for different grains near or at the grain boundaries, can be evaluated.

The light spot scans shown in this report have provided useful backup to the overall assessment, and provide a more realistic indication of the reasons for sheet behavior, e.g. whether reduced response was obtained as a function of the grain size or in relatively small areas across the sheet. In discussing the equipment we will indicate the possible features which can provide quantitative data. The measurement equipment is shown in the form of a block diagram in Figure V-1 and detailed techniques are discussed below.
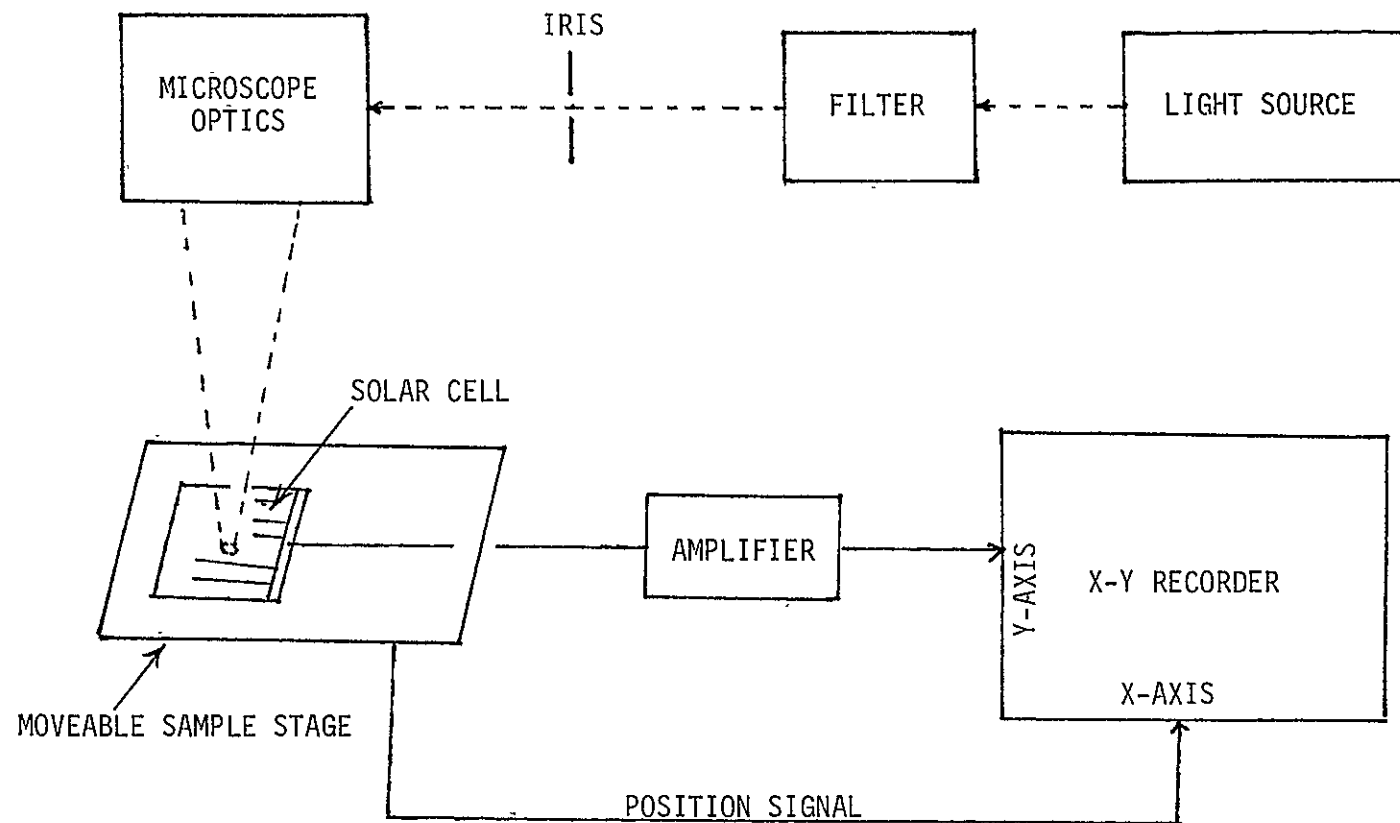
A BLOCK DIAGRAM OF A FINE LIGHT SPOT SCANNING APPARATUS

FIGURE V-1

Discussion of Components

(a) The light source should preferably contain long wavelength ($\lambda > 8000\overset{\circ}{A}$) components, to allow sampling of the silicon quality away from the surface. For alignment, à He-Ne laser has been used. For most measurements, a tungsten light is used, with a very thin Si filter to remove short wavelength components. Low intensities are useable. Even with the optical losses caused by the filter, the distance from the source to the cell (~ 6 ft), and the iris and demagnification through the microscope optics, the use of a built-in low noise amplifier near the cell stage provides sufficient signal to drive the x-y recorder.

(b) The use of a microscope provides direct observation of the area being scanned, to aid in correlation with visual features on the cells. The use of higher power objectives (with the irises) can provide spot sizes below 10 µm. However, at such small spot sizes, the depth of focus of the objectives is very small, and thus causes problems for sheet samples which do not have a high degree of flatness because the variable spot size provides variable areas of sampling. Therefore, a moderately high magnification objective was used mostly providing a spot ~ 20-50 µm in diameter. (For more detailed investigation in localized areas, it is planned to use smaller spots.)

(c) Even with the direct observation possibility, we use the gridlines on the cells as built-in distance (and locating) markers. Also by careful measurements of gridline width, and the shape of the intensity decrease while scanning over the gridline, an estimate can be made of the effective spot size.

(d) The cell is held in a pressure contact holder, on a platform which moves in and out, with speed adjusted by a variable control. The linear movement of the platform is fed into the x-axis of the controller; the amplified cell signal is fed into the y-axis.

(e) The x-y recorder is "calibrated" by using a control cell of good output; keeping the gain and light spot conditions. fixed, the cell under test is substituted and a comparison trace made.

It is possible to improve the quantitative comparison on this set-up, to calibrate the y-signal directly against the local diffusion length measurement. However, mostly the equipment has been used for broad-scale comparisons and overall confirmation of the results have been obtained from I-V curves, spectral response, or from separate diffusion length measurements.